Dihydroorotate dehydrogenase regulates ER membrane reorganisation and cell death in cancer

Thesis submitted in accordance with the requirements of the University of Liverpool for

the degree of Doctor in Philosophy

By

Govinda Raju Yedida

December 2019

DECLARATION

This thesis is the result of my own work. The material contained within this thesis has not been presented, nor is currently being presented, either wholly or in part for any other degree or qualification.

Govinda Raju Yedida

This research was carried out in the Department of Molecular and Clinical Cancer Medicine, University of Liverpool, UK.

Thesis contents

Publications

Govindaraju Yedida, Milani, M.,Cohen, G. M., and Varadarajan, S. 'Apogossypol-mediated reorganisation of endoplasmic reticulum antagonises mitochondrial fission and apoptosis.' Cell Death and Disease, July 2019 doi:10.1038/s41419-019-1759-y

Carter RJ, Milani M, Butterworth M, Alotibi A, Harper N, **Yedida G**, Greaves G, Al-Zebeeby A, Jorgensen AL, Schache AG, Risk JM, Shaw RJ, Jones TM, Sacco JJ, Hurlstone A, Cohen GM and Varadarajan S. 'Exploring the potential of BH3 mimetic therapy in squamous cell carcinoma of the head and neck', Cell Death and Disease, December 2019 doi:10.1038/s41419-019-2150-8

Abstract

The endoplasmic reticulum (ER) exists as an elaborated network of flat sheets and cylindrical tubules. ER network interacts with several other organelles, including mitochondria to play a vital role in membrane dynamics and other functions. However, the impact of ER-mitochondrial interactions on apoptosis is poorly understood. Cancer cells acquire resistance to anti-cancer agents through different mechanisms, including failure to undergo apoptosis. Therefore, better understanding of ER-mitochondrial communications and their impact on apoptosis could unravel mechanisms of drug resistance. We have previously observed a reversible reorganisation of ER membranes in cells exposed to several pharmaceutical agents. Hence, we conducted this study using ER membrane reorganisation as a tool to explore ER-mitochondrial communication and how it impacts mitochondrial-mediated apoptosis. This thesis is divided into three results chapters.

In the first results chapter, using apogossypol as a prototype tool compound, it is shown that ER membrane reorganisation occurs at the level of ER tubules but does not involve ER sheets. Moreover, further characterisation of the subcellular localisation of reorganised membranes reveal that other organelles, such as mitochondria, lysosomes, Golgi complex were not involved in ER membrane reorganisation. Next, the effect of ER membrane reorganisation with respect to mitochondrial membrane dynamics and apoptosis was studied. The results indicate that ER membrane reorganisation prevents DRP-1-mediated mitochondrial fission as well as BH3 mimetic-mediated BAX translocation, cytochrome c release and apoptosis.

In the next results chapter, the objective was to examine the impact of ER membrane reorganisation modulators on apoptosis. Inhibitors of dihydroorotate dehydrogenase (DHODH), such as teriflunomide and leflunomide, not only prevent ER membrane reorganisation, but also antagonise the protective effects of the reorganised ER membranes against BH3 mimetic-mediated apoptosis. Since DHODH inhibitors antagonised ER membrane reorganisation and enhanced BH3 mimetic-mediated apoptosis, in the next chapter, the therapeutic benefits of DHODH inhibitors was explored in head and neck squamous cell carcinoma (HNSCC). The results indicate that DHODH is highly expressed in HNSCC cell lines, and genetic as well as pharmacological inhibition of DHODH reduce clonogenic survival potential in several HNSCC cells. Although targeting DHODH could be a promising strategy in HNSCC, inhibitors of DHODH do not synergise with other potential chemotherapeutic agents namely, cisplatin, A-1331852, S63845, and CB-839. Further studies are required to assess whether DHODH inhibitors will be effective as single agents, or in combination with other novel chemotherapeutic agents.

Abbreviations

APAF-1	Apoptotic protease activation factor-1
ATF-6	Activating transcription factor-6
ATL	Atlastin
BAD	BCL-2 associated agonist of cell death
BAK	BCL-2 homologous antagonist killer
BAX	BCL-2 associated X protein
BCL-2	B cell lymphoma-2
BCL-w	BCL-2 like protein like proein-2
BCL-X_L	B-cell lymphoma-extra large
BID	BH3 interacting-domain death agonist
BIK	BCL-2-interacting killer
BIM	BCL-2-like protein 11
BMF	BCL-2-modifying factor
BIP	BIP binding immunoglobulin (BIP)
CCCP	carbonyl cyanide m-chlorophenyl hydrazine
CHOP	CCAAT/ enhancer-binding protein homologous protein
CLIMP63	CLIMP-63 cytoskeleton linking membrane protein 63
CLL	Chronic lymphocytic leukemia
DHODH	dihydroorotate dehydrogenase
DISC	death inducing signalling complex
DRP-1	Dynamin related protein-1
ER	Endoplasmic reticulum
ERGIC	ER-Golgi intermediate compartment
ERMR	Endoplasmic reticulum membrane reorganisation

FADD	Fas associated death domain protein
GRP75	Glucose regulatory protein 75
HMG-CoA reductase	3-hydroxy-3-methylglutaryl-CoA reductase
HNSCC	Head and neck squamous cell carcinoma
IP3R	Inositol 1,4,5-trisphophate receptors
IRE1	Inositol-requiring enzyme 1
KNT-1	Kinectin-1
LNP	Lunapark
MCL-1	Myeloid cell leukaemia 1
MCU	Mitochondria calcium uniporter
MFF	Mitochondrial fission factor
MFN	Mitofusions
MiD49	Mitochondrial dynamics of 49 kDa protein
MiD51	Mitochondrial dynamics of 51 kDa protein
NOXA	Phorbol-12-myristate-13-acetate-induced protein 1
OPA1	Optic atrophy1
ORAI1	Calcium release-activated calcium modulator 1
PC	Phosphatidylcholine
PDI	protein disulphide isomerase
PE	phosphatidylethanolamine
PERK	Protein kinase RNA-like ER kinase
PEX	Peroxisomal assembly proteins
PIP2	Phosphatidylinositol 4,5-bisphosphate
PUMA	P53 upregulated modulator of apoptosis
RTN-4	Reticulon-4

RHD	Reticulons have a specialised reticulon homology domains
RyR	Ryanodine receptor
SERCA	Sarcoendoplasmic reticulum calcium transport ATPase
SOCE	Store operated calcium entry
STIM	Stromal interaction molecule
TMEM	Transmembrane protein 16
VAP	Vesicle associated membrane protein-associated protein
VDAC	Voltage dependent anion channel
XBP1	X-box binding protein 1

List of figures

Chapter 4

Chapter 5

Chapter 1
General introduction

Contents

1.1. Structural domains of the endoplasmic reticulum

The endoplasmic reticulum (ER) is an important cellular organelle that is involved in many fundamental cellular processes[1]. Dysfunction of the ER has been associated with different diseases, including cancer[2–5]. The ER is widely spread throughout the cell and exists as a network with distinct morphological domains, such as the elongated ER tubules and flattened ER sheets[6,7]. ER tubules exhibit a cylindrical shape, which is maintained by specialised residential proteins, such as the members of reticulon family[8,9]. Reticulons have specialised reticulon homology domains (RHD), which forms a hairpin like structure for bending the ER membrane to maintain tubular architecture[10]. In contrast, ER sheets are flattened structures, which appear as a series of stacked flat sheets, and each stack connected by helical ramps[10]. This architecture helps to provide the wide space required for ribosomal binding, protein folding and other ER functions. ER sheets are maintained by several proteins, including CLIMP-63 (cytoskeleton linking membrane protein 63), kinectin-1 (KNT-1) and p180 [10,11]. Ribosomes localise on the ER sheets and are commonly referred to as the rough ER, which play an important role in protein synthesis[12,13]. In contrast, smooth ER is devoid of ribosomes and plays significant role in lipid synthesis and organelle interaction[2,14]. The lumen of ER is separated from the cytosol and provides the space required for important physiological functions like protein folding and other ER mediated functions[15]. In addition, recent studies have demonstrated that ER tubules form extensive branches resulting in the creation of three-way junctions. The key players from these junctions are proteins, such as the atlastins (ATL) and lunapark (LNP) [16,17]. These junctions maintain the ER shape and membrane dynamics[18,19].

1.2. ER membrane contacts

Owing to their widespread distribution throughout the cell, the ER membranes form contacts and/or cross-talks with various other cellular organelles, including the mitochondria, lysosomes and peroxisomes[6,20,21]. These interactions play critical roles in several cellular processes, including cell survival, lipid exchange and calcium signalling[20,21].
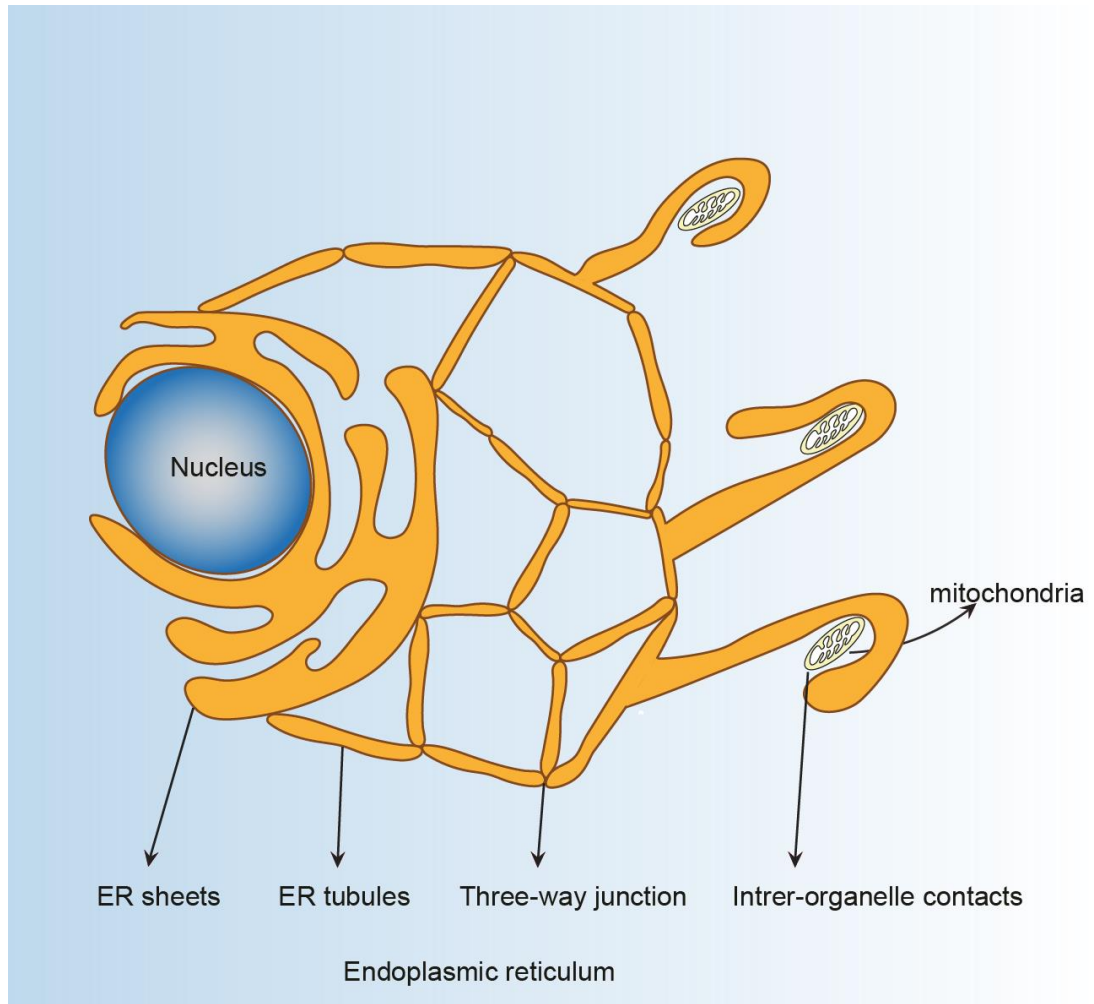
Figure 1.1. Schematic diagram of ER structural domains. The ER is widely spread throughout the cell with distinct morphological domains composed of flattened sheets and elongated tubules. ER tubules often form three-way junctions, as result of fusion among tubular membranes. Elongated ER tubules interact with several organelles, including mitochondria, which in turn regulate mitochondrial membrane dynamics and functions.
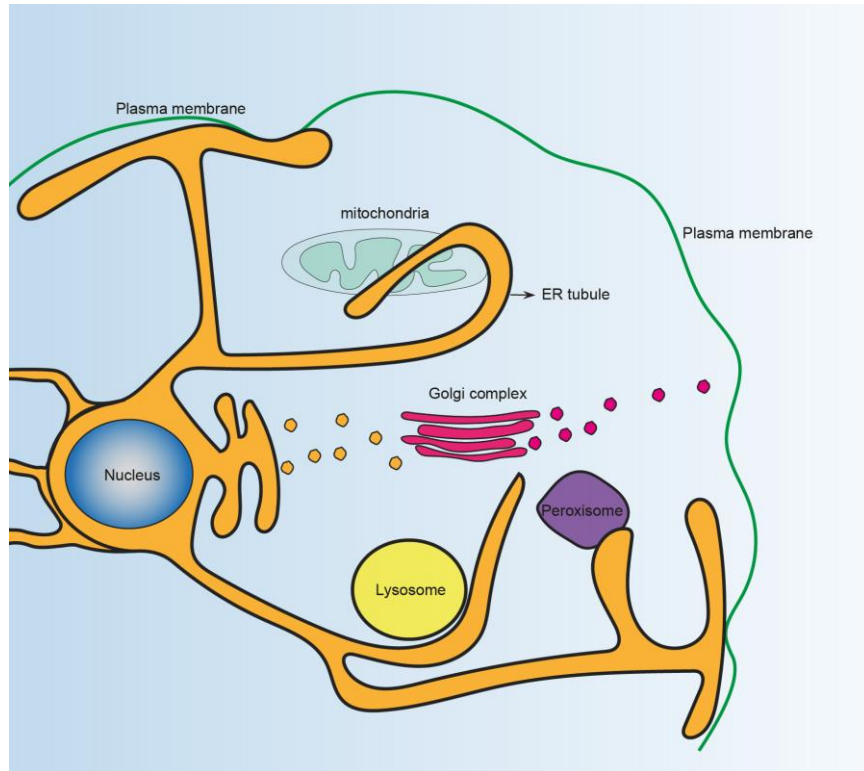
Figure 1.2. Schematic representation of ER membrane organelle contacts. ER tubules interact with other organelles, including mitochondria, lysosomes, peroxisomes and Golgi complex for maintaining cellular survival and cell death homeostasis.

1.2.1.   ER-mitochondrial contact sites

ER membranes interact with the mitochondria at mitochondrial-ER contact sites (MERCs) that are crucial hubs for lipid transfer, mitochondrial fission, calcium homeostasis, cellular stress, cell survival and cell death[22,23]. MERCs play a critical role in the transfer of calcium from the ER to mitochondria during cell death [24]. ER is the major site of calcium storage within the cell. The cytosolic calcium enters ER *via* SERCA ATPases and released from the ER *via* inositol trisphosphate receptors (IP3R)[25,26] . It has been reported that IP3Rs allow calcium transfer from ER to the mitochondria through outer mitochondrial localised voltage dependent anion channel (VDAC)[26].The coupling of IP3R and VDAC is stabilised by the ER-localised protein, Grp75[22,26] . This coupling system (IP3R-Grp75-VDAC) helps in the transfer of calcium from ER to outer mitochondrial membrane (OMM), which is then exchanged to inner mitochondria membrane (IMM) through mitochondria calcium uniporter (MCU)[22] . It has been reported that any alteration in ER-mitochondria molecular tether complex (IP3R-Grp75-VDAC-MCU) will influence cellular stress and cell survival mechanisms [24,26–30].

ER-mitochondrial interface also plays important roles in lipid transfer and mitochondrial membrane biogenesis [21,31]. In the context of lipid transfer, the major phospholipids of mitochondrial membranes, namely phosphatidylethanolamine (PE) and phosphatidylcholine (PC), are both synthesised in the ER and later translocated to the mitochondria to regulate mitochondrial membrane biogenesis and maintenance [21]. Similarly, ceramide is another lipid synthesised in ER and translocated to the mitochondria to act as a precursor for membrane sphingolipids in mitochondrial membrane biogenesis [24,32,33].

1.2.2.   ER-lysosomal contact sites

Lysosomes is one of the key organelles involved in intracellular digestion, it contains several acidic enzymes responsible for the breakdown of macromolecules into their individual molecules, thus regulating cellular homeostasis including cell death and survival[34–37]. ER-lysosomal contacts play important role in nutrient sharing, in this process ER tubule fuse with lysosomes *via* a SNARE mechanism achieved by

syntaxin-7 (STX-7) and VMP7, the ER also play a critical role in ER-lysosomal mediated calcium-induced-calcium-release (CICR) process[38].In this process, nicotinic acid adenine dinucleotide phosphate (NAADP) plays a key role to release lysosomal calcium from two pore channel (TPC) channels located in the lysosomal membrane[38]. Lysosomal released calcium further activates ER membrane calcium channels IP3R and RyR[38]. CICR process will help to amplify calcium levels and controlling adequate amount of calcium storage in lysosomes and ER. However, the composition of organelle interaction is clearly in metabolite exchange but exciting new functions in organelle interaction and communication have been discovered[38]
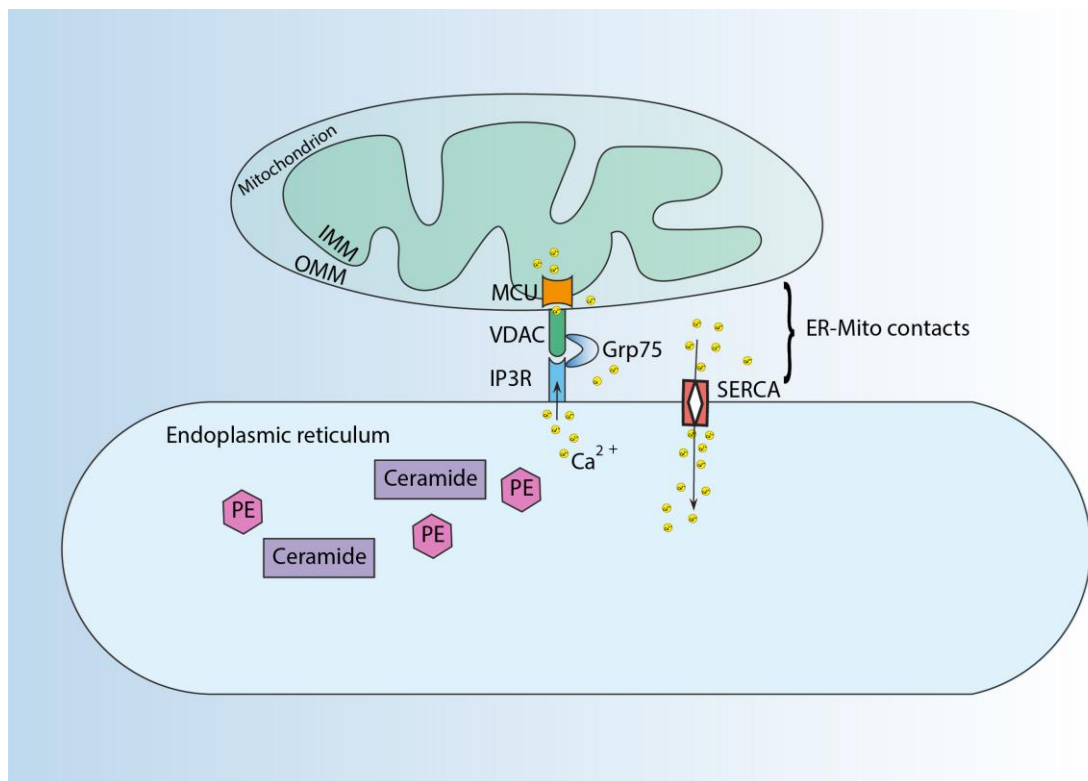
Figure. 1.3. Schematic representation of ER-mitochondrial contacts tether complex. ER-mitochondrial tethers often facilitate calcium transfer between ER-mitochondria through tether complex (IP3R-Grp75-VDAC-MCU).

1.2.3.　ER-Peroxisomal contacts sites

ER membranes interact with peroxisomes for membrane biogenesis[39,40] and lipid transfer[39,41,42]. PEX proteins, including PEX 3 and PEX19, are synthesised in the ER from they are translocated to peroxisomes for membrane maintenance[43]. However, precise molecular mechanism exist between ER-peroxisomal contact sites are still unclear[39,41,43,44].

1.2.4.　ER-plasma membrane contact sites

ER-plasma membrane contacts also play important roles in calcium homeostasis and the regulation of store operated calcium entry (SOCE)[45,46]. ER is the main calcium storage unit within the cell[47–50]. High levels of ER calcium facilitate proper protein folding[46]. Depletion of ER calcium levels results in the oligomerisation of an ER transmembrane stromal interaction molecule (STIM1), which in turn interacts with a plasma membrane-bound calcium release-activated calcium modulator 1 (ORAI1)[45,46]. Coupling of STIM1 and ORAI1 results in SOCE to facilitate the refilling of the depleted ER calcium stores[51–53]. Similarly, ER-plasma membrane contacts also play critical roles in lipid translocation[49,54]. It has been reported that lipid shuttling often uses tether complexes, such as vesicle associated membrane protein-associated protein (VAP) and transmembrane protein 16 (TMEM 16)[55].

1.3.　ER function

ER is involved in several cellular functions, including protein folding, protein quality control, calcium storage, lipid synthesis, sterol biosynthesis, drug detoxification and cell death[11,24,32,56–59]. In the context of lipid biosynthesis and regulation, ER synthesises several structural phospholipids, such as phosphatidylcholine (PC), phosphatidylethanolamine (PE), as well as ceramides and cholesterol[60]. The initial steps of ceramide synthesis take place within the ER, following which ceramides are transferred to the Golgi complex to aid in the formation of complex sphingosine[60]. Sphingosine is one of the major lipids in the lipid bilayer. Alterations in ER lipid synthesis leads to several disorders, including obesity and cancer[33,60]. ER also regulates cholesterol biosynthesis, as the rate-limiting step is catalysed by the ER resident protein, HMG-CoA reductase (3-hydroxy-3-

methylglutaryl-CoA reductase)[61]. Alterations in HMG-CoA reductase are associated with several diseases, including smith-lemi-opitz syndrome, Alzheimers disease and cardiovascular diseases[61].

Detoxification is the physiological process responsible for removal of toxic substances from body and is mainly carried out by the liver[59]. ER in the liver cells (hepatocytes) allows a larger surface area and space for detoxifying enzymes. Various detoxifying enzymes identified in the ER, such as cytochrome P450, metabolise toxic compounds, such as the anti-epileptic drug, phenobarbital[62]. Interestingly, chronic phenobarbital toxification often changes the entire ER morphology[62]. Such ER morphological changes referred to as anastomosing ER is an adaptive response to deal with high concentrations of phenobarbital [62].

1.4. Mitochondrial fission and fusion

Mitochondria are dynamic organelles and often undergo fission and fusion to control their shape and functions[7,27,31,63]. Mitochondrial fission is a highly co-ordinated process in which mitochondria are divided into two or more independent mitochondria[7,24]. During mitochondrial fission, ER tubules wrap around the mitochondria and marks the fission constriction site at the outer mitochondrial membrane (OMM) [7,31,64]. This is followed by the translocation of DRP-1 (dynamin related protein-1) from the cytosol to OMM[7,27,31]. DRP-1 is a GTPase super family protein, which upon mitochondrial translocation binds to its receptors, such as MFF (mitochondrial fission factor), MiD49 (mitochondrial dynamics of 49 kDa protein) and MiD51 (mitochondrial dynamics of 51 kDa protein)[31,65].

Mitochondria also undergo fusion, wherein two or more mitochondria fuse together to generate elongated mitochondria[31]. Several outer and inner mitochondrial proteins, such as mitofusions (MFN1 and MFN2) and OPA1 (optic atrophy1) aid in mitochondrial fusion[48].
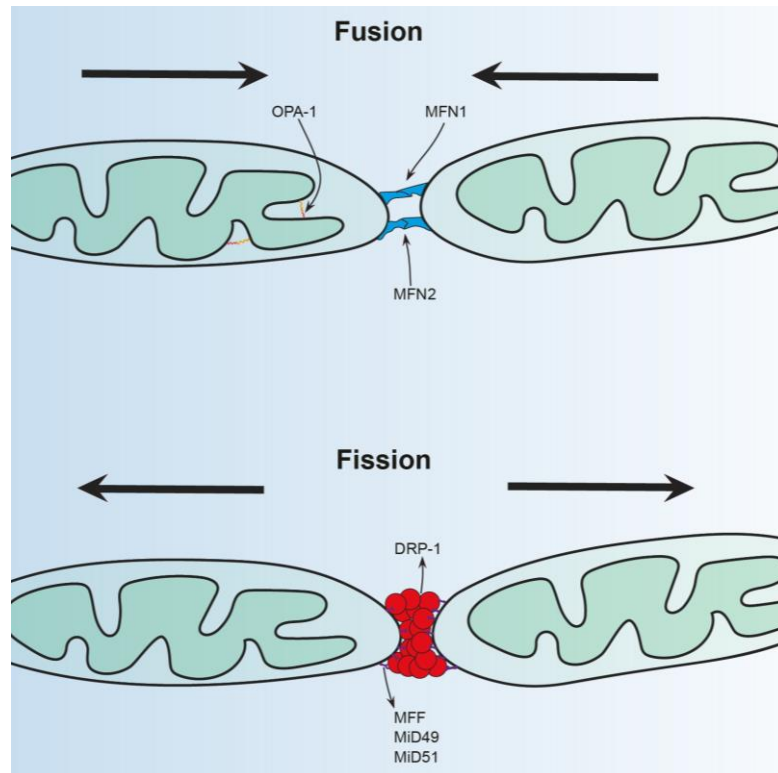
Figure 1.4. Schematic representation of mitochondrial fission and fusion. Mitochondria are dynamic organelles. Mitochondrial fusion process is mediated by MFN1 and MFN2 in the outer mitochondrial membrane and by OPA-1 in the inner mitochondrial membrane, whereas mitochondrial fission is mediated by binding of DRP-1 to its receptor in outer mitochondrial membrane.

1.5. Calcium signalling

ER calcium signalling is tightly controlled by several influx and efflux mechanisms [53,66,67]. The efflux of calcium is regulated by IP3Rs (inositol 1,4,5-trisphophate receptors)[68] and RyRs (ryanodine receptors)[69]. Increased ER lumenal calcium levels often activates IP3 signalling, which involves the cleavage of PIP2 (phosphatidylinositol 4,5-bisphosphate) to IP3 and DAG (diacylglycerol) with the help of phospholipase C [53]. Activated IP3 binds to its receptor to facilitate the release of ER calcium into cytosol. In contrast, RyRs act as calcium sensors, and get spontaneously activated when ER lumen is overloaded with calcium[50,66]. The influx of ER calcium is regulated by SERCA (sarcoendoplasmic reticulum calcium transport ATPase), which accumulates calcium inside ER lumen and regulates ER homeostasis[70–73], ER stress and apoptosis[50,53]. As detailed above, inhibition of SERCA activity depletes ER calcium stores and facilitates store operated calcium entry (SOCE) (Figure 1.5) [74–77] by the interactions of STIM and ORAI proteins (Figure 1.5)[50].
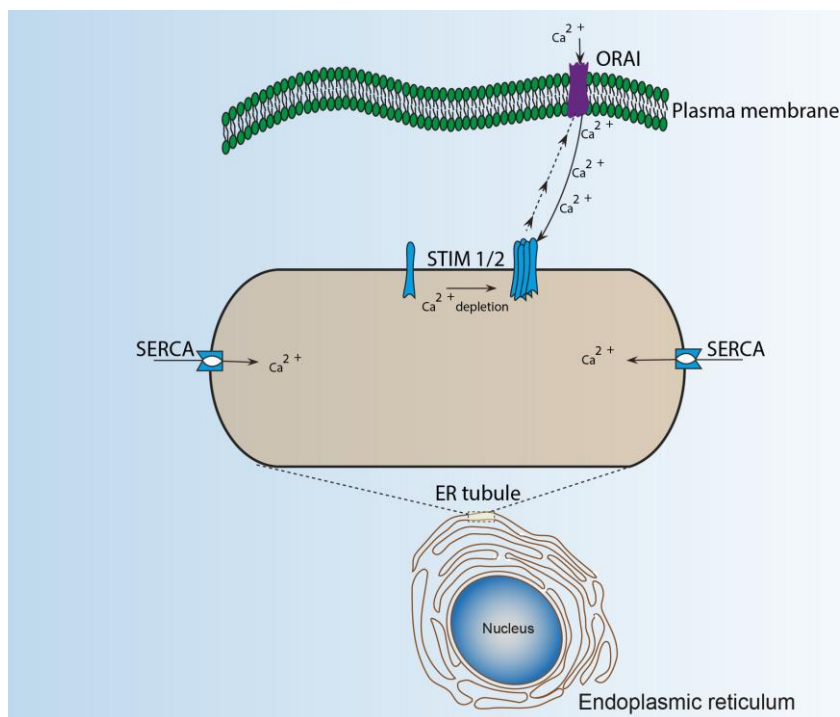
Figure.1.5. Schematic representation of store operated calcium entry. Normally ER calcium influx occurs through SERCA and stored inside ER lumen for maintaining ER functions and homeostasis. Inhibition of SERCA by thapsigargin reduces ER lumenal calcium levels, which are sensed by ER membrane proteins, such as STIM1/2. This helps to refill ER calcium by association with plasma membrane calcium channel proteins, such as ORAI1.

1.6.   ER stress and the unfolded protein response

The ER plays an important role in protein folding[78–81]. Newly synthesized polypeptides are translocated to the ER lumen *via* a large transmembrane channel called the ER translocon, which is composed of Sec61β protein complex[80] . Upon translocation, the polypeptides are carefully folded within ER lumen with the help of ER chaperones, such as binding immunoglobulin (BIP) and protein disulphide isomerase (PDI)[79,82] . Correctly folded proteins are then released from ER to the Golgi complex for further processing and maturation, and eventually translocated to their final destinations[4,83] . Proper protein folding is critical for maintaining cellular homeostasis, including cell survival and cell death[4,84].

Accumulation of misfolded proteins inside the ER lumen activates the unfolded protein response (UPR)[4] . The main goal of the UPR is to restore the protein folding capacity of the ER as quickly as possible by halting other cellular functions that are required for protein synthesis [84]. The UPR signalling pathway is controlled through three different stress-sensor proteins, namely PERK (protein kinase RNA-like ER kinase), IRE1 (inositol-requiring enzyme 1) and ATF6 (activating transcription factor 6)[80,84] . In normal conditions, PERK, IRE1 and ATF6 are found bound to BIP [82,85]. Upon UPR stimulation, these interactions are disrupted and BIP is released, which leads to the activation of PERK, IRE1 and ATF6 [4,80]. Activation of PERK involves its dimerization and phosphorylation, followed by the phosphorylation of a eukaryotic translation initiation factor 2 alpha (eif2α), which inhibits protein translation and enables the cells to restore ER homeostasis[4,86] . The active form of IRE1 induces the mRNA splicing of x-box binding protein 1(XBP1). Thereafter, the spliced XBP1 (sXBP1) is translocated to the nucleus, where it binds to an ER stress response element promoter and transcribes several UPR response genes[4] . Dissociation of BIP from ATF6 transports the full length ATF6 (p90) to the Golgi complex, where it is proteolytically cleaved to ATF6 (p50)[80,82] . The cleaved form of ATF6 (p50) also acts as a transcription factor and regulates transcription of UPR response genes[4,87] . While activated PERK, IRE1 and ATF6 signal to alleviate ER stress and restore ER homeostasis, this is not possible under prolonged ER stress. As a result, the UPR mechanisms lead to apoptosis[4,88] . It has been reported that CCAAT/ enhancer-binding protein homologous protein (CHOP) plays a crucial role in ER stress-mediated apoptosis[87,89] .
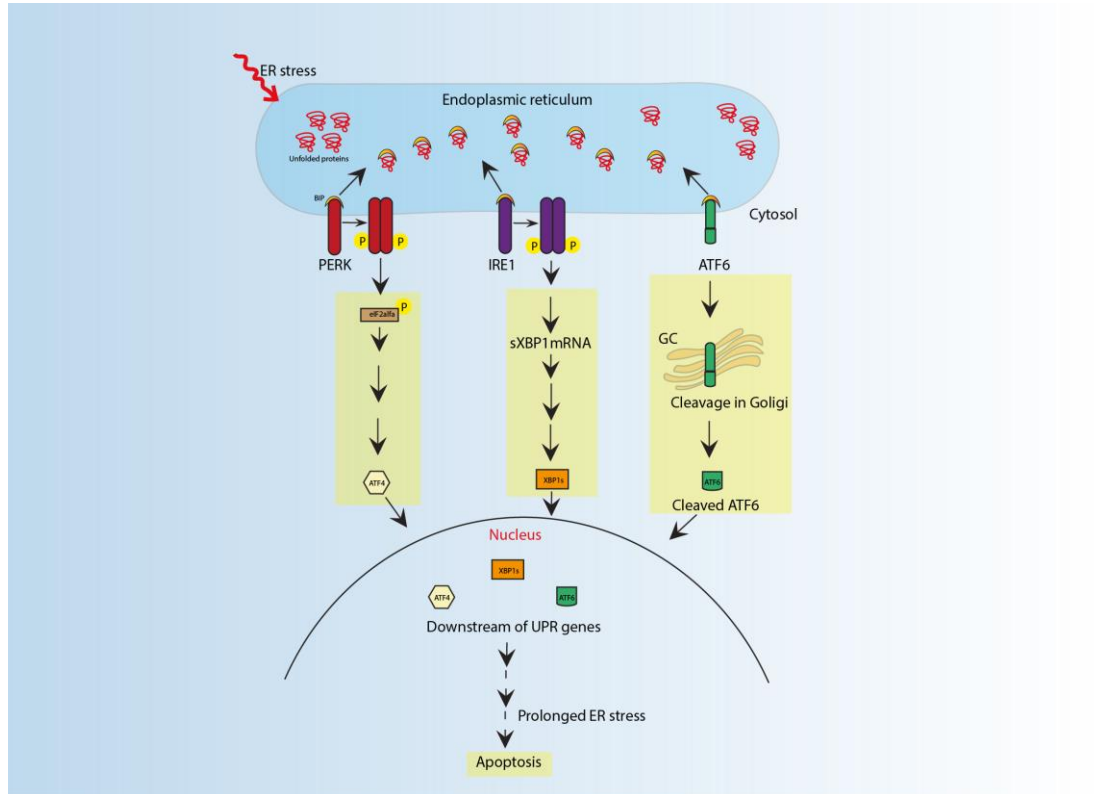
Figure.1.6. Schematic representation of ER stress and UPR signalling. Disrupted protein folding inside ER lumen often causes ER stress and activates an adaptive response called unfolded protein response (UPR). This response is mediated by the dissociation of BIP from three ER stress sensors. PERK, IRE1 and ATF6. Following dissociation of BIP from PERK becomes activated by dimerization process and its downstream activated signal helps to relieve ER stress. Activated IRE1 induces splicing of XBP1 mRNA into sXBP1 and its downstream signal process helps to relieve ER stress. ATF6 is translocated to the Golgi complex, where it is cleaved into an active transcription factor to relieve ER stress. Prolonged ER stress often triggers apoptosis *via* CHOP.

1.7. ER membrane reorganisation

Although the canonical ER stress response and the UPR have been extensively characterised, recent findings have demonstrated a novel form of ER stress, in which the ER membranes are reorganised by distinct pharmacological agents, such as apogossypol, ivermectin and NDGA (Figure 1.7)[90,91]. Such ER membrane reorganisation (ERMR) is evolutionary conserved from yeast to humans, as ERMR has been observed in fission yeast (*Schizosaccharomyces pombe*), Chinese hamster ovary cells (CHO), mouse embryonic fibroblasts (MEF) as well as in several human cell lines[91]. The induction of ERMR is rapid and occurs within 30 minutes of exposure to the reorganisation inducers[91]. Moreover, ERMR can be completely reversed when the drugs are washed out [91].

ERMR alters vesicular trafficking from ER/Golgi and also attenuates global protein synthesis[91]. Despite such effects, ERMR has been shown to be distinct from the UPR, as ERMR occurs even in the absence of new transcription and translation and also in cells lacking UPR regulators, such as PERK, IRE1, ATF6, XBP1 and CHOP[91]. It has been reported that reorganisation inducers target calcium homeostasis and may promote SOCE[91]. Overexpression of STIM1 can induce ERMR and inhibitors of SOCE, such as 2-APB (2-aminoethoxydiphenyl borate), can efficiently prevent apogossypol-mediated ERMR[90]. These findings suggested that there could be specific regulatory mechanisms between STIM and SOCE that could modulate ERMR. However, silencing the expression levels of SOCE regulators (STIM1 and ORAI1) does not alter apogossypol-mediated ERMR. In addition, extracellular supplementation of calcium also does not alter ERMR[90], further suggesting that 2-APB most likely regulates ERMR independent of calcium signalling.
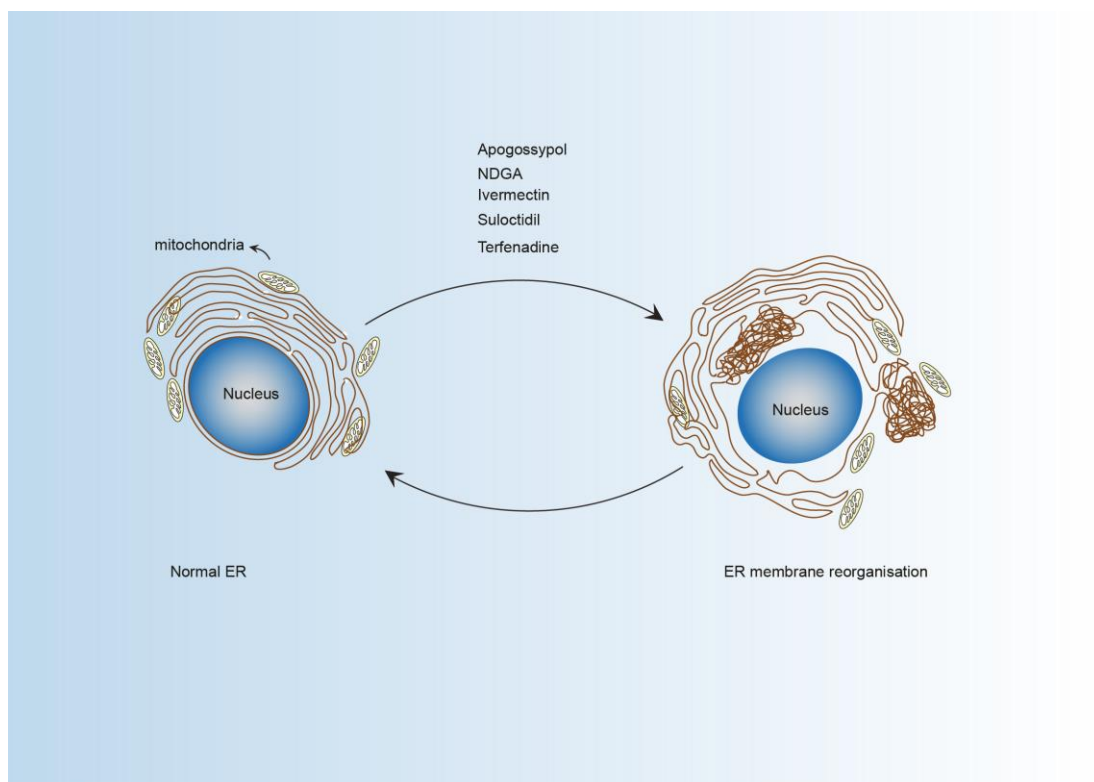
Figure. 1.7. Schematic representation of ERMR. ERMR is triggered by several chemical compounds, including apogossypol, NDGA, ivermectin, suloctidil and terfenadine. (Scheme adapted from Varadarajan et al., 2012 [91]).

1.8. Apoptosis

Apoptosis is highly conserved pathway and is critical for the development of tissues and organisms[92–94]. It is characterised by the condensation of nucleus, a decrease in cell size and plasma membrane blebbing[95]. An imbalance in apoptosis is a common feature of many diseases, including cancer[93,96,97]. Apoptosis pathway can be initiated by either the mitochondrial dependent (intrinsic) (Figure 1.10) or mitochondrial independent pathway (extrinsic) (Figure 1.10)[92,98–100]. The extrinsic pathway occurs at the level of cell surface and initiated by the binding of death ligands to its receptors. Death ligands like FasL binds to Fas receptor, recruit adaptor proteins like Fas associated death domain protein (FADD), to form the death inducing signalling complex (DISC), which eventually leads to the activation of caspases -8, -3 and -7[92,101] (Figure 1.10). In certain cells the activation of effector caspases by caspase-8 requires the cleavage of Bid, a member of the BCL-2 family proteins[102] (Figure 1.10). In contrast, the mitochondria play an important role in intrinsic pathway. This pathway initiated by the pore formation at outer mitochondrial membrane by a process known as mitochondrial outer membrane permeabilization (MOMP)[98]. This results in the release of cytochrome c from inner mitochondrial membrane to the cytosol[99] (Figure 1.10) . Released cytochrome c binds to an apoptotic protease activation factor-1 (APAF-1), which in turn recruits procaspase 9 to form the apoptosome[98,100]. This further cleaves procaspase 9 into active caspase 9 and initiates the caspase cascade. This pathway is regulated by different members of the BCL-2 family proteins[103] (Figure 1.10).

The BCL-2 family members share one or more common BCL-2 homology (BH) domains such as BH1, BH2, BH3 and BH4, and can be divided into anti-apoptotic proteins (BCL-2, BCL-X_L, BCL-w and MCL-1) and pro-apoptotic proteins (Figure 1.8)[92,96–98]. Proteins that possess only the BH3 domains are referred to as the pro-apoptotic BH3 only proteins (Figure 1.8), which can further sub-divided as activators (BIM, BID, PUMA) and sensitisers (BAD, NOXA, BIK, BMF). In addition, the pro-apoptotic BCL-2 family members include effector proteins, BAX, BAK (Figure 1.9). The activators of BCL-2 family, BIM, BID and PUMA are block the anti-apoptotic proteins and can interact with BAX and BAK then induce apoptosis (Figure 1.9). The effector proteins of BCL-2 family, BAX, and BAK are inhibited the anti-apoptotic proteins BCL-2, BCLX$_L$, MCL-1 (Figure 1.9). Upon induction of

apoptosis, the sensitisers BAD and NOXA are inhibit the anti-apoptotic proteins (Figure 1.9). For example, BCL-2, BCL-w, and BCL-X$_L$ can bind to and inhibit BAD, while MCL-1 cannot. Instead, MCL-1 can uniquely bind to NOXA (Figure 1.9). Pro-apoptotic protein that normally resides in the cytoplasm and upon apoptotic stimuli, undergoes conformational changes to translocate to OMM[96,98]. On the other hand, BAK is normally localised on OMM in healthy cells, upon apoptotic stimuli BAK undergoes conformational changes and eventually form pore on outer mitochondrial membrane[92,98]. Upon disruption of outer mitochondrial membrane, cytochrome *c* released into cytosol which finally triggers the apoptosis by promoting caspase activation (Figure 1.10).

Cytochrome *c* is an important component of the mitochondrial electron transport chain[104–106]. The electron transport chain consists of several complexes such as, complex I. Complex II, complex III, cytochrome *c* and complex IV. It has been reported that electron transport chain components critically affect cell death and survival process[105]. For example, the loss of electron transport chain components, such as cytochrome *c* affects mitochondrial function and could result in cell death[107]. Under normal conditions, cytochrome *c* resides inside mitochondrial cristae and this is regulated by optic atrophy 1 (OPA-1)[108,109]. During apoptosis, OPA-1 is proteolysed, which eventually facilitates the release of cytochrome *c* from the inner mitochondrial membrane to the cytosol *via* BAX and BAK pores[110]. Released cytochrome *c* then binds to an apoptotic protease activation factor-1 (APAF-1), which eventually recruits procaspase 9 to form the apoptosome[111].

Targeting BCL-2 family of proteins is made possible using BH3 mimetics, which are small molecule inhibitors that mimic the BH3 domains of BH3-only proteins (Figure 1.8)[102,112–116]. BH3 mimetics bind to the hydrophobic groove of the anti-apoptotic members to prevent their function and trigger apoptosis[102,113]. Specific BH3 mimetics have now been developed to selectively inhibit BCL-2 (ABT-199)[114], BCL-X$_L$ (A-1331852)[117,118] and MCL-1 (A-1210477)[118]. ABT 199 (venetoclax), a specific BCL-2 inhibitor, was developed for the treatment of CLL and is the first FDA-approved BCL-2 inhibitor for CLL treatment[114119,120].
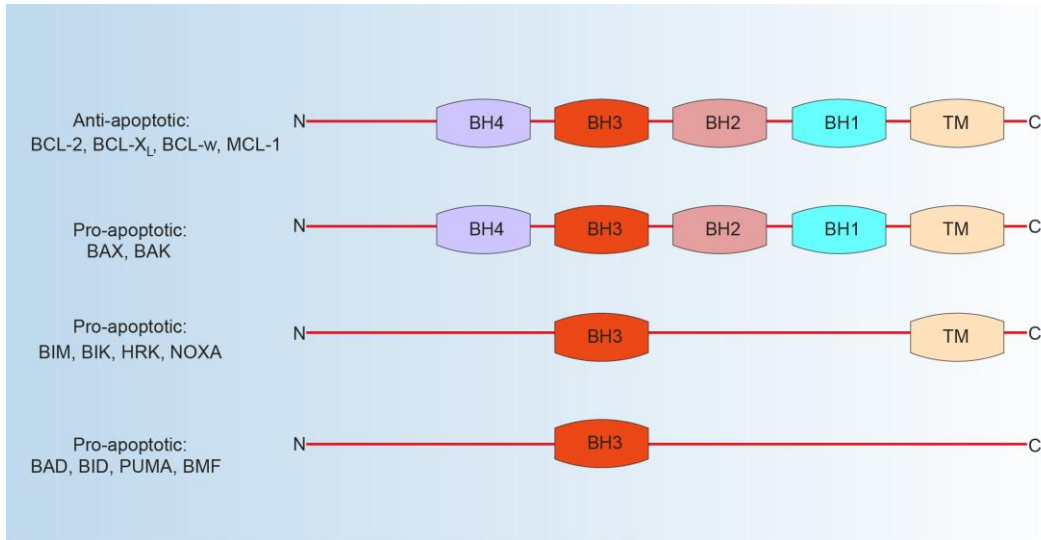
Figure. 1.8. The schematic representation of the structural features of anti-apoptotic and pro-apoptotic BCL-2 proteins. The BCL-2 family proteins have different homologue domains (BH1-4) and the carboxy terminal transmembrane domain (TM)[102,121].
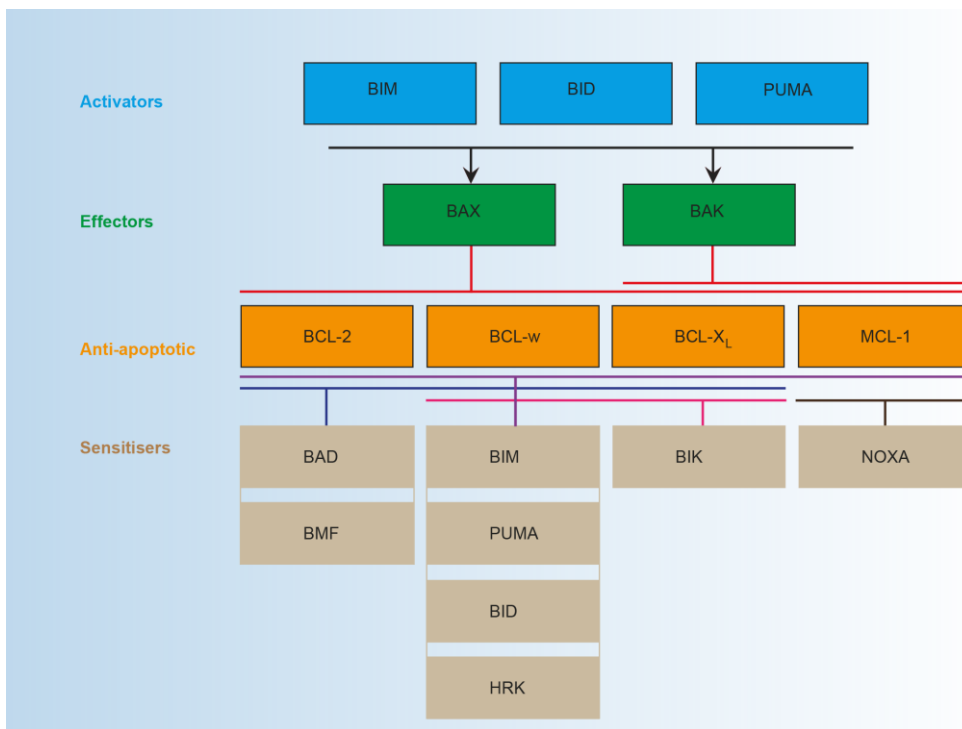
Figure. 1.9. The schematic representation of the major members of BCL-2 family of proteins and their interactions. The anti-apoptotic BCL-2 family of proteins (BCL-2, BCL-w, BCL-X$_L$ and MCL-1 are suggested to interacted with both sensitisers, activators and effector members to facilitate the regulation of apoptosis within a cell. The activators (BH3-only proteins) exhibit more specific interaction patterns for each anti-apoptotic member. For example, the anti-apoptotic members such as BCL-2, BCL-w and BCL-X$_L$ can interact with and inhibit BAD. While MCL-1 have a specific interaction with NOXA[122].
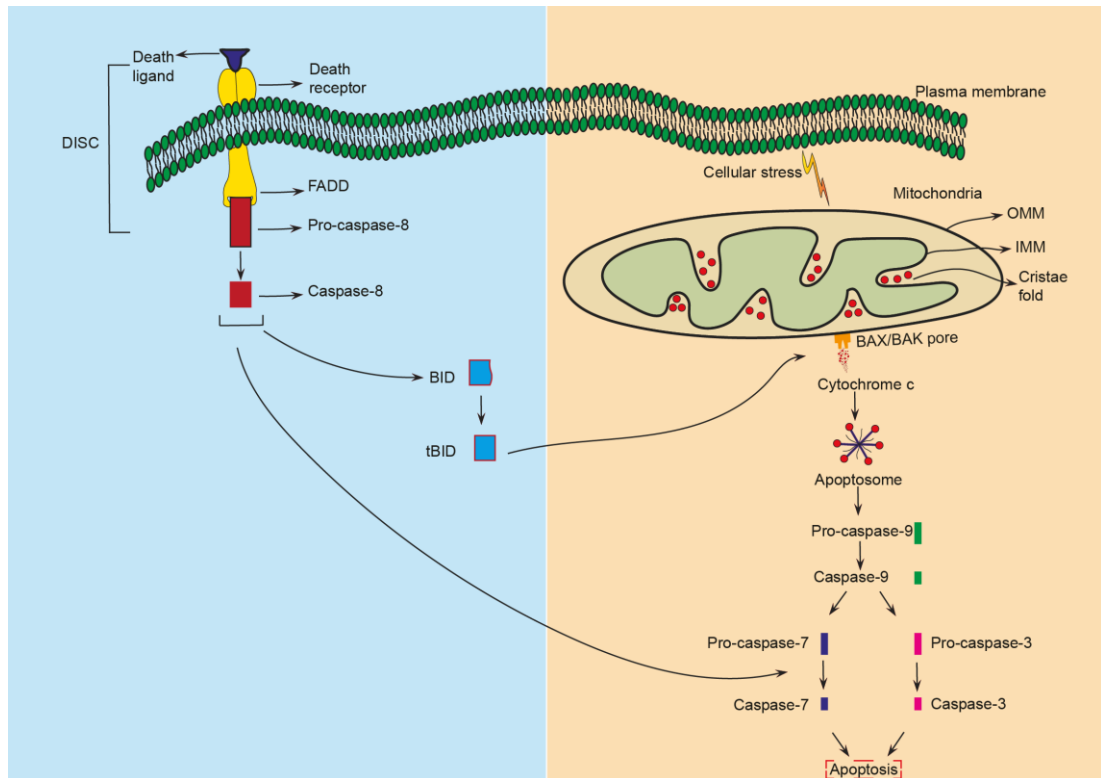
Figure 1.10. The schematic representation of apoptosis. Cells undergo apoptosis either *via* the extrinsic or intrinsic pathway. Extrinsic apoptosis pathway is initiated by the death receptors and ligands in the plasm membrane. Binding of death ligand to death receptor facilitates DISC assembly, which eventually activates procaspase-8 and BID. Upon activation, truncated BID is eventually translocated to the mitochondria and facilitates BAX/BAK-mediated release of cytochrome *c*. Intrinsic apoptosis occurs at the level of mitochondria, resulting in BAX/BAK activation and oligomerisation at the OMM to facilitate cytochrome *c* release from mitochondria to cytosol, which eventually activates apoptosome and caspase-9.

1.9. Pyrimidine metabolism

Pyrimidine synthesis is an essential metabolic pathway in the cells. Intermediates of this pathway include CTP, TTP and UTP, all of which act as essential building blocks for DNA and RNA[123–128]. Pyrimidines also act as precursors for UDP-sugars (glycogen synthesis), energy source (CTP) and cofactors (NAD, FAD)[123,127]. Pyrimidine biosynthesis also plays critical roles in various diseases, including cancer[127–131]. Cancer cells use high levels of pyrimidines[127,128] and any alteration in pyrimidine synthesis lowers the pyrimidine pool and suppresses growth of the cancer cell[132].

Pyrimidine biosynthesis is regulated either by salvage or *de novo* pathways[123,127]. In salvage pathway, pyrimidine nucleotides are obtained from recycled bases that are released during degradation of RNA and DNA[123,127]. *De novo* pyrimidine biosynthesis is a coordinated process which begins with glutamine and carbon dioxide, which synthesise carbamoyl phosphate by carbamoyl phosphate synthase (Figure 1.11)[123,127]. Carbamoyl phosphate then combines with aspartate to form carbamoyl aspartate, a reaction catalysed by aspartate transcarbamoylase[123,127]. Carbamoyl aspartate, thus formed, is then converted to dihydroorotate by dihydroorotase (Figure 1.11)[123,127]. Dihydroorotate is then converted to orotate by the enzyme dihydroorotate dehydrogenase (DHODH)[126]. DHODH enzyme present inside mitochondria and its activity has been used a target in treating several diseases included cancer, rheumatoid arthritis, malaria, and multiple sclerosis[128,131,132]. Finally, orotate is synthesised by orotate phosphoribosyl transferase, which eventually forms UMP, UDP and UTP by phosphate exchange mechanism (Figure 1.11)[123].

DHODH consists of N-terminal and C-terminal domains interconnected with a loop to form an active catalytic region (Figure 1.12)[130,133]. This catalytic region is widely targeted using different DHODH inhibitors (Figure 1.12).
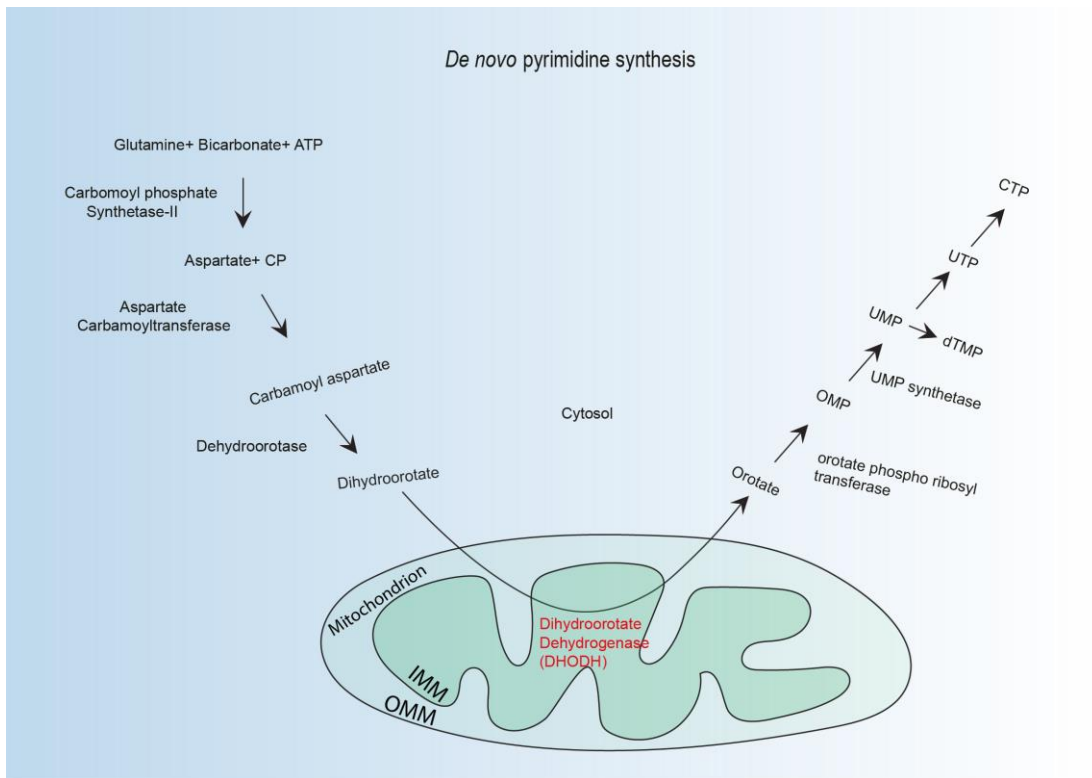
Figure 1.11. *De novo* **biosynthesis of pyrimidine nucleotide.** The pathway consists of the six enzymatic reaction catalysed by carbamoyl phosphate synthase, aspartate carbomoyltransferase, dihydroorotase, dihydroorotate dehydrogenase, and finally UMP synthetase.
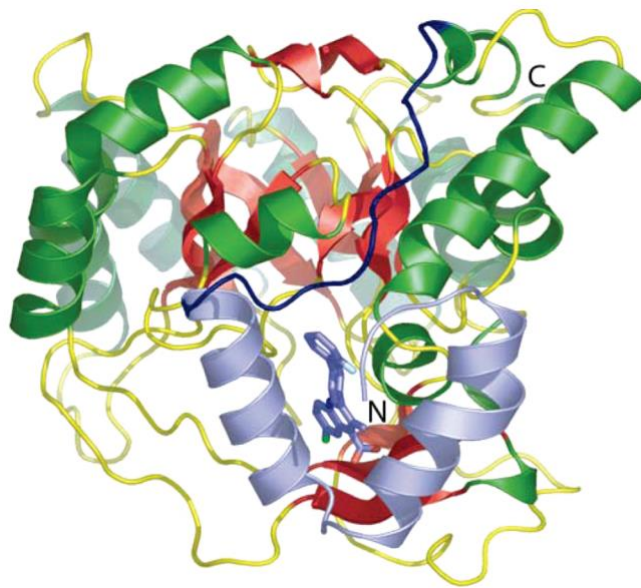
Figure. 1.12. DHODH structure. The N-terminal helical domain is coloured light blue. The N and C terminal connected loop is coloured dark blue, helices are coloured green, strands red, loop region yellow. (PyMOL figure adapted from Walse et al, 2008[134])

1.10. DHODH inhibitors

DHODH inhibitors were designed to inhibit pyrimidine biosynthesis and deplete pyrimidines to inhibit DNA and RNA synthesis[129,135–138] . There are several inhibitors developed against DHODH enzyme, including brequinar[137], leflunomide[136], teriflunomide[139,140], Bayer (BAY2402234)[129] and ASLAN003 (Figure 1.13)[138]. DHODH inhibitors have proven to be efficient in the treatment of several diseases, including rheumatoid arthritis and haematological cancers[127127,128]. Brequinar has been used to treat rheumatoid arthritis, head and neck cancer and other cancers[137]. Reports suggested that Brequinar has not shown significant effect on early phase clinical trials of head and neck , breast and ovarian cancer[137,141,142]. In addition, the toxicity and narrow therapeutic window of this compound has limited its clinical use[127]. Leflunomide (Arava) was later designed against DHODH for treating rheumatoid arthritis and this drug successfully gained FDA approval in 1999[143–145] . Several findings report that leflunomide has a short half-life and its treatment often causes severe liver toxicity within 6 months[145] . Due to liver toxicity and weak potency, this compound was later withdrawn from FDA approval list and discontinued. Later, leflunomide was structurally modified into another compound and named as teriflunomide[145,146] . Teriflunomide is the active derivative of leflunomide and the only difference between these two drugs is the opening of the isoxazole ring. Upon oral administration, the isoxazole ring of leflunomide opens and teriflunomide is formed (Figure 1.14).[139] Teriflunomide was successfully investigated in clinical trials and received FDA approval in 2012.

Although numerous inhibitors are currently available to selectively target DHODH (Figure 1.13), it is unclear as to how these inhibitors inhibit tumor growth. Recent studies using the CRISPR/Cas9 gene knockout strategy reveals that genetic knockout of DHODH effectively inhibited tumor growth[130,147]. This could well be due to their roles in pyrimidine biosynthesis, but more studies need to be performed to confirm this theory.
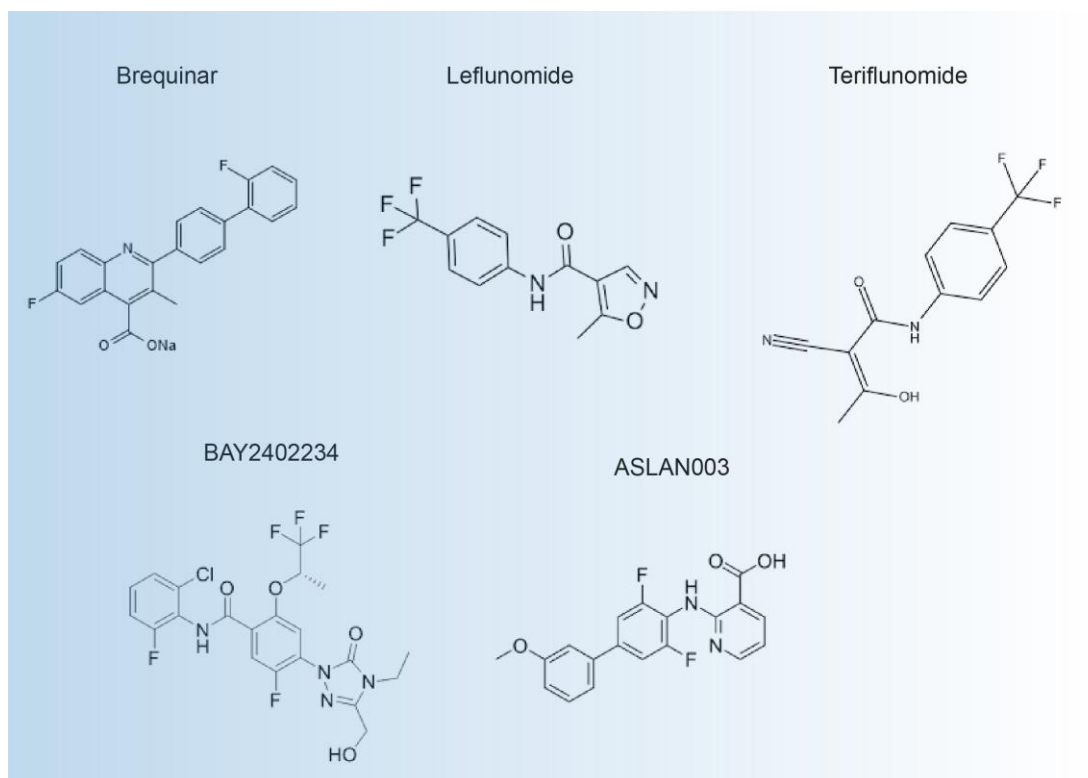
Figure. 1.13. The chemical structure of DHODH inhibitors.
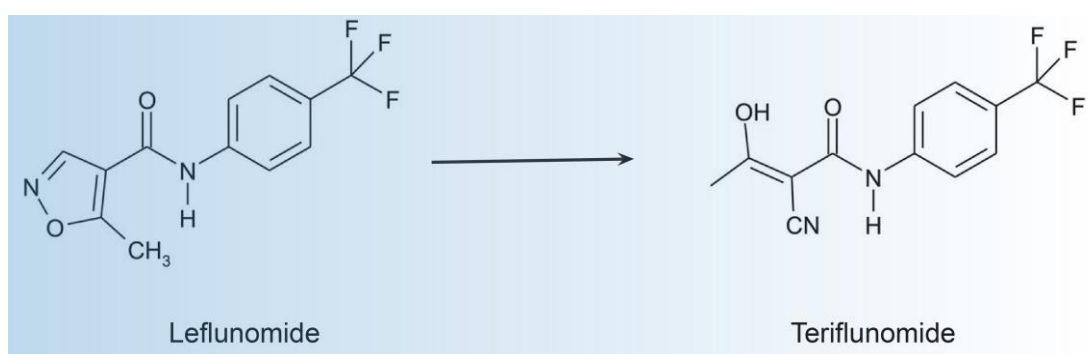
Figure 1.14. Chemical structure of leflunomide and its metabolite teriflunomide.

1.11. Objectives of this study

A current challenge in cancer therapy is drug resistance. Growing reports suggest that cancer cells acquire resistance to chemotherapeutic drugs through different mechanisms, which include a failure to undergo apoptosis. Since ER-mitochondria communication has been reported to have a significant impact on apoptosis, this study is aimed at gaining a better understanding of the functional consequences of ER-mitochondria communication in the context of cancer cell death. In this study, reorganisation of ER membranes (ERMR) is used as a tool to study ER-mitochondria communication further. In addition, this study is further extended to examine the therapeutic benefits of *de novo* pyrimidine synthesis inhibitors in head and neck squamosal cell carcinoma.

The following question have been addressed in this thesis:

1. To examine whether ERMR-induced reorganisation is restricted to ER membranes or other organelles.

2. To investigate impact of ERMR on mitochondrial-mediated apoptosis.

3. To investigate whether ERMR inhibitors modulate ERMR regulated apoptosis.

4. To explore the potential of *de novo* pyrimidine biosynthesis inhibitors in improving the effectiveness of current treatments in head and neck cancer.

Chapter 2

Materials and methods

Contents

2.1. Cell culture

All cell culture work was carried out using standard aseptic techniques and maintained according to the guidelines provided by the vendors. Briefly, cell lines were grown in culture flasks with recommended growth media containing 10 % foetal bovine serum (Life Technologies, catalogue number: 10270106). The cells were monitored daily and cells were passaged when they reached at 60-70 % confluency. Upon reaching confluence, the suspension cells were dispersed and split further using fresh media. For adherent cells, the media was aspirated from the flask and cells washed with phosphate buffered saline (PBS; Fisher Scientific, catalogue number: 11510546) before adding the trypsin-EDTA solution (Life Technologies, catalogue number: 15400054) and incubated for 2 min at 37°C to allow cells to detach from flask. Upon detachment, fresh media was added to cells to stop trypsinisation and cells were passaged further. All cultured cells were maintained in an incubator at 37°C with 5% carbon dioxide (CO_2).

2.2. Cell lines

All cell lines used in this study are categorised into individual culture media, cell line origin and supplier information as summarised in the table 2.1 below. RPMI indicates Roswell Park Memorial Institute 1640, purchased form Life Technologies, catalogue number: 61870044. DMEM indicates Dulbecco's Modified Eagle Medium purchased from Life Technologies, catalogue number: 32430100. MEM indicates Minimum Essential Medium Eagle, purchased from Sigma, catalogue number: M2279. BME indicates β-mercaptoethanol, NEAA indicates non-essential amino acids.

Cell Line	Culture media	Tumour origin	Source
H1299	RPMI	Non-small cell lung carcinoma (NSCLC)	ATCC (American Type Culture Collection)
MAVER-1	RPMI	Mantle cell lymphoma (MCL)	Dr. J. Slupsky (University of Liverpool)

RS4;11	RPMI	Acute lymphoblastic leukemia (ALL)	Prof. M. Dyer (University of Leicester)
KCL-22	RPMI	Chronic myeloid leukaemia (CML)	Prof. R. Clark (University of Liverpool)
K562			
H929	RPMI + BME	Multiple myeloma	ATCC
HeLa	DMEM	Cervical carcinoma	ATCC
MDCKII	DMEM	Madin-Darby canine kidney	Prof. M. Pirmohamed (University of Liverpool)
UM-SCC - 1	DMEM + NEAA	Head and neck squamous cell carcinoma (HNSCC); Isolated form oral cavity	Prof. T. Carey (University of Michigan, USA)
UM-SCC - 11B	DMEM + NEAA	HNSCC isolated form larynx	
UM-SCC - 81B	DMEM + NEAA	HNSCC isolated form oropharynx	
FaDu	EMEM + NEAA	HNSCC isolated form hypopharynx	ATCC

Table 2.1 Table showing all the cell lines used throughout this study.

2.3.   Cell line authentication

Total genomic DNA was isolated using DNA isolation kit (Qiagen, Cambridge, UK) according to manufacturer's recommendation. Isolated samples were then sent to the University of Liverpool cell line authenticity facility. Briefly, samples were subjected to short tandem repeat (STR) profiling using GenePrint 10 (Promega, Madison, WI, USA). Cells were required to have at least an 80 % match (Table 2.2).

Cell Line	% Match with cell line specific databases
H1299	100%
MAVER-1	94%
RS4;11	100%
KCL-22	100%
K562	83%
H929	100%
HeLa	100%
MDCKII	Not-tested
UMSCC - 1	100%
UMSCC - 11B	100%
UMSCC - 81B	100%
FaDu	Newly purchased/ Not-tested

Table 2.2. Table showing cell lines were authenticated using STR profiling and matched against multiple databases.

2.4.   Reagents and compounds

Reagents, chemicals and buffers were obtained from Sigma-Aldrich/ Merck (Darmstadt, Germany) unless otherwise specified, such as Selleck (Houston, TX, USA), Abbvie (Chicago, IL, USA), Sigma (Darmstadt, Germany) and Apex Biotechnology (Houston, TX, USA). Reagents and compounds and supplier information are summarised in the table 2.3 below.

Inhibitors	Target/ Function	Source
ABT- 199	BCL-2	Selleck
A-1331852	BCL-X_L	Abbvie
A-1210477	MCL-1	Abbvie
S63845	MCL-1	Selleck
Z-VAD.fmk	Caspases	Selleck

CCCP	Mitochondrial uncoupler	Sigma
Apogossypol	ER membrane reorganisation inducer (ERMR inducer)	APExBIO
NDGA (Nordihydroguaiaretic acid)	ERMR inducer and antioxidant	Sigma
Ivermectin	ERMR inducer and anthelmintic	Sigma
Terfenadine	ERMR inducer and antihistamine	Sigma
Suloctidil	ERMR inducer and vasodilator	Sigma
Teriflunomide	DHODH	Sigma
Leflunomide	DHODH	Sigma
Orotate	Intermediate of pyrimidine pathway	Sigma
Uridine	Intermediate of pyrimidine pathway	Sigma
Cisplatin	Covalent DNA adducts*	Selleck
CB 839	Glutaminase 1 (GLS 1)	Selleck

Table 2.3. Inhibitors used this study.

*Cisplatin is a covalent DNA adduct, which induces DNA damage by covalently binding to the DNA at N7 position of purine.

2.5. Antibodies

Antibodies were purchased from Abcam (Cambridge, UK), Sigma (Darmstadt, Germany), BD BioSciences (CA, USA), CST (Cell Signalling Technology, MA, USA), Enzo Biochem Inc (NY, USA), Calbiochem Research Biochemicals (now Merck), Santa Cruz Biotechonology (CA, USA) or DSHB (Developmental Studies Hybridoma Bank, The university of Iowa, Iowa). ICC indicates immunocytochemistry. WB indicates western blot. FACS indicates fluorescence-activated cell sorting. Antibodies information are summarised in the table 2.4 below.

Antibody	Source	Catalogue number	Isotype	Application
Endoplasmic reticulum				
BAP31	Abcam	Ab37120	Rabbit IgG	ICC
RTN4	Abcam	Ab47085	Rabbit IgG	ICC
CLIMP 63	Enzo	ALX-804-604	Mouse IgG2a	ICC
KNT-1	Sigma	HPA003178	Rabbit IgG	ICC
Bip	Abcam	21685	Rabbit IgG	ICC, WB
PDI	Abcam	Ab2792	Mouse IgG2a	ICC, WB
CHOP	Abcam	Ab11419	Mouse IgG	WB
Golgi complex and lysosomes				
GM130	BD	610822	Rabbit IgG	ICC
LAMP 1	DSHB	AB 528127	Mouse IgG1	ICC
Mitochondria				
HSP60	BD	611562	Mouse IgG1	ICC
DRP-1	BD	611113	Mouse IgG1	WB
DRP-1	CST	8570	Rabbit IgG	ICC
MFN-1	CST	13196	Rabbit IgG	WB
MFN-2	CST	9482	Rabbit IgG	WB
Opa1	BD	612607	Mouse IgG1	WB
Apoptosis				
BAX (6A7)	Enzo	ALX-804-224-C100	Mouse IgG1	FACS
BAK (AB-1)	Calbio	AM-03	Mouse IgG2a	ICC, FACS
Cytochrome *c*	CST	4272	Rabbit IgG	ICC, WB
Caspase 3	CST	9662	Rabbit IgG	WB
Caspase 7	CST	9494	Mouse IgG1	WB
cl. caspase 9	CST	9505	Rabbit IgG	WB
cl. PARP	CST	5625	Rabbit IgG	WB
Miscellaneous				
GAPDH	SC	Sc-25778	Rabbit IgG	WB
Actin	SC	Sc-1616R	Rabbit IgG	WB
DHODH	Sigma	HPA011942	Rabbit IgG	WB

Table 2.4. List of antibodies used in this study.

2.6.   RNA interference

Small interfering RNAs (siRNAs) were obtained from Qiagen (Cambridge, UK). Transfection were carried out according to the manufacturer's instructions. siRNAs were transfected into cells using a final concentration of 10 nM, using optiMEM reduced serum media (Life Technologies) and interferin transfection reagent (Polyplus, Illkirch, France). RNA interference and sequence targeted information are summarised in the table 2.5 below.
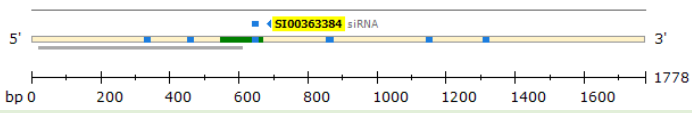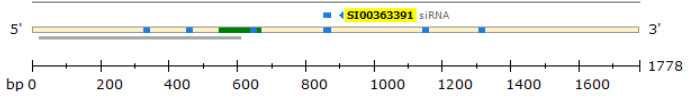
Protein targeted	Catalogue number	Sequence targeted
DHODH	S100363391	 CAGGGCTTTGGCGGAGTCACA
DHODH	S100363384	 CTCCGGGATTTATCAACTCAA
Non-targeting control	1027310	AACTGGGGGAGGATTGTGGCC

Table 2.5. List of siRNAs used in this study.

2.7.   Transient transfection

Plasmid transfection was performed as per manufacturer's instructions. Briefly, cells were seeded one day before transfection at determined density to reach 80% confluence. Cells were then transfected with Sec61β-GFP plasmid (from Prof. T. Rapoport, Harvard, Boston, USA; Addgene plasmid 15108) using TransIT-LT-1 transfection reagent (Mirus Bio LLC, Madison, WI, USA). The ratio DNA (μg): transfection reagent (μl) was 1:3. Transfection efficiency was observed in an EVOS Floid cell imaging station (Thermo Fisher Scientific, MA, USA).

2.8.   Western blotting

Western blotting was carried out according to a standard protocol. Briefly, gels were made in-house with Protogel acrylamide (30%) (National Diognostics, Atlanta GA, USA), lower gel buffer (1.5 M Tris-HCL, 0.4% SDS, pH 8.8), upper gel buffer (Tris-HCL 0.5 M, 0.4% SDS, pH 6.8), 10% ammonium persulphate (APS) and tetramethylethyllenediamine (TEMED). Cells were collected and pellets were lysed with radioimmunoprecipitation assay (RIPA) lysis buffer (10 mM Tris- (pH 8.0), 1mM EDTA, 0.5 mM EGTA, 1% Triton X-100, 0.1 % sodium deoxycholate, 0.1% sodium dodecylsulfate (SDS), 140 mM NaCl, 20 μM MG-132 and one protease inhibitor tablet (Roche, Basel, Switzerland). After lysis, total protein content was determined using calorimetric protein assay (Bio-Rad protein assay Dye reagent, BioRad, CA, USA) and readings were measured with a spectrophotometer (Eppendorf, Hamburg, Germany). After protein concentration determination, samples were prepared using 4X NuPAGE LDS sample buffer (Life Technologies) and boiled for 5 min at 70°C. Cell lysates were fractionated by SDS-PAGE (sodium dodecyl sulfate polyacrylamide gel electrophoresis) in electrode buffer (25mM Tris-HCL, 192 mM glycine, 10% SDS) at 130 V for 120 min and then transferred to a nitrocellulose membrane (VWR, Radnor, PA, USA) in transfer buffer (25 mM Tris-HCL, 192 mM glycine, 20% methanol) at 100 V for 100 min. After transfer, membranes were blocked with 5% (W/V) non-fat milk with TBS-T (Tris-buffered saline with 0.1% Tween, 20 mM Tris-HCL, 150 mM NaCl, 0.1% Tween-20) for 30 min. The blocked membrane was washed once with TBS-T and incubated with primary antibodies at 4° C overnight. Membranes were washed with TBS-T 3 times for 5 min and incubated with anti-mouse or anti-rabbit IgG HRP-linked secondary antibodies (Cell Signalling Technology) for 1 h, and developed with ECL system (GE Healthcare, IL, USA) using a ChemiDoc imaging system (BioRad, CA, USA).

2.9.   Cytochrome *c* release

Harvested cells were washed with ice-cold PBS and resuspended in mitochondrial isolation buffer (250 mM sucrose, 20 mM HEPES, pH 7.4, 5 mM $MgCl_2$ and 10 mM KCL) containing 0.05 % digitonin. Cells were left on ice for 10 min followed by centrifugation at 13000 g for 3 min. The supernatant contained the light

membrane and cytosolic fraction whereas the pellet contained the heavy membrane fraction that is enriched with mitochondria. Both isolated fractions were analysed by western blotting.

2.10. Clonogenic survival

Cells were seeded at a recommended density in a 12 well plate. On the first day after seeding, the growth medium was replaced with new growth medium and then cells were exposed to drugs as per experimental design. Subsequently, cells were daily monitored for colony formation. Once the colonies are grown (corresponding to nearly 50-60 cells per colony), they were washed with PBS then fixed with fixing solution (1:7 v/v ratio acetic acid to methanol) for 5 min at room temperature. Following fixation, colonies were stained with staining solution (20 ml methanol, 80 ml H_2O, 0.5 g crystal violet) for 1 h at room temperature. Then, colonies were washed with tap water and left for drying. Colonies were later counted using a Gel Count instrument (Oxford Optronix, Oxford, UK), and survival fraction was calculated using the following formula:

Platting efficiency (PE)* = Colony counted/ cells pated

% Survival Fraction = Colony counted/ (Cells plated x Plating efficiency) x100

*Plating efficiency is one of the parameters normally used to determine number of colonies originate from single cells.

2.11. Flow cytometry

To measure the extent of apoptosis by assessing phosphatidylserine (PS) externalisation, adherent cells were collected and trypsinised before being pelleted, whereas the suspension cells were collected directly into tubes. Cell pellets were resuspended in 500 µl of 1X annexin binding buffer (10 mM HEPES, 140 mM NaCl, 2.5 mM $CaCl_2$, pH 7.4) with annexin-V-FITC (made in-house; 1:20,000 dilution; dilution was optimised to generate similar results against commercially purchased annexin V) and incubated at room temperature for minimum 8 min. 5 µl of 1 mg/ml propidium iodide (PI) (Sigma-Aldrich/Merk, Darmatadt, Germany) was added to cell suspension just before analysis. For BAX and BAK activation, cells were collected and fixed with 1% paraformaldehyde (PFA) at room temperature for 10 min. The cells

were then re-suspended in FACS buffer (0.1% saponin, 0.5% bovine serum albumin (BSA) in PBS) for 10 min. The fixed cells were then incubated with the primary antibody (anti-BAK AB-1 or anti-BAX 6A7; 0.1 mg/ml) diluted in FACS buffer for 1 h at 4°C. Cells were then pelleted by centrifugation before incubation with species-specific secondary antibody (goat-anti-mouse IgG-AlexaFluor-488 conjugated secondary antibody), diluted in FACS buffer for 1 h at 4°C. The extent of apoptosis, BAK/ BAX activation was detected by Attune NxT flow cytometer (ThermoFisher). 10,000 events per sample were recorded and a minimum of 3 replicates were assessed for each experiment.

2.12.   Immunocytochemistry

One day prior to experiment, cells were seeded on sterile coverslips in a 24 well plate to reach 60-70% confluence at the time of experimental treatment. Cells were fixed with 4% (w/v) PFA for 10 min at room temperature. Cells were permeabilised with 0.5% (v/v) Triton X-100 in PBS for 10 min at room temperature. After permeabilization, cells were incubated with primary antibody, diluted in 3% BSA in PBS for 1 h. After washing, cells were then incubated with species-specific secondary antibody (AlexaFluor, Life Technologies) diluted in 3% BSA in PBS for 1 h, followed by nuclear staining with Hoechst 33342 in 3% BSA in PBS. The coverslips were then mounted in glass slides with Polymount (Polysciences, PA, USA). Finally, cells were imaged in 3i Marianas spinning disk confocal microscope fitted with a plan-Apochromat 63x/1.4NA Oil objective, M27 and a Hamamatsu ORCA-Flash4.0 v2 sCMOS Camera (all from Intelligent Imaging Innovation, GmbH, Germany).

2.13.   Visualisation and Quantification of ER membrane reorganisation

Cells exposed to ER membrane reorganisation inducers for indicated times were first immunostained with ER membrane antibodies (RTN4 or BAP31). After, immunostaining, cells were imaged with 3i Marians spinning disk confocal microscope to assess ER membrane reorganization. Normal ER looks widely spread within the cell whereas reorganised ER appears like membranous bundles of aggregates within the cells. Upon exposure to apogossypol, a cell may contain

anywhere from 20-100 ER membrane aggregates, when visualised under confocal microscopy. Since the number of ER membrane aggregates was highly inconsistent among the different cells, cells that exhibited ER membrane aggregates regardless of the number of aggregates, were quantified as cells exhibiting ERMR. Cells that contained no detectable ERMR was identified as normal ER. Thus, the quantification of ERMR was performed by counting the extent of ERMR (number of cells exhibiting ERMR) from several pictures acquired in a confocal microscope of at least 100 cells from 3 independent experiments.

2.14. Statistics

For time-course studies, a two-way ANOVA was performed. All other studies were analysed for statistical significance with one-way ANOVA and the asterisks depicted correspond to the following p values: * for $p \leq 0.05$, ** for $p \leq 0.005$ and *** for $p \leq 0.001$.

Chapter 3

Characterising the interrelationship between the endoplasmic reticulum and mitochondria

Contents

3.1. Background

ER-mitochondria contacts control multiple cellular processes, including calcium signalling, lipid synthesis, mitochondrial fission and cell death[27,31,33,60,148,149]. Recent studies have suggested that ER membranes play a significant role in regulating mitochondria structural dynamics and functions[22,30,51]. ER membranes achieve this by physically wrapping around the mitochondria, thus aiding in mitochondrial division and other mitochondrial functions[7,31]. The link between the ER-mitochondrial contacts and apoptosis remains poorly understood. An understanding of how ER-mitochondria contacts regulate mitochondrial apoptosis is critical to improve therapy in several cancers, as most chemotherapeutic agents kill cancer cells by inducing the intrinsic apoptotic pathway. Previous studies have demonstrated a novel cellular stress response characterised by reversible reorganisation of ER membrane reorganisation (ERMR), following exposure of cells to wide variety of drugs, such as apogossypol, ivermectin, terfenadine, suloctidil and other agents[90,91] (Figure 3.1).

Normally, ER is widely spread throughout the cell whereas reorganised ER membranes appear as clusters of ER membrane aggregates within the cell[91]. From electron microscopy, the aggregates appear to be largely devoid of ribosomes, and could therefore be part of smooth ER (Figure 3.1). It does not appear to have a consistent shape as they often manifest as bundles of membranes. Although the composition of these membranes is yet to be characterised, the reversible nature of these aggregates indirectly reveal that the chemical composition of these lipid membranes may not be too different from regular ER membranes. Nevertheless, it is striking to note that this phenomena is evolutionary conserved from yeast to humans, as ERMR has been observed in fission yeast (*schizosaccharomyces pombe*), Chinese hamster ovary cells (CHO), mouse embryonic fibroblasts (MEF) as well as in several human cell lines[91]. Furthermore, ERMR modulates ER associated functions, such as the vesicular trafficking between ER exit sites and the Golgi complex. A drastic attenuation of global protein synthesis has also been associated with ERMR[91]. Although these events result in a stress response, ERMR appears to be distinct from classical ER stress pathway and the unfolded protein response (UPR). UPR is well-studied pathway associated with the transcription, translation and activation of specific

genes and transcriptional factors, which are aimed at maintaining ER homeostasis, and under prolonged stress, triggering cell death[150]. ERMR occurs even in the absence of transcription and translation and also in cells lacking UPR regulators, such as PERK, IRE1, ATF6, XBP1 and CHOP[151]. It has been reported that ERMR can be induced by downregulation of an anterograde transport protein (α SNAP), retrograde transport protein (syntaxin 18), anti-apoptotic protein (MCL-1) as well as by an upregulation of a SOCE protein (STIM 1)[90]. This indicates that ERMR could be associated with diverse physiological functions, such as vesicular trafficking, calcium signalling as well as apoptosis.
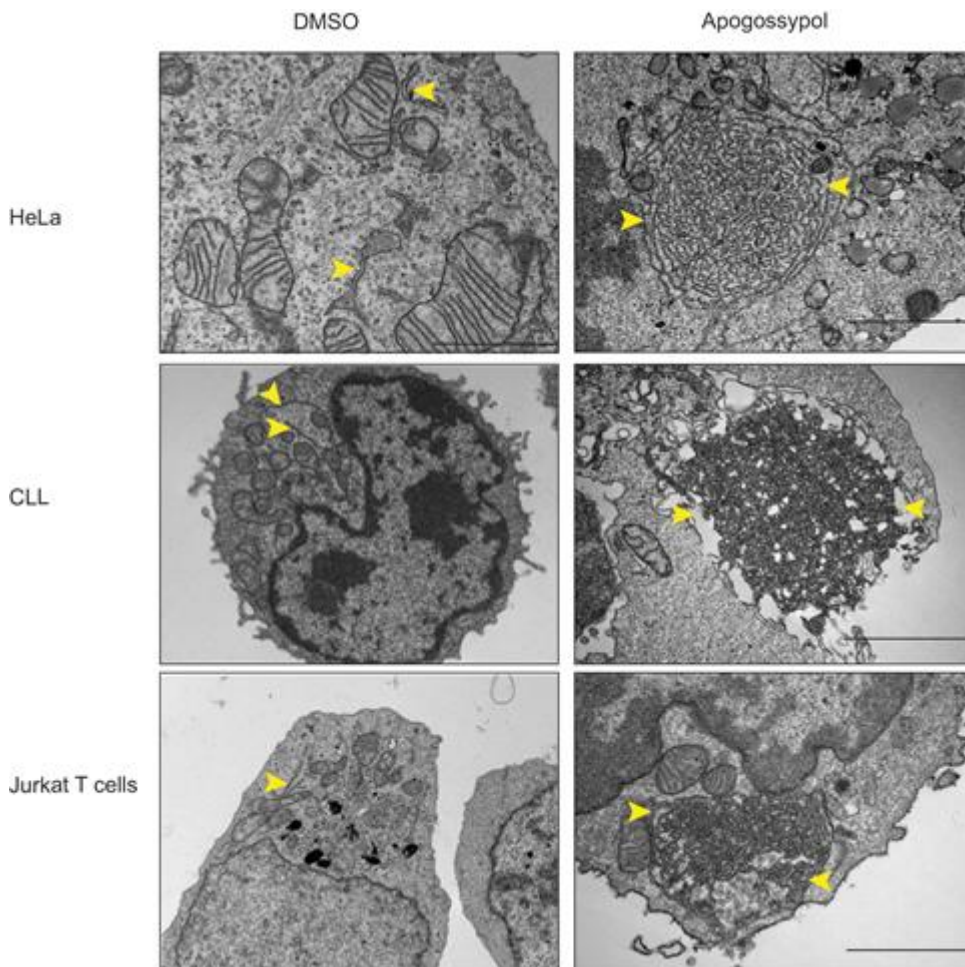
Figure 3.1. Apogossypol induces extensive ERMR in several cell lines. HeLa, CLL and Jurkat T cells were exposed to apogossypol (20 μM) for 16 h and subjected to electron microscopy. The yellow arrow heads indicate ER membranes. Scale bar: 10 μm. (Image adapted from Varadarajan et al., 2019)[90].

The original study describing ERMR observed that mitochondrial structure largely remained unchanged in cells exposed to ERMR inducers[91] . However, given the recent literature linking ER membranes and mitochondrial dynamics. It was speculated that modulation of ER membrane morphology might affect ER-mitochondria contacts, mitochondrial dynamics and as a result, the intrinsic pathway of apoptosis. To study this hypothesis, apogossypol was used as a tool compound to induce ERMR and then studied its impact on apoptosis.

The specific questions that will be addressed in this chapter are as follows:

(1) Do the reorganised ER membranes localise to specific subsites of the ER (such as the lumen, tubules or sheets)?

(2) What is the effect of ERMR on other closely related organelles, such as the ER-Golgi intermediate compartment, Golgi complex, lysosomes and mitochondria?

(3) Do the reorganised ER membranes regulate mitochondrial membrane fusion-fission dynamics?

(4) Do the reorganised ER membranes regulate the mitochondrial apoptotic pathway?

3.2. ERMR appears to occur at the site of ER tubule

To confirm whether apogossypol induced ERMR, MDCKII cells were transfected with a widely recognised ER membrane marker, sec61β[7,152], that is fused with a GFP-tag. Sec61β is a translocon that spans across the ER membranes[152], and facilitates the translocation of nascent polypeptides across ER membranes for further protein maturation. MDCKII cells were chosen for this study because the ER membranes are extensively spread in these cells with well-defined tubules and sheets, as evident in Figure 3.2. Most cell lines (other than MDCKII and COS-7) do not have clearly distinguishable ER tubules and sheets, and scientists often rely on super resolution microscopy to make this distinction. However, in the Sec61β-transfected MDCKII cells, exposure of apogossypol (20 μM) for 4 h (time of exposure optimised based on previous findings[90]) resulted in a dramatic reorganisation of ER membranes, at the ER tubules, and the sheets remained largely excluded from the reorganised ER membranes (Figure 3.2).
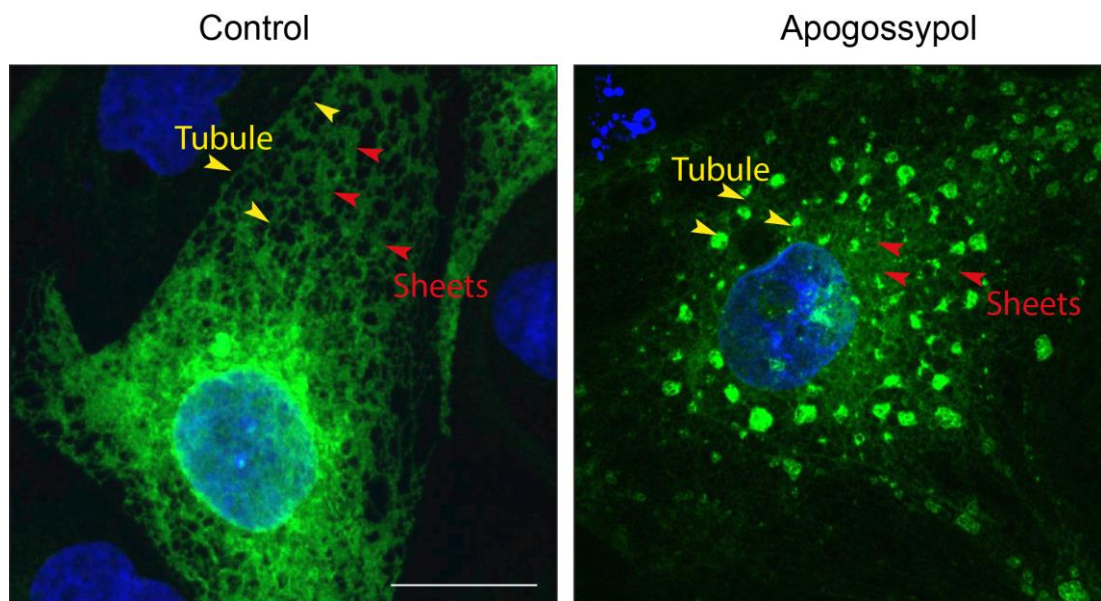
Figure 3.2. Apogossypol induces extensive ERMR in Sec61 overexpressed cells. MDCKII cells were transfected with Sec61β-GFP (ER marker) and then cells were exposed to apogossypol (20 μM) for 4 h. After treatment, the cells were fixed and imaged with 3i Marians spinning disk confocal microscope to assess ER membrane reorganization. Yellow arrow indicates ER tubule; red arrow indicates ER sheets. All experiments were independently performed three times. Scale bar:10 μm.

3.3.   ERMR involves the reorganisation of ER tubules

Although the previous observations in the MDCKII cells revealed that ERMR occurred at the levels of ER tubules and not sheets, further confirmation was required to convincingly demonstrate this. RTN4 (reticulon-4) is a protein that is localised to the tubular ER and is responsible for regulating ER tubular morphogenesis through promoting tubular production and extension[14,153–155]. BAP31 (B- cell receptor associated protein of 31kDa) is another protein that is localised to the tubular ER[8,156–158]. Hence, these tubular markers were used to check whether apogossypol-induced ERMR localised within ER tubules. For this experiment, cells were exposed to apogossypol (20 µM) for 4 h, and then immunostained with ER tubule markers RTN4 or BAP31. In these cells, exposure to apogossypol resulted in extensive ERMR, to which both RTN4 and BAP31 appeared to redistribute (Figure 3.3 a-b). Moreover, RTN4 and BAP31 exhibited a perfect colocalisation on the reorganised ER membranes (Figure 3.4). Taken together, these results strongly suggested that ER tubules played a significant role in ERMR. However, whether other parts of ER, such as the sheets or lumen are involved in ERMR remains to be studied.

3.4.   ERMR does not involve ER sheets or ER lumen

ER sheets are relatively flat in structure and appear stacked together[7]. ER sheets have several resident proteins, including CLIMP-63 (cytoskeleton linking membrane protein 63), also referred as CKPA-4 (cytoskeleton associated protein 4)[159]. CLIMP-63 is widely distributed throughout the ER sheets and responsible for the generation and maintenance of ER sheets. Kinectin-1 (KNT-1)[159] and p180[159] are other ER sheet-resident proteins. KNT-1 widely spans throughout the ER sheets and acts as a scaffold protein to maintain ER sheets[7]. To assess whether ERMR is localised to the ER sheets, cells were exposed to apogossypol (20 µM) for 4 h and co-stained with ER sheets markers (CLIMP-63 or KNT-1). As a positive control, cells were also stained with previously mentioned ER tubule markers (RTN4 or BAP31). The results showed that unlike BAP31or RTN4 that immediately redistributed to the ERMR, neither CLIMP-63 nor KNT-1 resulted in a similar redistribution (Figure.3.5 a-b). Thus, it was concluded that apogossypol-induced ERMR does not occur within ER sheets, and that ERMR was restricted to ER tubules.
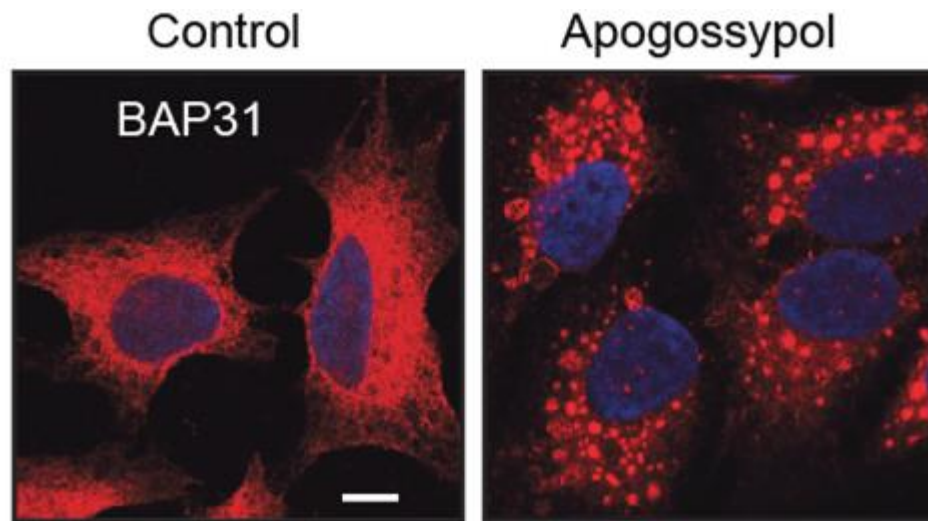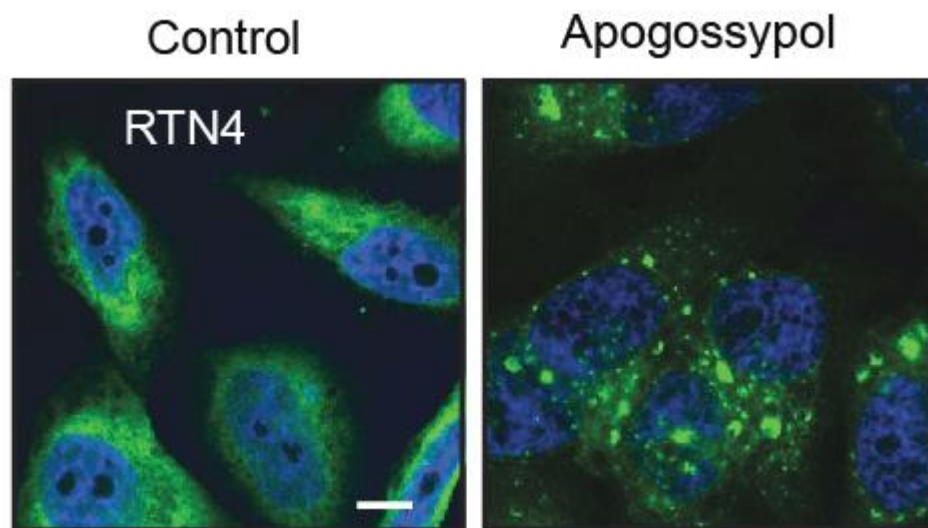
Figure 3.3. ERMR colocalises with ER tubule markers. HeLa cells were exposed to apogossypol (20 μM) for 4 h. The cells were then immunostained with ER tubule markers a) BAP31 and b) RTN4. All experiments were independently performed three times. Scale bar:10 μm.
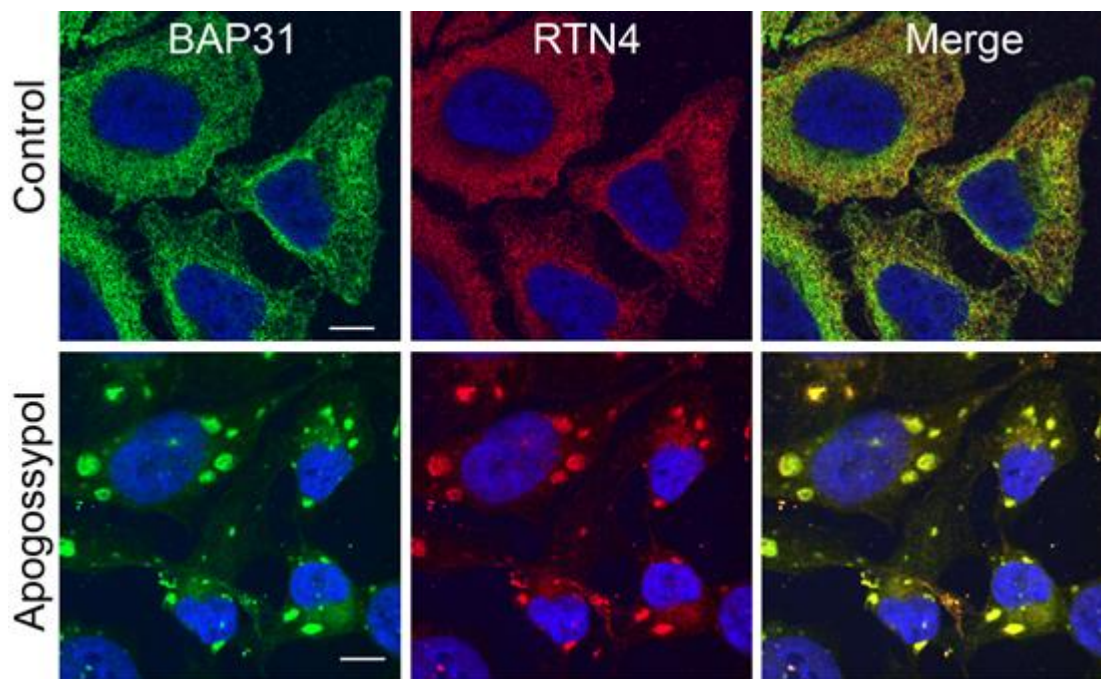
Figure 3.4. ERMR occurs at the level of ER tubules. HeLa cells were exposed to apogossypol (20 μM) for 4 h. The cells were then immunostained for ER tubule markers BAP31 and RTN4. All experiments were independently performed three times. Scale bar:10 μm.

Next, I examined whether ERMR involved the lumenal portions of the ER. ER lumen provides lumenal space for several important cellular processes, including protein folding. The ER lumen is enriched with several ER lumenal resident proteins, including BIP[83,156,160,161] (binding immunoglobulin protein) and PDI[161] (protein disulphide isomerase). BIP acts as an ER stress sensor[43]. Upon ER stress, BIP dissociates from other ER stress response proteins, such as PERK, IRE1, ATF6 and eventually triggering an adaptive signal to recover the cells from ER stress[162,163]. Similarly, PDI functions as a molecular chaperone and aids in protein folding process to maintain ER homeostasis[163] . Hence, these proteins were used as lumenal markers to check whether apogossypol-induced ERMR localised to the ER lumen. For this, cells were exposed with apogossypol (20 µM) for 4 h and then co-stained with ER lumen markers (BIP or PDI) along with an ER tubule marker (BAP31). The results showed that unlike BAP31 that immediately redistributed to the ERMR, neither BIP nor PDI resulted in a similar redistribution (Figure.3.6). Thus, it was concluded that apogossypol-induced ERMR does not occur within ER lumen, and that ERMR was restricted to ER tubules.

3.5.   ERMR does not colocalise with ER tubule but alters the distribution of ERGIC and Golgi complex

ERGIC, located between ER and Golgi complex, helps to transport cargo proteins from the ER to the Golgi complex for further processing[14]. ERGIC-53[164,165] is a protein predominantly localised to the ERGIC and responsible for the export of glycoproteins from ER to Golgi complex. GM130 is a widely distributed protein in the Golgi complex[166,167]. To check whether apogossypol-induced ERMR formed inside ERGIC and Golgi complex, cells were exposed to apogossypol (20 µM) for 4 h and labelled with ERGIC-53 or GM130, along with RTN-4, as an ER tubule marker. The results showed that unlike BAP31 that immediately redistributed to the ERMR, neither ERGIC-53 nor GM130 redistributed to the reorganised ER membranes (Figures 3.7 a and b). However, apogossypol-induced ERMR dispersed the Golgi complex (Figure 3.7 b), as previously observed[91]. Similarly, a modest dispersal of ERGIC-53 was also observed (Figure 3.7 a).
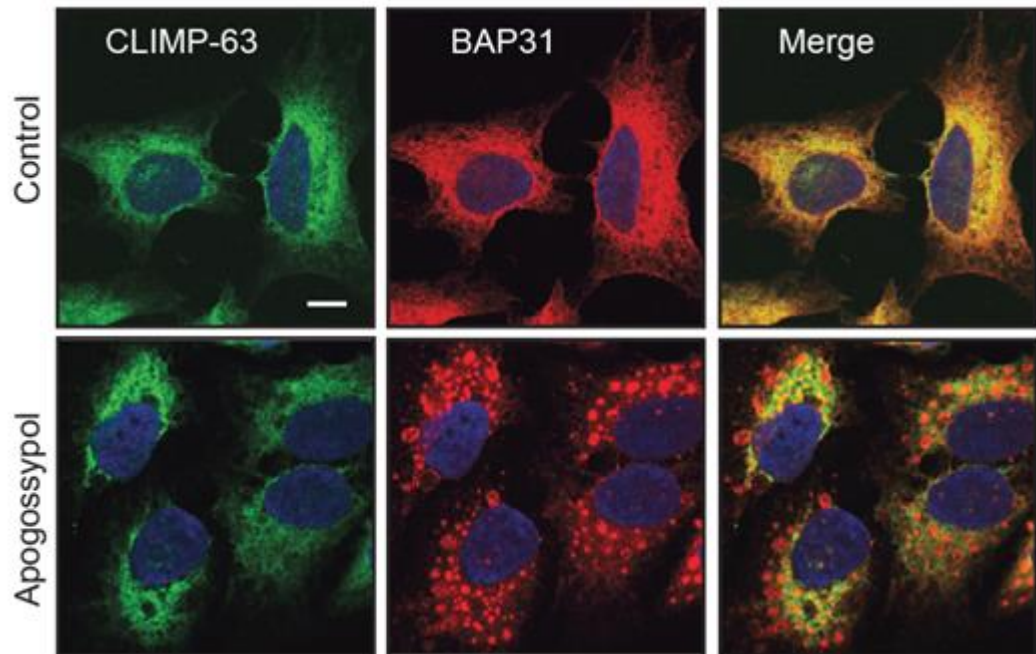
Figure 3.5. ERMR does not involve ER sheets. HeLa cells were exposed to apogossypol (20 μM) for 4 h. Cells were then co-stained for an ER sheet marker (CLIMP-63 or KNT-1) or an ER tubular marker (BAP31 or RTN4). All experiments were independently performed three times. Scale bar: 10 μm.
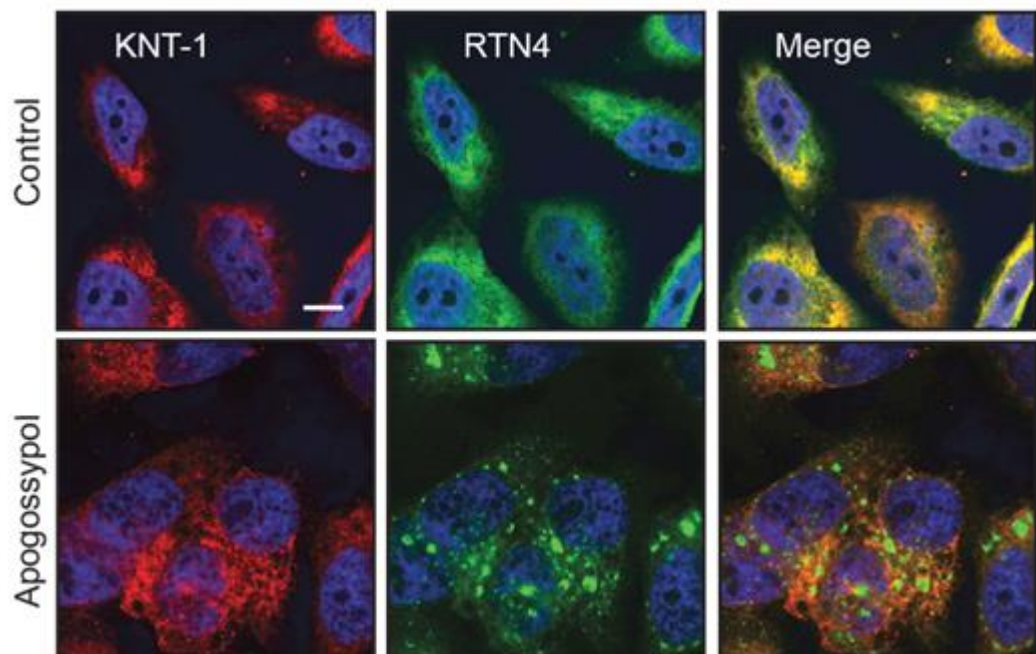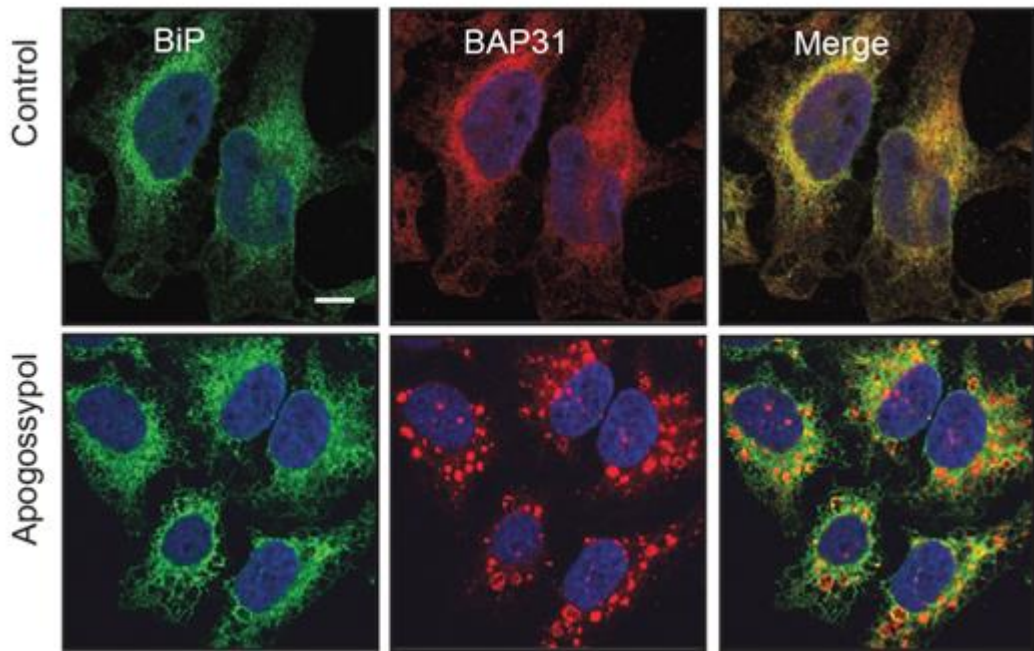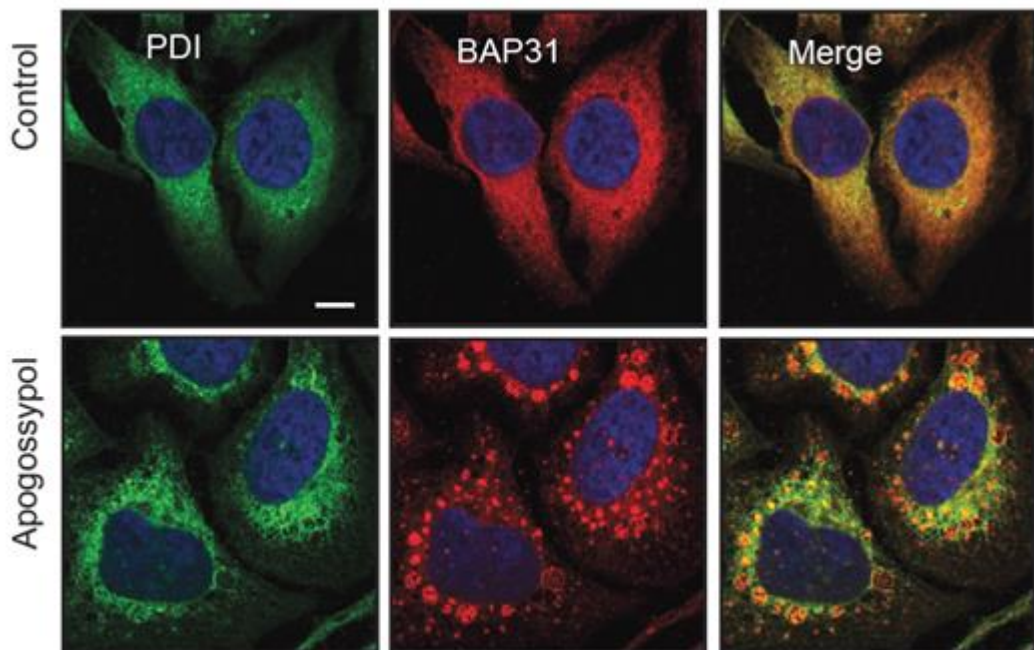
Figure 3.6. ERMR does not occur within the ER lumen. HeLa cells were exposed to apogossypol (20 μM) for 4 h. Cells were then co-stained for an ER lumenal marker (BIP or PDI) with an ER tubular marker (BAP31). All experiments were independently performed three times. Scale bar: 10 μm.

3.6. ERMR does not colocalise with membranes of mitochondria or lysosomes

ER has been shown to interact with other organelles, including lysosomes and mitochondria[168,169]. Lysosomal-associated membrane proteins (LAMP) including LAMP 1 and 2 are predominately distributed in the lysosomes and responsible for maintaining lysosomal structure[169]. Similarly, a mitochondrial chaperone, HSP60 (heat shock protein 60) was used as a mitochondrial marker[170]. Cells, transiently transfected with an ER marker (Sec61β-GFP), were exposed to apogossypol (20 µM) for 4 h and then immunostained with the chosen lysosomal and mitochondrial markers. The results showed that apogossypol-induced ERMR does not result in the redistribution of LAMP 1 or HSP60 (Figure 3.8), thus confirming that ERMR is only restricted to ER tubules and not to other cellular organelles, such as the lysosomes and mitochondria.

3.7. ERMR antagonises CCCP and A-1210477-mediated mitochondrial fission

Previous results strongly suggested that ERMR is restricted to ER tubules (Figure 3.2-3.8). It has been reported that ER tubules play an important role in mitochondrial dynamics[7,171], during which ER tubules wrap around mitochondria to facilitate mitochondrial fission[31,168]. Since, mitochondrial proton uncoupler (CCCP; carbonyl cyanide m-chlorophenyl hydrazine)[172,173] and A-1210477 (MCL-1 inhibitor) induce extensive mitochondrial fission[174,175], cells were pre-exposed to apogossypol (20 µM) for 1 h (apogossypol still present throughout the experiment) and then exposed to CCCP or A-1210477. The cells were then co-stained with HSP60 (mitochondria marker) and RTN4 (ER marker). The results showed both CCCP and A-1210477 mediated mitochondrial fission as evidenced by the HSP-60 staining (Figure.3.9 a-c) , consistent with previous findings reporting mitochondrial fission[174]. Apogossypol-induced ERMR did not result in mitochondrial fission on its own but was efficient in preventing both CCCP and A-1210477-mediated mitochondrial fission (Figure.3.9 b-c). The extent of mitochondrial fission (appeared as fragmented mitochondria) was quantified by counting around 100 cells from 3 independent experiments. (Figure.3.9 d).
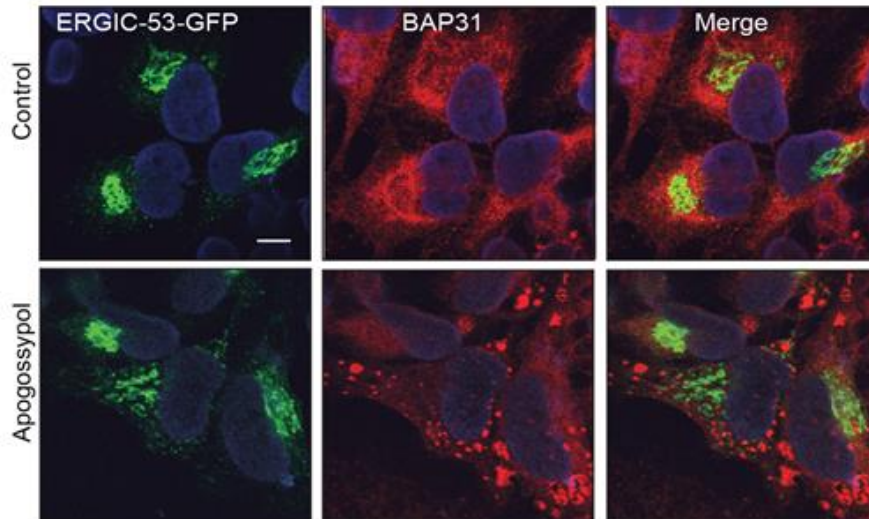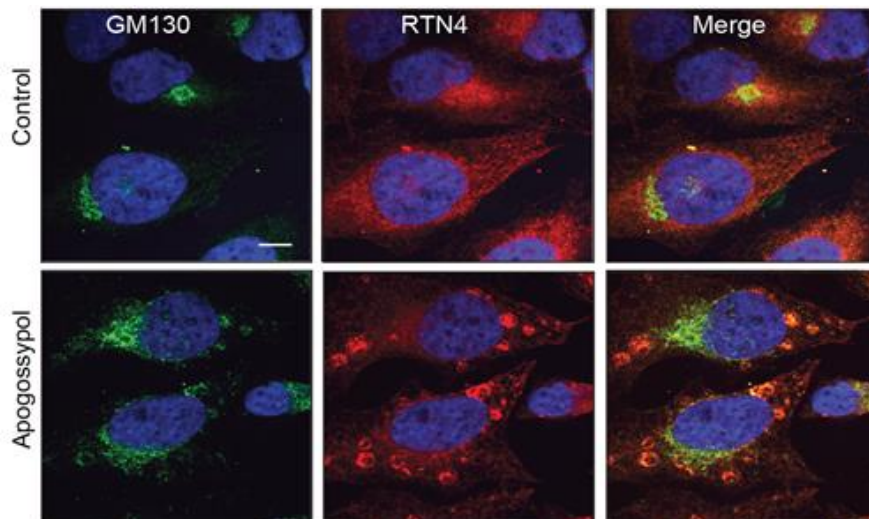
Figure 3.7. ERMR does not occur within the ER-Golgi intermediate compartment and Golgi complex. a) HeLa cells were transfected with ERGIC-53-GFP. Following transfection, the cells were exposed to apogossypol (20 μM) for 4 h. After treatment, cells were immunostained with the ER tubular marker BAP31. b) HeLa cells treated as before were co-stained for GM130 and RTN4. All experiments were independently performed three times. Scale bar: 10 μm.
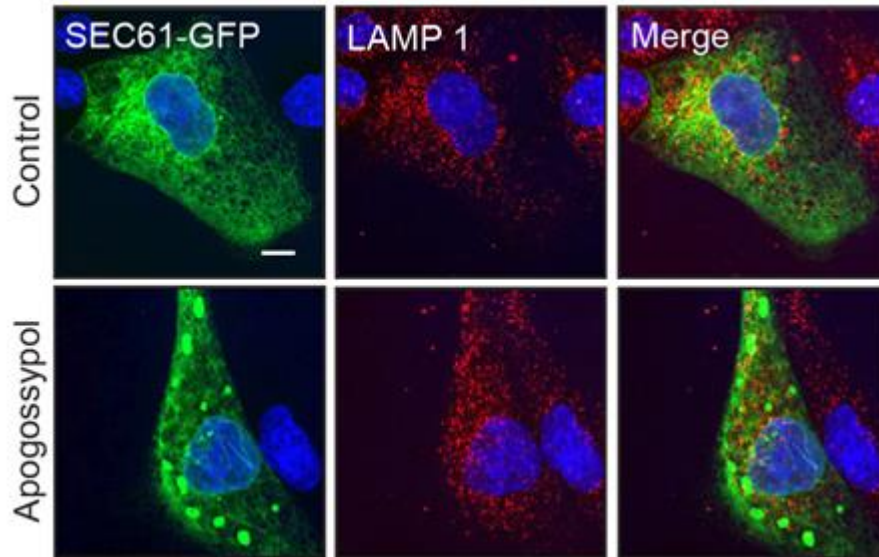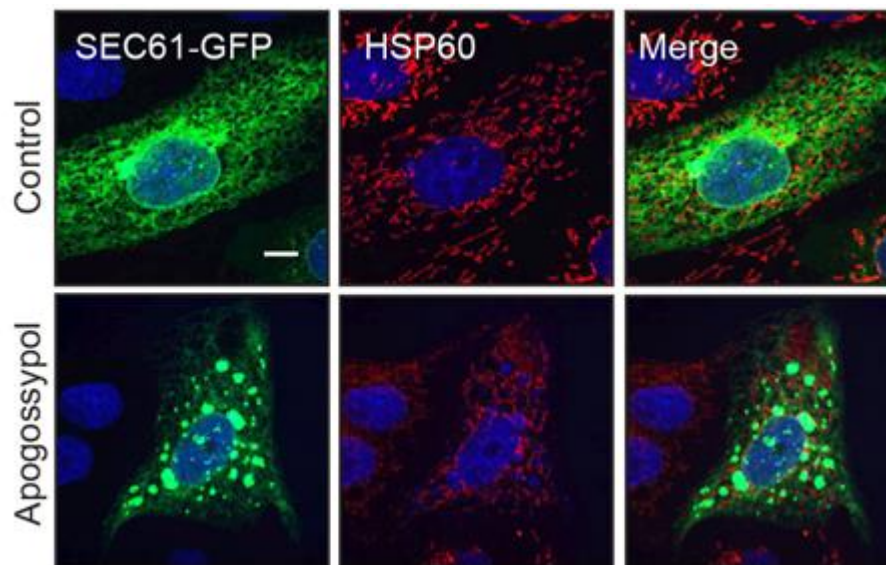
Figure 3.8. ERMR does not appear to involve lysosomes or mitochondria. HeLa cells were transfected with an ER marker (Sec61β-GFP). Following transfection, the cells were exposed to apogossypol (20 μM) for 4 h. After treatment, cells were immunostained for a) lysosomal marker; LAMP 1, b) mitochondria marker; HSP60. All experiments were independently performed three times. Scale bar: 10 μm

3.8. ERMR does not alter expression levels of mitochondrial fission and fusion proteins.

MFN (mitofusin) and OPA1 (optic atrophy1) are the main regulators of the mitochondrial fusion[31,48]. The two isoforms of MFN (MFN1 and MFN2) are localized to the outer mitochondrial membrane, whereas OPA1 is localised to the inner mitochondrial membrane[31]. As a loss of fusion results in the proteolytic processing of the higher molecular weight, long isoforms (L1 and L2) of OPA1 to yield three short isoforms (S1-S3)[48]. To check whether apogossypol-mediated ERMR regulated the expression levels of different mitochondrial fission-fusion proteins, cells were exposed with apogossypol (20 µM) for 1 h and then to CCCP (10 µM) for 1 h or A-1210477 (20 µM) for 4 h and western blotting was carried out. In the control DMSO treated cells OPA1 existed as two long and three short isoforms (Figure.3.10), A-1210477 did not shown any alteration in OPA1 processing compared to the control (DMSO treated) cells. In contrast, exposure to CCCP resulted in a clear processing of the long isoforms of OPA1 to yield more of the short isoforms (Figure.3.10). In contrast, MFN1 and MFN2 protein expression levels did not change following the different treatments. Similarly, mitochondrial fission GTPase, DRP1 or its receptors, including MFF (mitochondrial fission factor), MID49 (mitochondrial dynamic protein of 49 kDa) and MID51 (mitochondrial dynamic protein of 51 kDa) also remained unchanged. Interestingly, exposure to apogossypol resulted in small decrease in the phosphorylation status of DRP1 (at S616, which is associated with mitochondrial fission) in cells exposed to either A-1210477 or CCCP. Taken together, apogossypol-mediated ERMR does not appear to regulate the expression levels of mitochondrial fission or fusion proteins.

53

a

DMSO

	RTN4	HSP60	Merge
Control			
Apogossypol			

b

CCCP

	RTN4	HSP60	Merge
Control			
Apogossypol			

54
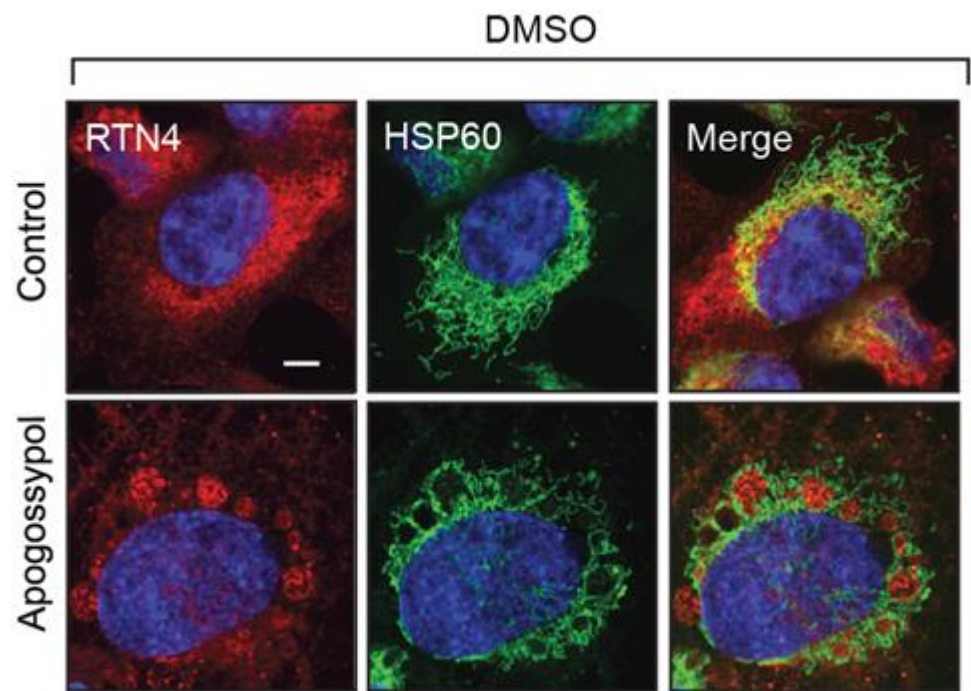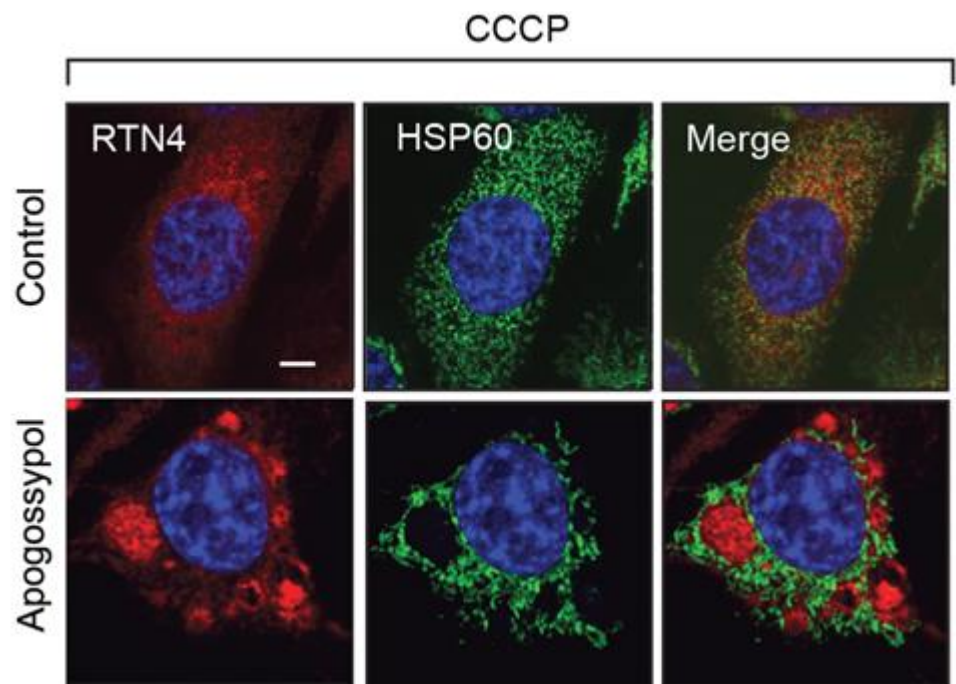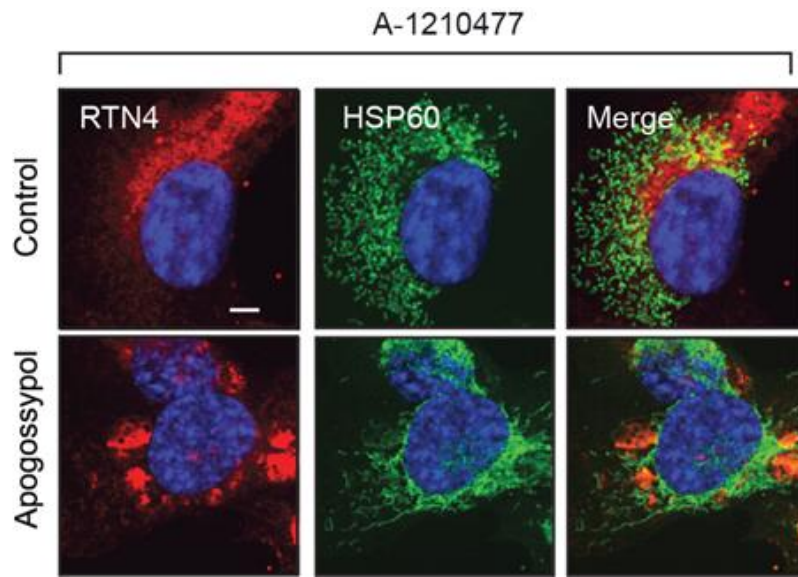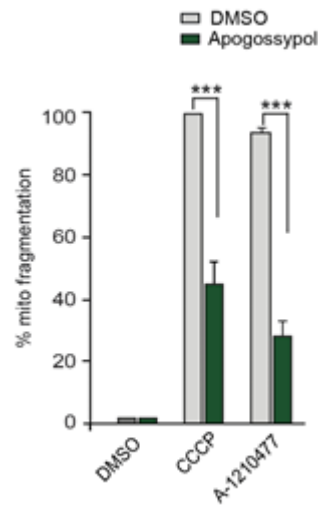
Figure 3.9. ERMR prevented CCCP- and A-1210477-mediated mitochondrial fragmentation. HeLa cells were exposed to apogossypol (20 µM) for 1 h. After pre-treatment cells were exposed to b) CCCP (20 µM) for 1 h or c) A-1210477 for 4 h. Cells were then co-stained with a mitochondrial marker (HSP60) and an ER tubular marker (RTN4). All experiments were independently performed three times. Scale bar: 10 µm. d) Quantification of CCCP- or A-1210477-mediated mitochondrial fragmentation was performed by counting around 100 cells, that exhibited mitochondrial fragmentation, from 3 independent experiments. Error bars = Mean ± SEM. *** $p \leq 0.001$.
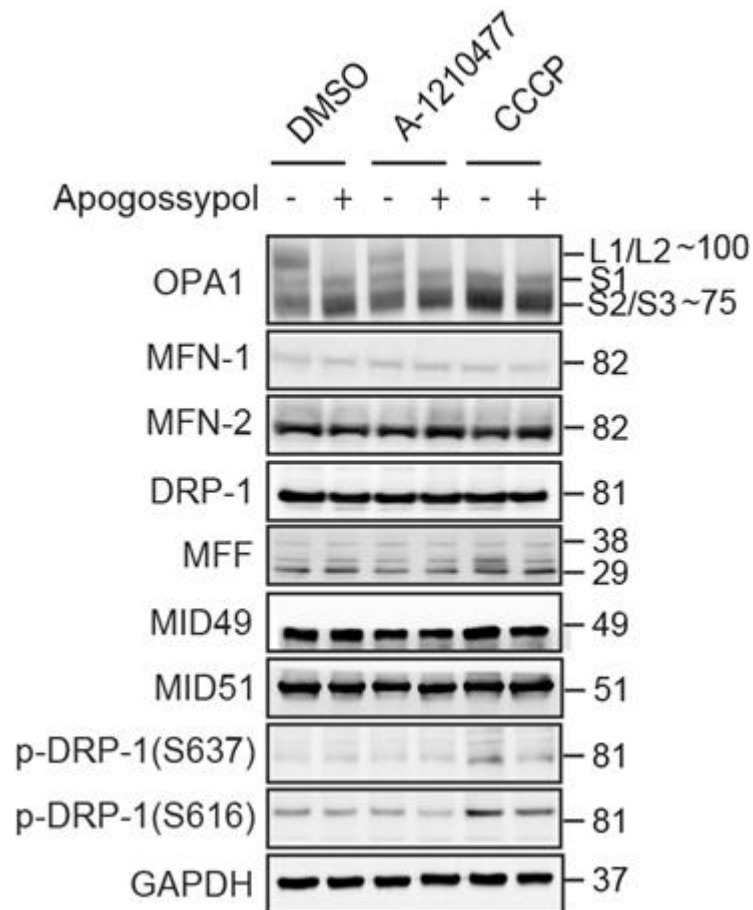
Figure 3.10. Western blot analysis of mitochondrial fission and fusion proteins. H1299 cells were pre-treated with apogossypol (20 μM) for 1 h then treated with A-1210477 (10 μM) for 4 h or CCCP (10 μM) for 1 h. After treatment, cells were lysed and subjected to western blot analysis using the indicated antibodies.

3.9. ERMR alters DRP-1 distribution

Since DRP-1 translocation from the cytosol to mitochondrial membranes is a key event for mitochondrial fission[27,48], it is possible that ERMR antagonises mitochondrial fission by preventing DRP-1 translocation. For this, cells were stained for endogenous DRP-1 or transfected with a DRP-1-GFP plasmid, followed by exposure to apogossypol (20 µM) for 4 h. Interestingly, the normal punctate distribution of endogenous DRP1 or overexpressed DRP-1-GFP was significantly altered following apogossypol-mediated ERMR (Figure.3.11). These results suggested that apogossypol-induced ERMR altered DRP-1 distribution. Interestingly these results suggested that DRP-1 is trapped within ERMR.
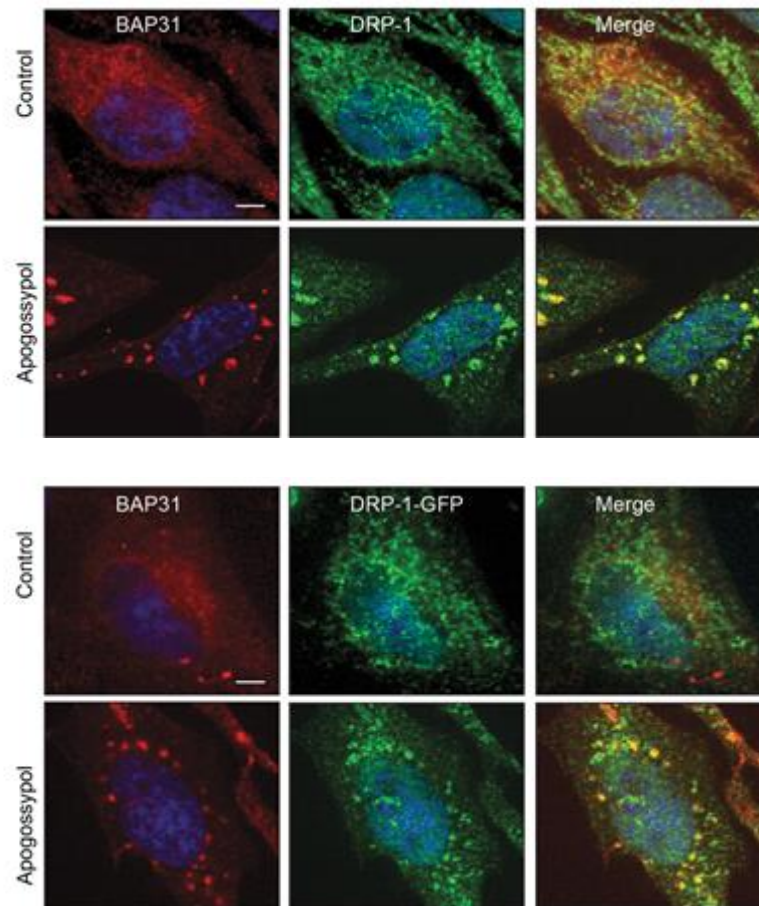
Figure 3.11. ERMR effects DRP-1 distribution. a) HeLa cells were exposed to apogossypol (20 µM) for 4 h. Cells were then co-stained with DRP-1 and an ER tubular marker (BAP31). b) HeLa cells were transiently transfected with wild type DRP-1-GFP. Following transfection, the cells were exposed to apogossypol (20 µM) for 4 h. After treatment, cells were then immunostained with ER tubular marker (BAP31). All experiments were independently performed three times. Scale bar: 10 µm.

3.10.   ERMR antagonises BAX translocation from cytosol to mitochondria

Previous results showed that ERMR played a crucial role on DRP1-mediated mitochondrial fission (Figure.3.11). DRP-1-mediated mitochondrial fission could be linked to apoptosis induction due to the recruitment of BAX (BCL-2 associated X protein) to the mitochondrial membrane with some assistance from ER membranes[98,174,176,177]. Upon apoptotic stimuli, cytosolic BAX translocates to the mitochondria, where it is activated to form oligomeric channels that result in cytochrome *c* release[177]. Therefore, to check whether the reorganised ER membranes would alter BAX translocation, cells were exposed to a combination of BH3 mimetics (A-1331852; BCL-XL inhibitor and A-1210477) in the presence of apogossypol. In the absence of BH3 mimetics, BAX appeared largely cytosolic (Figure.3.12), whereas following exposure to BH3 mimetics, BAX translocated to the mitochondrial membranes, characterised by its punctate staining[174]. Such punctate staining was drastically reduced in cells treated with a combination of apogossypol and BH3 mimetics (Figure.3.12). These results demonstrated that apogossypol-mediated ERMR prevented the mitochondrial translocation of BAX.

3.11.   ERMR does not antagonise BAK activation

In addition to BAX, BAK also has the ability to form pores on mitochondria membranes and eventually triggers cytochrome *c* release from mitochondria to cytosol[177–179]. Since ERMR prevented the mitochondrial translocation of BAX, it is possible for ERMR to also modulate BAK activation and pore formation. However, unlike BAX, BAK is generally localised within OMM and upon apoptotic stimuli, it undergoes conformational changes, such as the exposure of AB1 epitope, to form pores[178]. Therefore, cells were exposed to a combination of BH3 mimetics (A-1331852; BCL X_L inhibitor and A1210477; MCL-1 inhibitor) in the presence of apogossypol and the extent of BAK activation was measured. The punctate staining of BAK, which corresponds to BAK activation, was only present in cells exposed to BH3 mimetics (Figure.3.13). Such BAK punctate were not reduced in cells treated with a combination of apogossypol and BH3 mimetics but mitochondrial co-localisation appears to, revealing that apogossypol-mediated ERMR does not influence BAK activation.
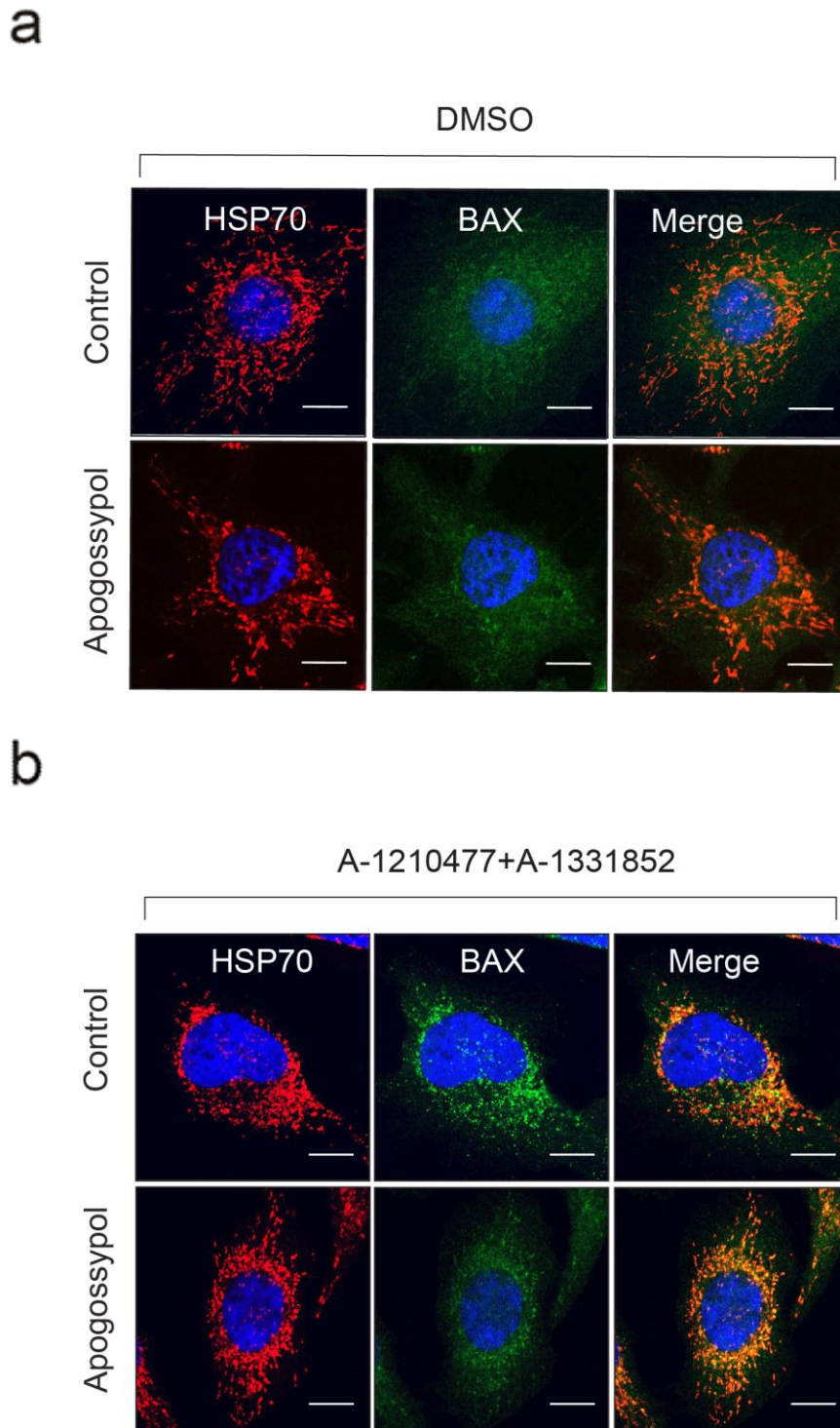
Figure 3.12. ERMR prevented BAX translocation. a) HeLa cells were pre-treated with Z-VAD.fmk (30 μM) for 30 min then treated with apogossypol (20 μM) for 1 h. b) After treatment, cells were exposed to A-1210477 (10 μM) + A-1331852 (0.1 μM) for 4 h. Cells were immunostained with HSP60 and BAX antibodies. The box regions in the image are enlarged to show BAX localising on the mitochondria. All experiments were independently performed three times. Scale bar: 10 μm.
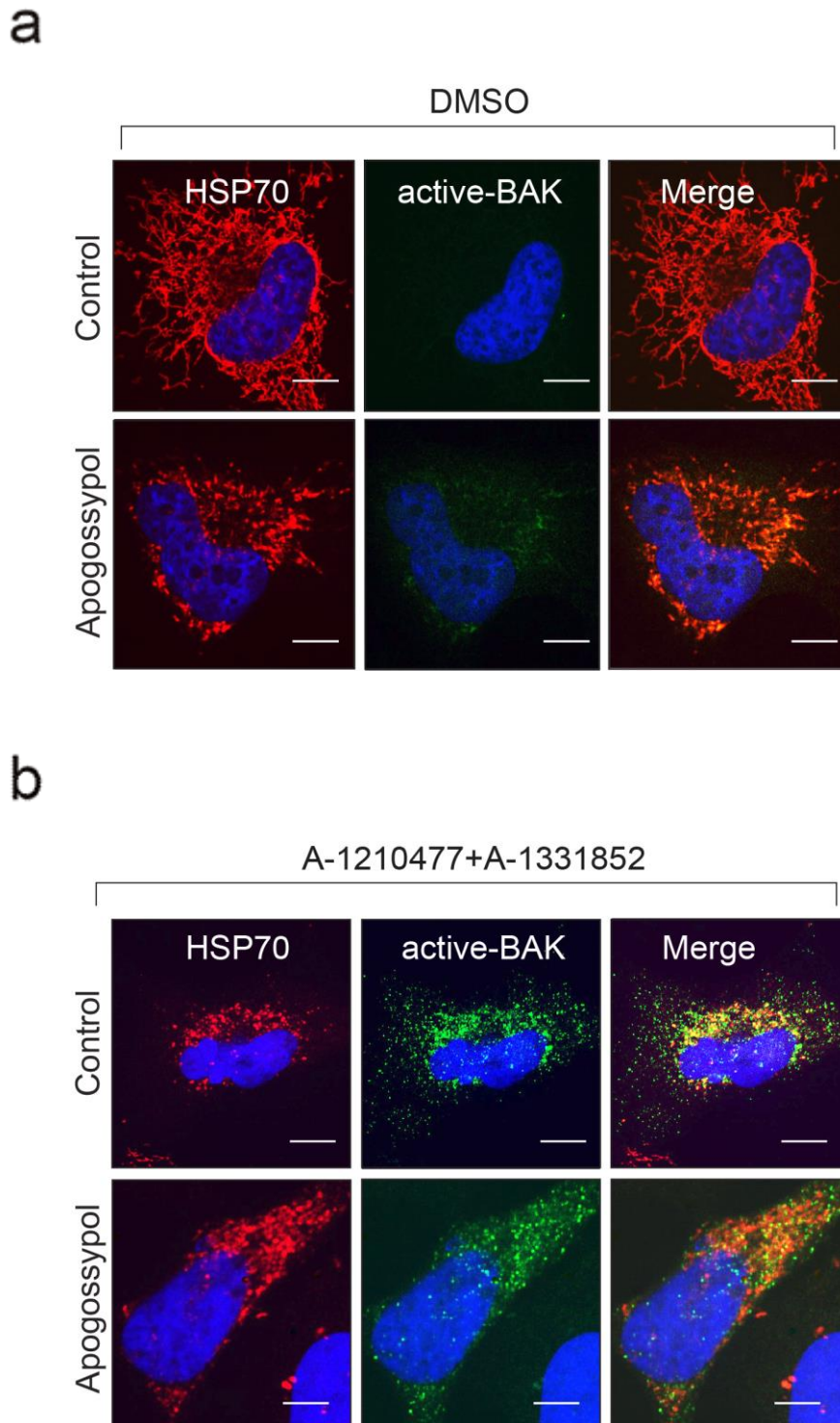
Figure 3.13. ERMR does not affect BAK activation. a) HeLa cells were treated with Z-VAD.fmk (30 μM) for 30 min and then with apogossypol (20 μM) for 1 h. b) After treatment, cells were exposed to A-1210477 (10 μM) + A-1331852 (0.1 μM) for 4 h and immunostained with HSP60 and active-BAK antibodies. All experiments were independently performed three times. Scale bar: 10 μm. The box regions in the image are enlarged to show active BAK on mitochondrial membranes in the indicated cells.

3.12. ERMR selectively antagonises BAX but not BAK activation

Previous results suggested that apogossypol-mediated ERMR prevented BAX translocation (Figure.3.12). To check whether ERMR also prevented BAX activation, cells were exposed to BH3 mimetics (A-1331852; BCL X_L inhibitor and A1210477; MCL-1 inhibitor) in the presence of apogossypol and stained with anti-BAX 6A7 antibody. This antibody specifically recognises the α-1 helix of BAX, which is only exposed following apoptotic stimuli[180–183]. Following exposure to BH3 mimetics higher levels of BAX activation were determined (Figure.3.14 a). Exposure to apogossypol reduced BAX activation (Figure. 3.14 a), suggesting that apogossypol-mediated ERMR prevented both BAX translocation and activation. In agreement with previous results (Figure.3.12), apogossypol-mediated ERMR did not prevent BAK activation (Figure.3.14 b). These results confirmed that apogossypol-mediated ERMR preferentially prevented BAX activation but not BAK activation.
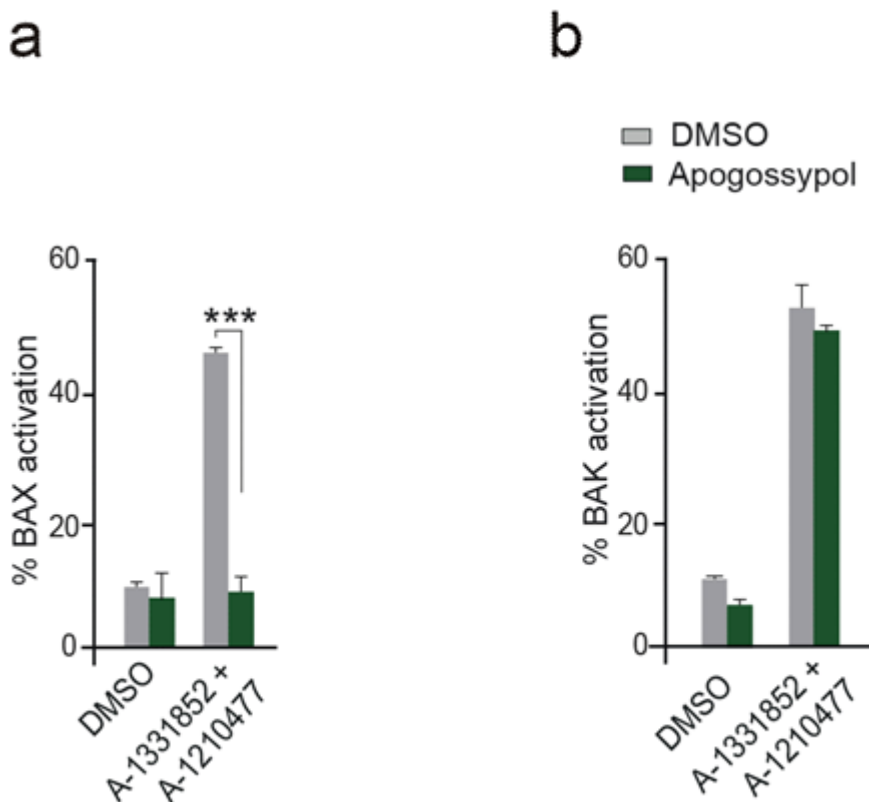
Figure 3.14. ERMR preferentially prevented BAX but not BAK activation. HeLa cells were exposed to apogossypol (20 μM) for 1 h. Cells were exposed to A-1210477 (10 μM) + A-1331852 (0.1 μM) for 4 h. Cells were stained with a) active BAX (6A7) antibody or b) active BAK (AB-1) antibody and, the extent of BAX and BAK activation assessed by flow cytometry. All experiments were independently performed three times. Error bars = Mean ± SEM. *** $p \leq 0.001$.

3.13. ERMR antagonises BH3 mimetics-mediated release of cytochrome *c*

Since apogossypol-mediated ERMR prevented BAX activation and mitochondrial translocation, it is possible that ERMR could affect BH3 mimetic-mediated release of cytochrome *c*. Following exposure to a combination of BH3 mimetics (A-1331852; BCL X_L inhibitor and A1210477; MCL-1 inhibitor), an extensive release of cytochrome *c* was observed from the mitochondria to cytosol (Figure.3.15). Exposure to apogossypol prevented BH3 mimetic-mediated cytochrome *c* release, as observed in western blots (Figure 3.15 a and b) as well as immunocytochemistry (Figure 3.15 c and d).
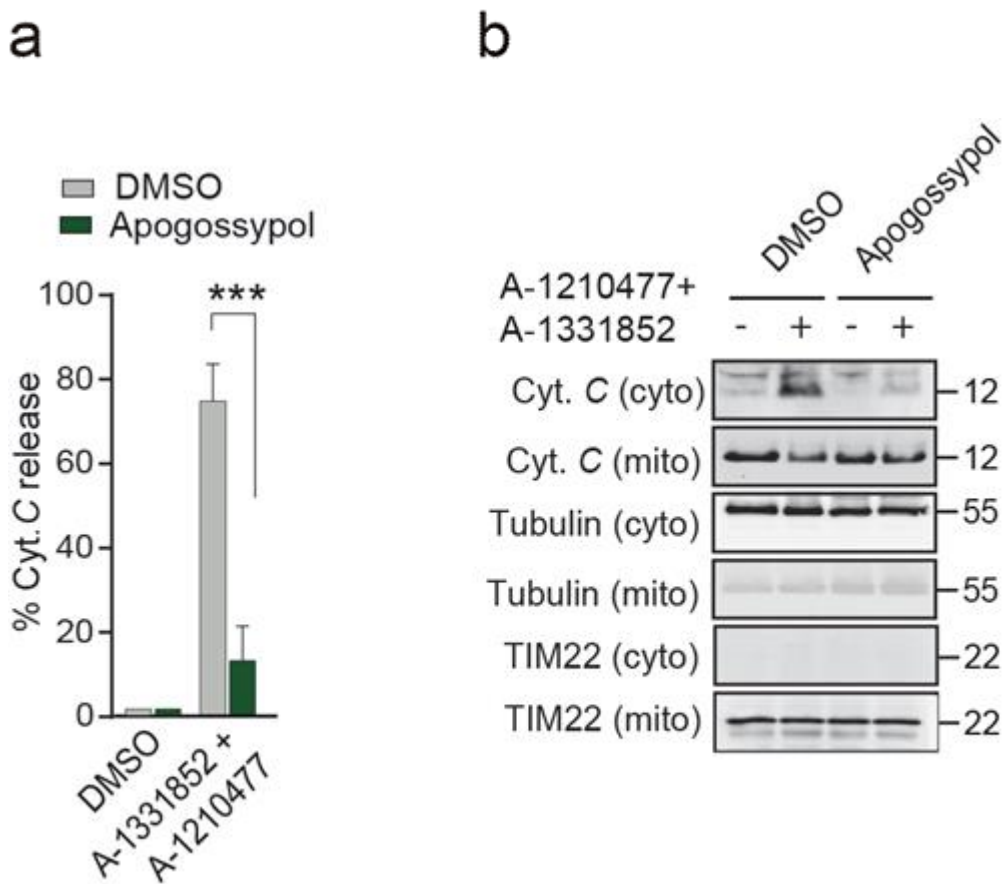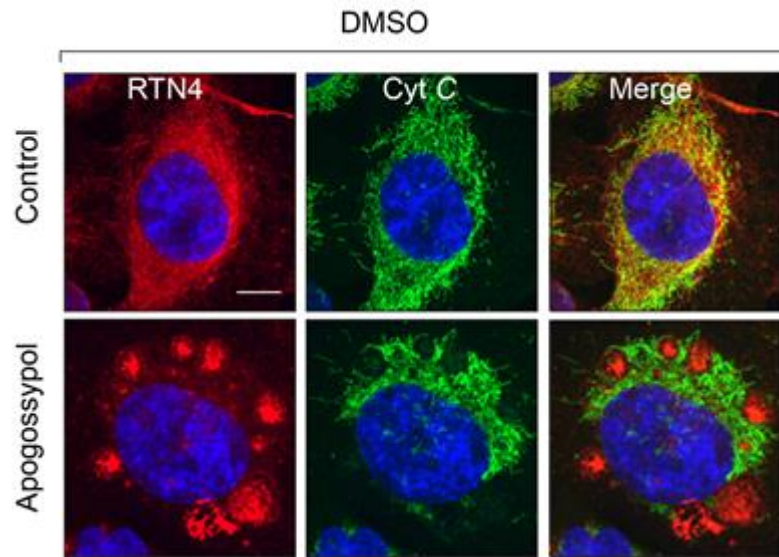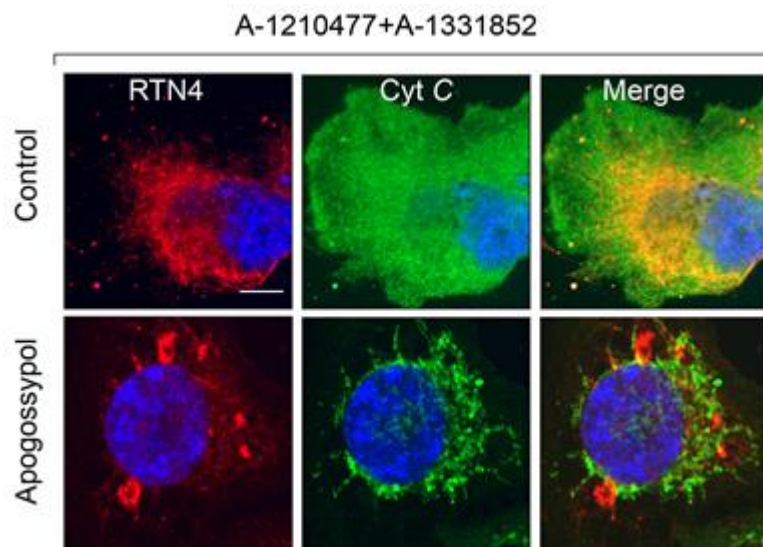
Figure 3.15. ERMR prevented cytochrome *c* release. HeLa cells were pre-exposed to Z-VAD.fmk (30 μM) for 30 min and then exposed to apogossypol (20 μM) for 1 h. Cells were exposed to A-1210477 (10 μM) + A-1331852 (0.1 μM) for 4 h. a) Quantification of extent of cytochrome *c* release was performed by counting ~100 from 3 independent experiments. Error bars = Mean ± SEM. *** $p \leq 0.001$. b) After treatment, mitochondrial and cytosolic fraction were subjected to western blot analysis using indicated antibodies. c) Cells were treated as before and co-stained with the cytochrome *c* and an ER tubular marker (RTN4). All experiments were independently performed three times. Scale bar: 10 μm.

3.14.   ERMR antagonises BH3 mimetics-mediated apoptosis in several cell lines

Since apogossypol-mediated ERMR prevented cytochrome c release, it is possible that ERMR could affect BH3 mimetic-mediated apoptosis. Maver-1 (derived from mantle cell lymphoma) and RS 4;11 (derived from acute lymphoblastic leukaemia) cell lines are primarily dependent on BCL-2 for survival[118,184]. Exposure to ABT-199; BCL-2 inhibitor triggers extensive apoptosis in these cells[118], which was prevented when exposed to a combination of apogossypol and ABT-199 (Figure.3.16 a-b). These results suggested that apogossypol-mediated ERMR prevented ABT-199-dependent apoptosis. Similarly, in BCL-X_L dependent cell lines, KCL-22 and K562 (chronic myeloid leukaemia cell lines), exposure to A-1331852; BCL-X_L inhibitor[118,185] triggers extensive apoptosis which was prevented in cells exposed to a combination of apogossypol and A-1331852 (Figure.3.16 c-d). In H929 (derived from multiple myeloma) primarily dependent on MCL-1 for survival, exposure to apogossypol prevented A-1210477-mediated apoptosis. (Figure.3.16 e). Finally, in H1299 (derived from non-small lung carcinoma) and HeLa (derived from cervical cancer) that primarily depend on both MCL-1 and BCLX$_L$ for survival, exposure to apogossypol prevented BH3 mimetic-mediated apoptosis (Figure.3.16 f-g). Taken together, these results suggested that ERMR played a significant role on BH3 mimetic-mediated apoptosis in several cancer cell lines.
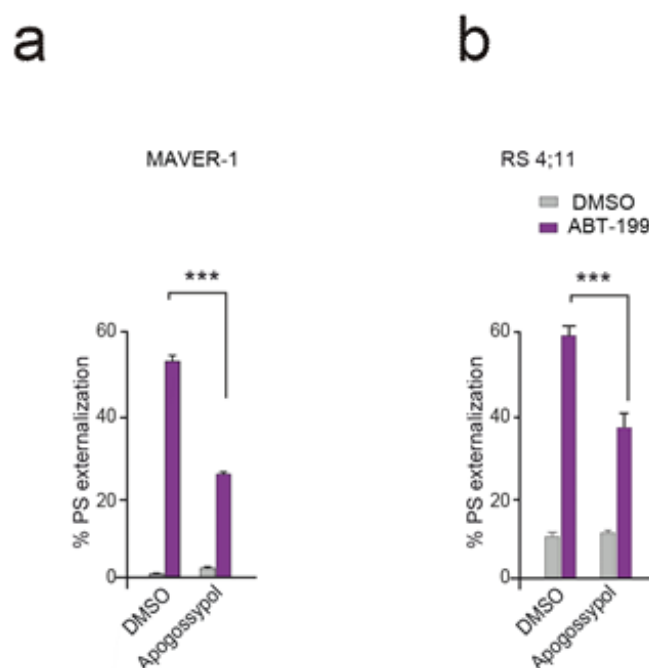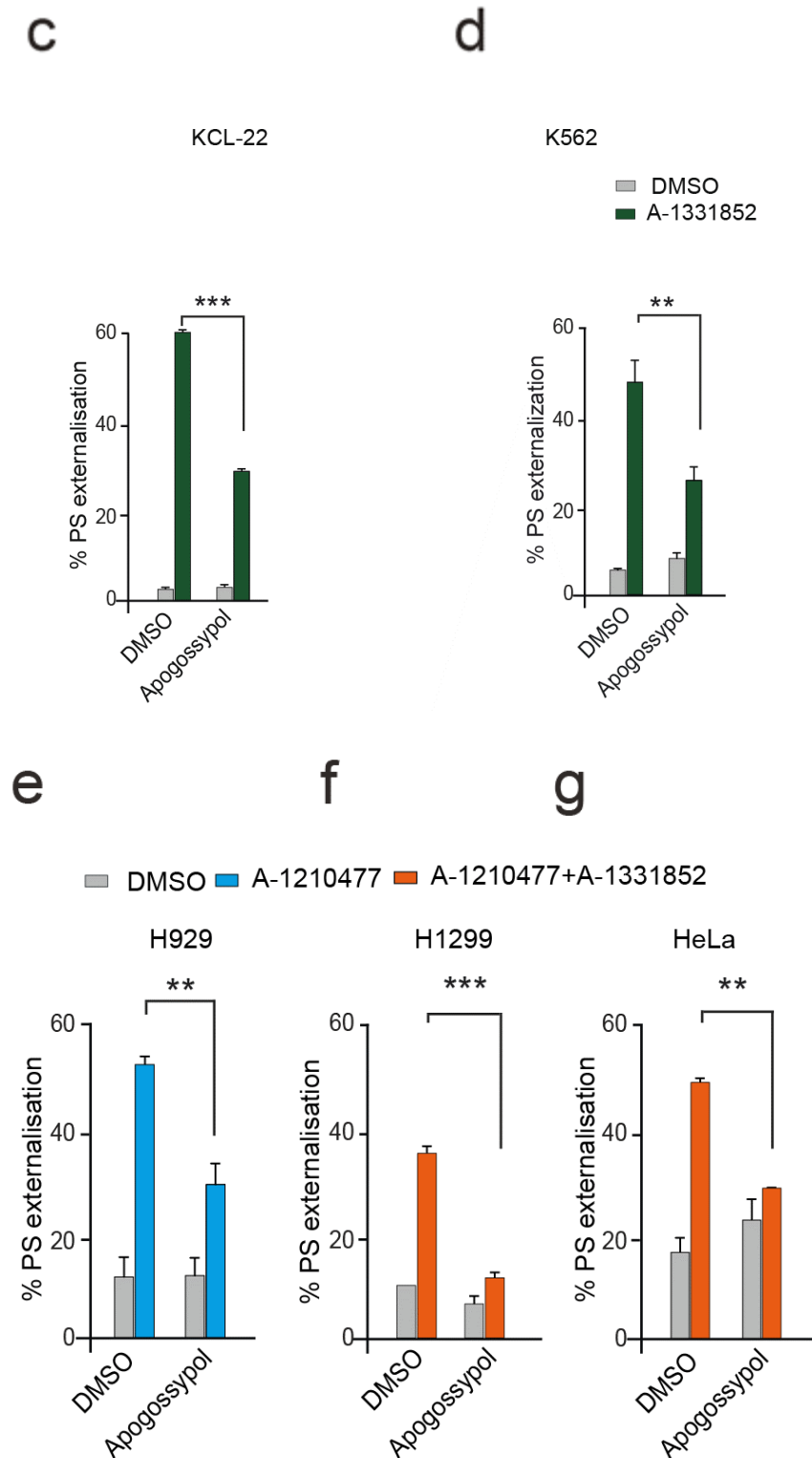
Figure 3.16. ERMR prevented BH3 mimetic-mediated apoptosis. a-b) BCL-2 dependent cells (MAVER-1, RS 4;11), c-d) BCL-X$_L$ dependent cells (KCL-22, K562), e) MCL-1 dependent cell (H929) and f-g) BCLX$_L$ and MCL-1 dependent cells (H1299, HeLa) were exposed to apogossypol (20 µM) for 1 h, exposed to specific BH3 mimetics for 4 h and assessed for apoptosis by PS externalisation. All experiments were independently performed three times. Error bars = Mean ± SEM. ** for $p \leq 0.005$, *** $p \leq 0.001$.

3.15. Different pharmacological agents showing extensive ERMR also prevents BH3 mimetic-mediated apoptosis.

Since apogossypol is capable of inducing ERMR as well as preventing BH3 mimetic-mediated apoptosis, it is important to assess whether the anti-apoptotic effect of apogossypol was due to its ability to induce ERMR.

Previously reports have identified other structurally diverse compounds that also induced ERMR[90,91]. It is possible that these compounds could also prevent BH3 mimetic-mediated apoptosis. Therefore, to investigate this, cells were exposed to structurally diverse reorganisation inducers, such as NDGA (antioxidant), ivermectin (anthelmintic), terfenadine (antihistamine) and suloctidil (vasodilator). All compounds induced ERMR, with suloctidil being the least efficient compared to the other three compounds (Figure.3.17 a,b). In agreement, the protective effect of the different compounds mimicked their ability to induce ER membrane reorganisation (Figure.3.17 b), thus probably explaining why suloctidil was not as potent as the other agents in protecting against BH3 mimetics mediated apoptosis. However, we cannot exclude the possibility that suloctidil might have its off-target effect on anti-apoptotic function. Overall, our data demonstrated that ERMR antagonised mitochondrial fission and BH3 mimetic-mediated apoptosis.
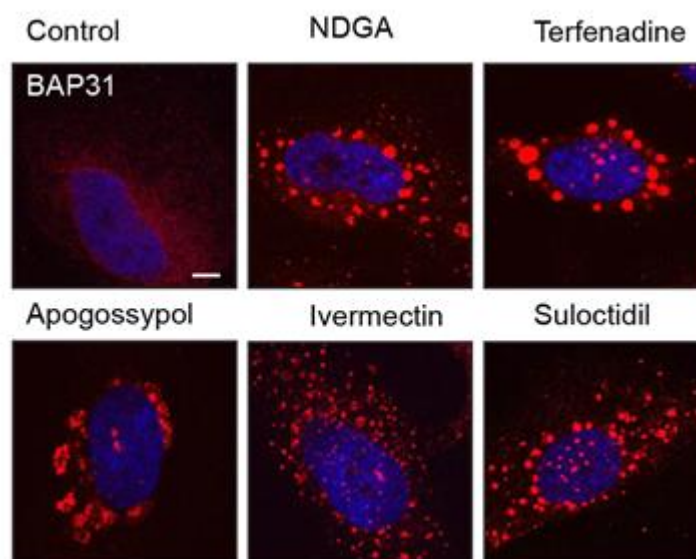
b
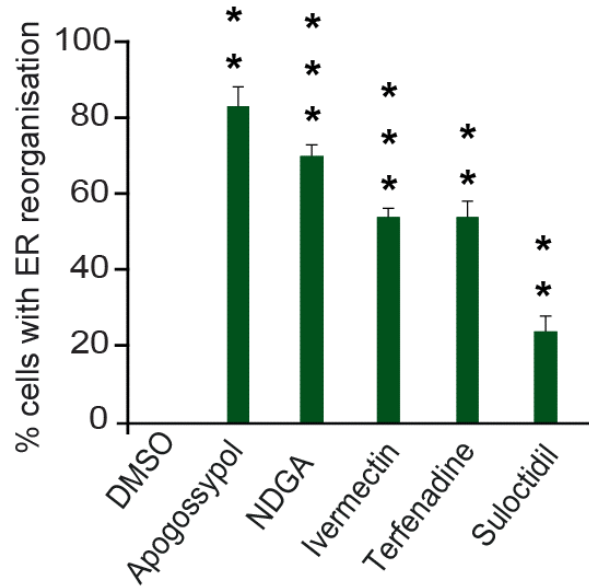
c
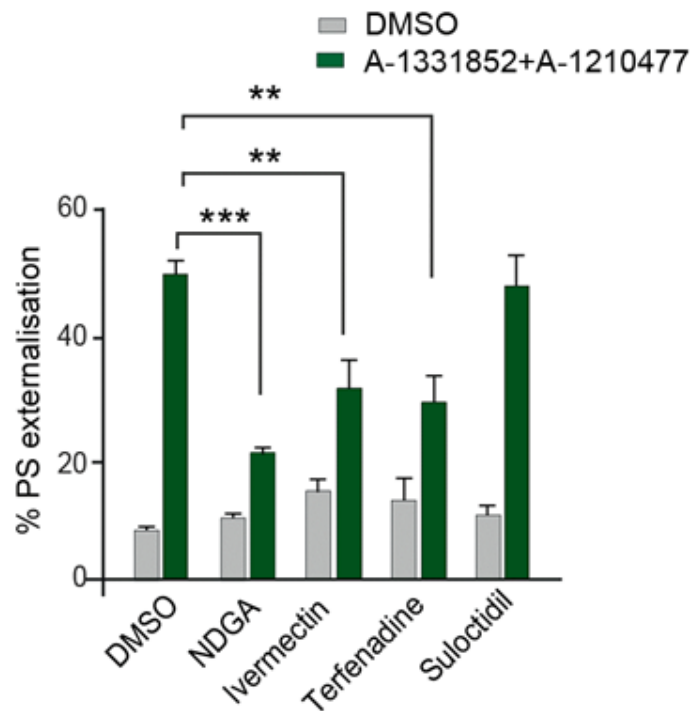
Figure 3.17. Other ERMR inducers induced ERMR and antagonised BH3 mimetic-mediated apoptosis. a) HeLa cells were pre-treated with NDGA (50 μM), ivermectin (20 μM), terfenadine (5 μM) or suloctidil (5 μM) for 4 h. The cells were then immunostained for an ER tubule markers (BAP31). b) Quantification of extent of ERMR was performed by counting around 100 cells from 3 independent experiments. Error bars = Mean ± SEM. ** for $p \leq 0.005$, *** p ≤ 0.001. c) Cells were exposed to indicated ERMR inducers for 1 h followed by a combination of A-1210477 (10 μM) and A-1331852 (0.1 μM) for 4 h and assessed for apoptosis by PS externalisation.

3.16.   Discussion

ER-mitochondria contacts have been previously shown to play important roles in calcium signalling, mitochondrial structural dynamics and apoptosis[7,48]. Growing evidence suggests that ER tubules regulate mitochondrial fission by physically wrapping around the mitochondria for initiating mitochondrial constriction, which is followed by the recruitment of DRP-1 onto the constriction sites. Thus, recruited DRP-1 further undergoes conformational changes to finally result in mitochondrial fission[27,48,186]. These events are also linked to cell fate decisions, including autophagy and apoptosis[92,187,188]. Understanding the impact of ER-mitochondria interactions on apoptosis is essential to improve cancer therapy, as most of the anti-cancer agents kill cancer cells through the mitochondrial apoptotic pathway. Since mitochondria are closely associated with the ER for maintaining their structural dynamics and important physiological functions, it is possible that disrupting this association may alter mitochondrial structural dynamics and functional homeostasis. One way to achieve this is by remodelling ER structure using inducers of ER membrane reorganisation (ERMR)[90,91] (Figure 3.1).

Initial characterisation of ERMR study focused on investigating the domains within ER that contributed to ERMR. It is well known that ER appears as different structural domains. These include the elongated and filamentous ER tubules as well as the flattened ER sheets. Previous studies demonstrated that proteins that reside in ER tubules such as, RTN4 (reticulon-4)[91] and BAP31 (B- cell receptor associated protein of 31KDa)[156] colocalised with ERMR (Figure 3.3 and 3.4). In this study, using two marker proteins that reside in ER sheets, namely CLIMP-63 (cytoskeleton linking membrane protein 63) and kinectin-1 (KNT-1) (Figure 3.5) , it has been convincingly shown that ERMR is almost exclusively from ER tubules and ER sheet proteins do not contribute to these structures (Figure 3.4 and 3.5). In addition, ER also have luminal spaces, which are responsible for creating a suitable environment for important cellular process, including protein synthesis and folding. Chaperones, such as BIP[189] (binding protein) and PDI (protein disulphide isomerase)[190] reside in the lumen and regulate protein folding[163]. This study demonstrates that apogossypol-induced ERMR is restricted to ER tubular proteins but not lumenal proteins (Figure 3.6). Since ER tubules and sheets are interconnected and may share continuous luminal space, it is

hard to speculate why the lumenal space is not involved in the ERMR. It is possible that ER lumen may be compartmentalised within specific regions of the ER tubules and all of ER sheets. Therefore, regions that form ERMR may not have the lumenal space/ proteins, thus forming compact membranous bundles. Even at the level of electron microscopy, the reorganised ER bundles appear to be largely devoid of lumen. Moreover, the fact that the UPR occurs exclusively at ER lumen and that ERMR is distinct from the UPR adds further support to this theory. This can be proved definitively by either performing high resolution confocal microscopy or correlative immunogold labelling studies.

Although ERMR colocalised with ER tubule markers, the reorganised membranes do not seem to share membranes from other subcellular organelles, including the Golgi complex, lysosomes and mitochondria (Figures 3.7 and 3.8). However, Golgi complex seems to be dispersed upon exposure to apogossypol, in agreement with previous work[91]. Dispersed Golgi is the one of the hallmarks for ERMR and indicates defective ER-Golgi vesicular trafficking[91]. Unlike Golgi, ERMR does not seem to alter the structure of lysosomes and mitochondria, despite sharing close contacts with these organelles. Therefore, initial studies suggested that ERMR may not influence mitochondrial or lysosomal structure. This was because mitochondria appeared filamentous in both control (DMSO-treated) as well as apogossypol-treated cells (Figure 3.8). However, recent reports suggest that ER tubules play an important role on regulating mitochondrial fission by physically wrapping around mitochondria and marking constriction sites[7,91]. In agreement, apogossypol-mediated ERMR prevented CCCP- and BH3 mimetic-mediated mitochondrial fission (Figure 3.9). These results suggested that ERMR altered mitochondrial membrane dynamics, which was evident only when cells were exposed to mitochondrial fission inducers. Such an effect was not observed in control cells, possibly because in HeLa and H1299 cell lines, mitochondria are already hyper filamentous. So, the effect of apogossypol to further enhance fusion was not clear. This can of course be overcome by using cells, such as MCF7, which generally have fragmented mitochondrial network.

It has been reported that CCCP- and A-1210477-mediated mitochondrial fission were strongly dependent on DRP-1[174]. Normally, DRP-1 resides within the cytosol, and upon fission, translocates to the mitochondria to induce mitochondrial

fission. The effect of apogossypol to prevent mitochondrial fission might be due to the inability of DRP-1 to translocate to the mitochondrial fission site. This was evident by the sequestration of DRP-1 within the reorganised ER membranes (Figure 3.11). Therefore, this suggests that DRP-1 is possibly localised to specific regions within ER, which upon fission stimuli, gets translocated to mitochondrial membranes while the ER wraps around the construction site. This could not be proved by confocal microscopy. Solid conclusions can be drawn only following subcellular fractionation to isolate mitochondrial, cytosol and ER fractions. Efforts to perform this study were largely unsuccessful due to technical reasons.

During fission DRP-1 translocated to mitochondria and coupled with its receptors, MFF, MiD49, and MiD5 which reside on mitochondrial fission sites to facilitate mitochondrial fission[31,51,191]. Although ERMR does not change the proteins expression levels of DRP-1 or its receptors, ERMR appears to alter the phosphorylation status of DRP-1. It has been reported that phosphorylation at serine 616 (pDRP1 S616) is associated with mitochondrial fission[48,192], whereas phosphorylation at serine 637 (pDRP1 S637) is associated with mitochondrial fusion[48,193,194]. This was more promising in cells exposed to CCCP and A-120477, which resulted in an increase in serine 616 phosphorylated DRP-1 that was antagonised by apogossypol (Figure 3.10). These results suggested that apogossypol-mediated ERMR could be regulating DRP-1 S616 phosphorylation. On the contrary, exposure to CCCP also increased serine 637 phosphorylation of DRP-1, which decreased when cells were also exposed to apogossypol (Figure 3.10). Although this was not observed following BH3 mimetics, these findings were counterintuitive. Further studies will have to be carried out in this area, as these preliminary findings suggest that apogossypol-mediated ERMR may be regulating mitochondrial fission through a complex mechanism.

This was more apparent with OPA1 protein levels, as this mitochondrial fusion protein has been shown to exist as different isoforms[48,108], and upon fission, undergoes proteolysis during which the long isoforms (L1 and L2) of OPA1 are cleaved into three short isoforms (S1, S2 and S3)[195]. In agreement, a mitochondrial fission inducer (CCCP) cleaved the long OPA1 isoforms into more shorter isoforms (Figure.3.10), such proteolytic cleavage was not reversed in cells exposed to apogossypol. In fact, apogossypol alone appeared to induce OPA1 proteolysis in cells. Taken together, these

results suggested that apogossypol-mediated ERMR plays a complex role in OPA1 proteolysis and mitochondrial membrane dynamics.

Since ERMR altered DRP-1 distribution, it is possible that ERMR might also alter BAX translocation, as DRP-1 and BAX have been shown to interact at the constriction sites[48]. This study demonstrates that ERMR specifically prevented BAX, but not BAK, activation and translocation to outer mitochondrial membrane (Figure 3.12). Although, HeLa cells express both BAX and BAK, it is unclear as to why these cells do not undergo apoptosis even when BAK is fully active in the presence of apogossypol. Clearly, in this study, HeLa cells appear to rely only on BAX and not BAK for apoptosis induction. This is not surprising as BH3 mimetic-mediated apoptosis seem to depend almost exclusively on BAX. Therefore, it is possible that unless BAX is available, active BAK cannot initiate apoptosis, at least under this condition. Further studies in a panel of cell lines will have to performed to better understand this phenomenon.

Collectively, this study demonstrates the ability of apogossypol-mediated ERMR to antagonise BH3 mimetic-mediated mitochondrial fission, BAX translocation, cytochrome *c* release and apoptosis (Figure 3.18). Although the experiments carried out with other ERMR inducers are largely in agreement with the effects of apogossypol-mediated ERMR, it is hard to uncouple the anti-apoptotic effects of apogossypol from those of ERMR. Therefore, the next results chapter will be aimed at uncoupling these events to prove that the anti-apoptotic effects are indeed due to ERMR.
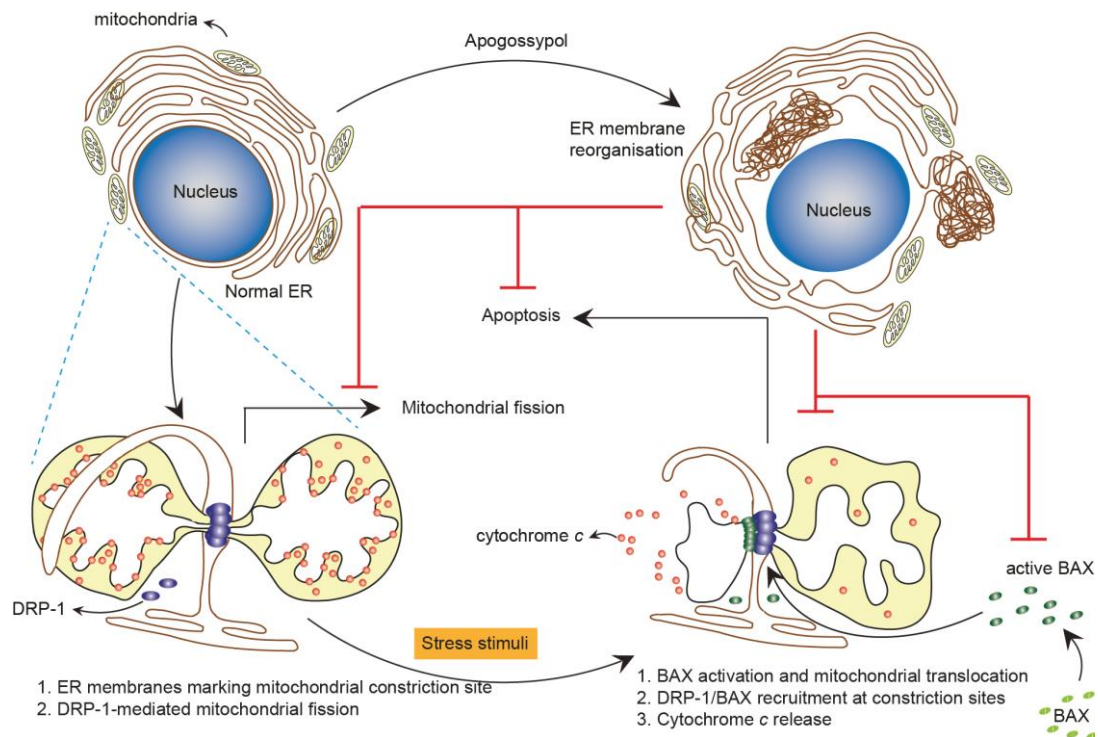
Figure 3.18. Schematic representation of the mitochondrial changes regulated by ERMR. Generally, ER and mitochondria are closely associated with each other and these interactions are extremely important for cellular homeostasis, bioenergetics and cell survival. ER tubules achieve these by wrapping around mitochondria and facilitating DRP-1-mediated mitochondrial fission. Apoptotic stimuli cause BAX translocation on mitochondrial membranes to trigger cytochrome *c* release and apoptosis. Apogossypol-induced ERMR disrupts such communication between ER and mitochondria, decreasing mitochondrial fission, BAX translocation, cytochrome *c* release as well as apoptosis. (Scheme adapted from Varadarajan et al., 2012)

Chapter 4

DHODH modulates both ERMR and

BH3 mimetics-mediated apoptosis

Contents

4.1.   Background

Since ERMR appears to regulate important physiological functions, like mitochondrial fission and apoptosis (Chapter 3), it is important to understand the initiation process of ERMR to uncouple the effects of apogossypol from ERMR in these functions. ER is widely extended throughout the cells and responsible for regulating various physiological functions, including calcium signalling[70,71,196], protein folding[197] and lipid synthesis[21,25,31,33,47,168,198]. It has been reported that ER becomes reorganised upon exposure to apogossypol[91,199], as well as several other agents that target calcium homeostasis[90]. Intracellular calcium stores ar maintained by several pumps, including the sarco/endoplasmic reticulum calcium ATP ases (SERCA), which facilitates calcium influx into the ER lumen[25,26]. Impairment or inhibition of SERCA activity prevents calcium influx to the ER lumen and depletes ER calcium stores[52,200–202]. Depleted ER calcium stores initiates an adaptive signalling and invokes the store operated calcium entry (SOCE) to refill ER lumenal calcium[21,25,26]. SOCE is mediated by ER resident proteins, STIM1 (stromal interaction molecule 1) and STIM2 (stromal interaction molecule 2). Both these proteins act as calcium sensors to detect reduced ER lumenal calcium store and helps to refill emptied ER calcium stores, through coupling with specific plasma membrane calcium channel proteins, such as ORAI1, ORAI2 and ORAI3 (calcium release-activated calcium channel protein 1,2 and 3)[45,46]. The interaction between STIMs and ORAI is crucial for maintaining calcium homeostasis[201,202].

It has been reported that overexpressed STIM1 can induce ERMR[90,91]. Moreover, apogossypol-mediated ERMR has been associated with SOCE [90], and 2-APB (2-aminoethoxydiphenyl borate), an inhibitor for SOCE, can efficiently prevent apogossypol-mediated ERMR[90]. These findings suggested there could be specific regulatory mechanisms between STIM and SOCE that could modulate ERMR. However, a previous study suggested that silencing the expression levels of SOCE regulators (STIM1, ORAI1 and STIM1) does not alter apogossypol-mediated ERMR[90]. In addition, extracellular supplementation of calcium also does not alter ERMR, further suggesting that 2-APB most likely regulated ERMR independent of calcium signalling. Nevertheless, 2-APB could be an important tool to identify whether the anti-apoptotic effects of apogossypol are indeed due to ERMR.
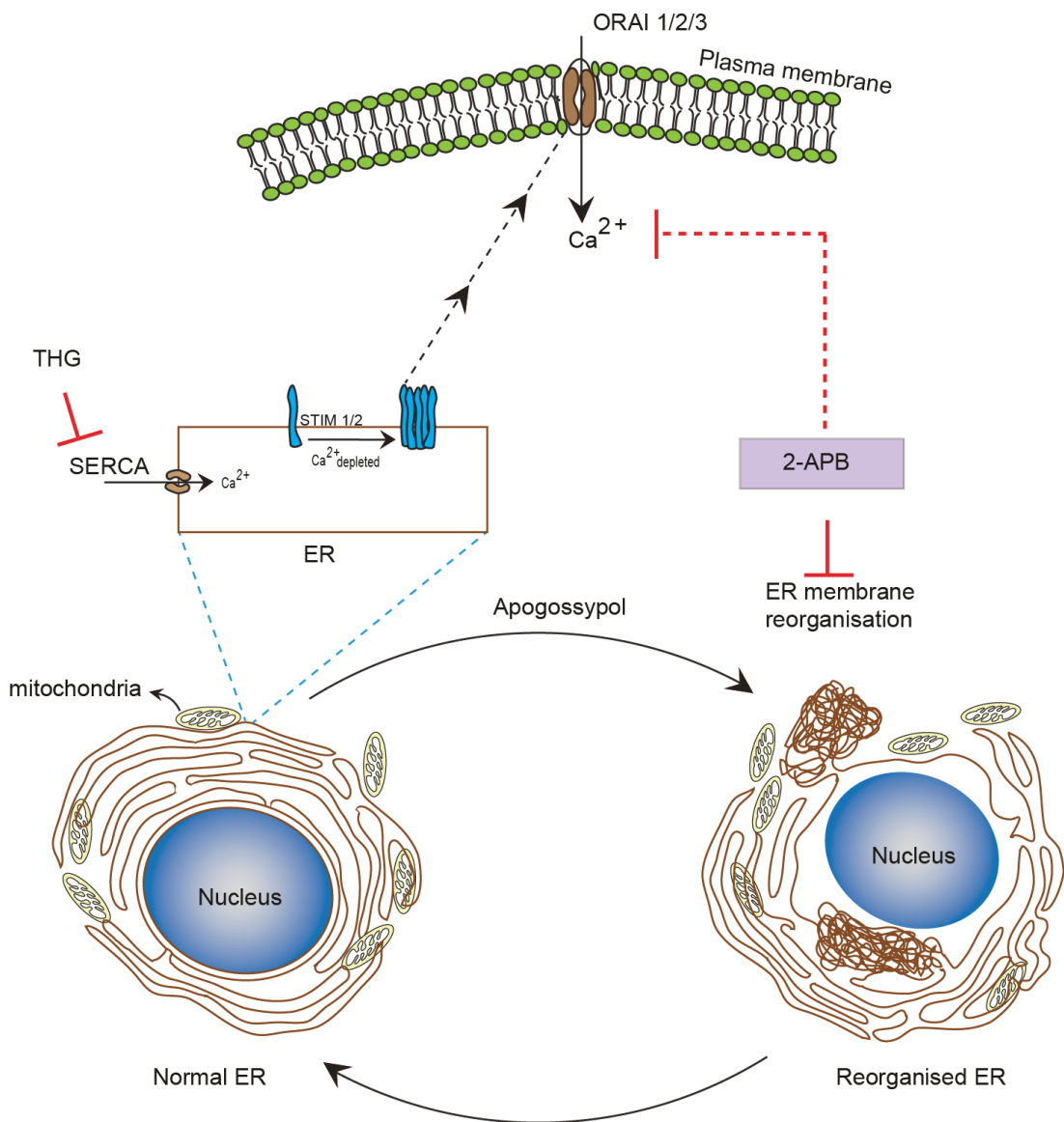
Figure 4.1 Schematic representation of regulatory process of apogossypol-induced ERMR. Under normal conditions, ER is spread throughout the cell and functions in maintaining calcium homeostasis. Exposure to thapsigargin (THG) inhibits SERCA ATPase, which depletes ER calcium, thus driving STIM1/2 and ORAI1/2/3-mediated store-operated calcium influx into the cell. 2-APB inhibits this calcium influx but also prevents apogossypol-mediated ERMR. (Scheme adapted from Varadarajan et al., 2013)[90]

Recently, Rhaman et al[203] examined a large panel of FDA approved drugs to identify specific SOCE inhibitors. Their study found that inhibitors of DHODH, such as teriflunomide and leflunomide, were strong modulators of SOCE. Therefore, in this chapter, the experiments will examine whether these agents would prevent apogossypol-mediated ERMR, thus uncoupling the protective effects of ERMR from apogossypol. Since the primary function of teriflunomide and leflunomide is to modulate the *de novo* pyrimidine biosynthesis *via* inhibition of enzyme DHODH (dihydroorotate dehydrogenase)[133,136,140,204], experiments in this chapter will focus on addressing the following questions:

(1) Can the SOCE inhibitors abolish apogossypol-mediated ERMR and revert the anti-apoptotic effects of ERMR?

(2) Could the inhibition of DHODH be coupled with ERMR and/or apoptosis?

4.2.   2-APB prevents apogossypol-mediated ERMR

It has been reported that 2-APB, an inhibitor of SOCE, is capable of diminishing apogossypol-mediated ERMR. It is possible that 2-APB-mediated decrease in ERMR could also abolish the anti-apoptotic functions of ERMR. Therefore, to check this, cells were exposed to increasing concentrations of 2-APB for 1 hr and treated with apogossypol (20 µM) for 4 h. It must be noted that cells were exposed to 2-APB throughout the course of this experiment. Then, ERMR was assessed using confocal microscopy. In agreement with previous findings, 2-APB prevented apogossypol-mediated ERMR in a concentration- dependent manner (Figure 4.2). In addition, the minimum concentration of 2-APB required to abolish ERMR was 100 µM (Figure 4.2). Therefore, this concentration was used for further investigation.
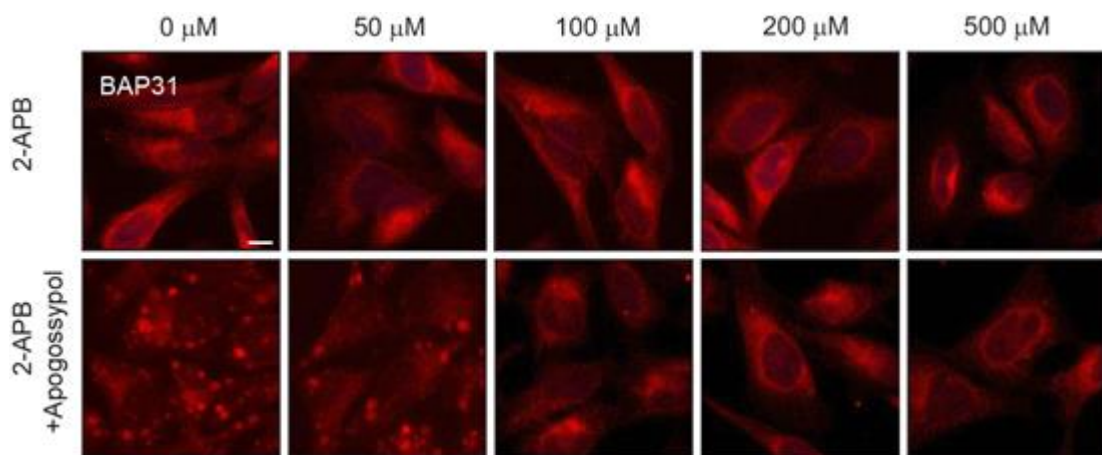
Figure 4.2 2-APB prevents apogossypol-mediated ERMR. HeLa cells were exposed with indicated concentrations of 2-APB for 1 h and treated with apogossypol (20 µM) for 4 h. The cells were then immunostained for ER tubule marker BAP31. All experiments were independently performed three times. Scale bar: 10 µm.

4.3. High concentration of 2-APB is cytotoxic to cells

Since 2-APB abolishes apogossypol-mediated ERMR, it is possible that 2-APB could also reverse the anti-apoptotic functions of ERMR. To test this possibility, cells were exposed to 2-APB (100 μM) for 1 h, in the presence of apogossypol (20 μM) and BH3 mimetics (A-1331852; BCL X_L inhibitor and A1210477; MCL-1 inhibitor) for 4 h. The ability of apogossypol to antagonise BH3 mimetic-mediated apoptosis, in the presence of 2-APB, was then assessed by flow cytometry. While BH3 mimetics induced extensive apoptosis, apogossypol diminished the extent of apoptosis, in agreement with previous findings (Figures 3.17 and 4.3). However, 2-APB as a single agent induced extensive apoptosis, which further enhanced cell death in the presence of BH3 mimetics and apogossypol (Figure 4.3 b). Taken together, these results suggested that 2-APB, whilst suitable to modulate ERMR, was not useful to study the anti-apoptotic functions of ERMR. Therefore, 2-APB was excluded from further investigation.

4.4. Leflunomide and teriflunomide prevent apogossypol-mediated ERMR

Since 2-APB could not be used to study the anti-apoptotic functions of ERMR, there was a need to find alternative tools to study these functions. A recent study by Rhaman et al[203] examined a large panel of FDA-approved drugs to identify specific SOCE inhibitors and concluded that leflunomide and teriflunomide could potentially inhibit SOCE. Since 2-APB prevented apogossypol-mediated ERMR, most likely *via* its ability to inhibit SOCE, it is possible that leflunomide and teriflunomide could also prevent apogossypol-mediated ERMR. To test this, cells were exposed to increasing concentrations of leflunomide or teriflunomide (0 – 200 μM) for 1 h and then exposed to apogossypol (20 μM) for 4 h. Both leflunomide and teriflunomide abolish apogossypol-mediated ERMR in a concentration-dependent manner (Figures 4.4 and 4.5). The minimum concentration of leflunomide and teriflunomide required to abolish ERMR was 200 μM (Figures 4.4 and 4.5).
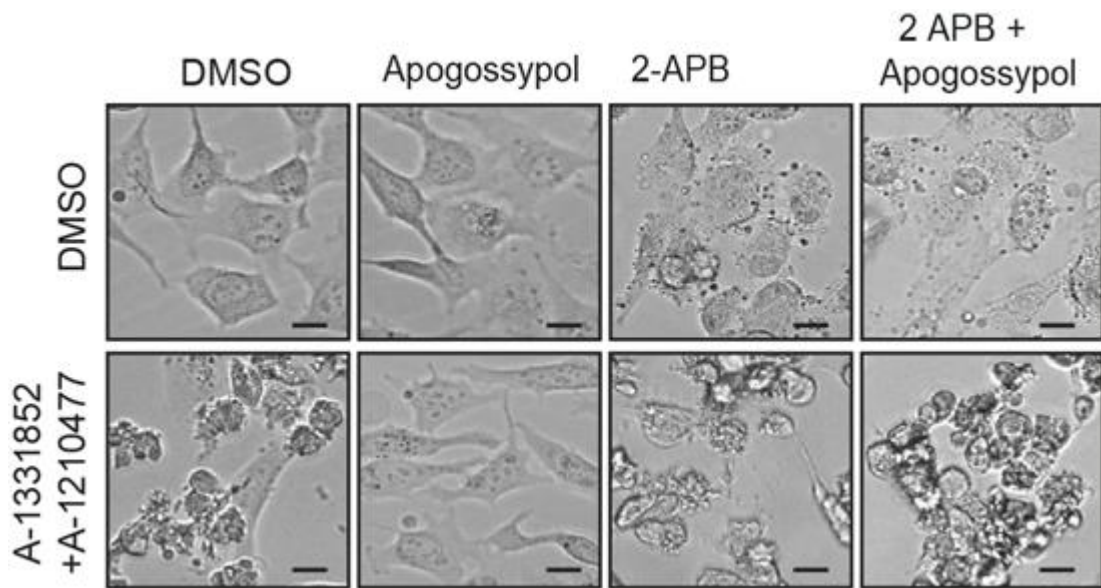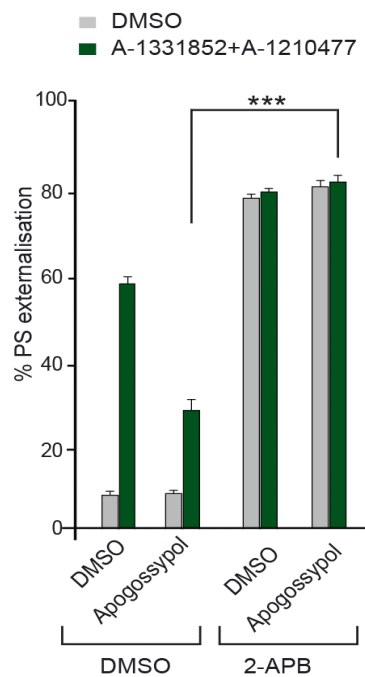
Figure 4.3 2-APB induces apoptosis. HeLa cells were exposed to 2-APB (100 µM) for 1 h, then exposed to apogossypol (20 µM) for 1 h and finally exposed to A-1210477 (10 µM) and A-1331852 (0.1 µM) for 4 h. After treatment, cells were assessed for apoptosis by PS externalisation. All experiments were independently performed three times. Error bars = Mean ± SEM. *** p ≤ 0.00.
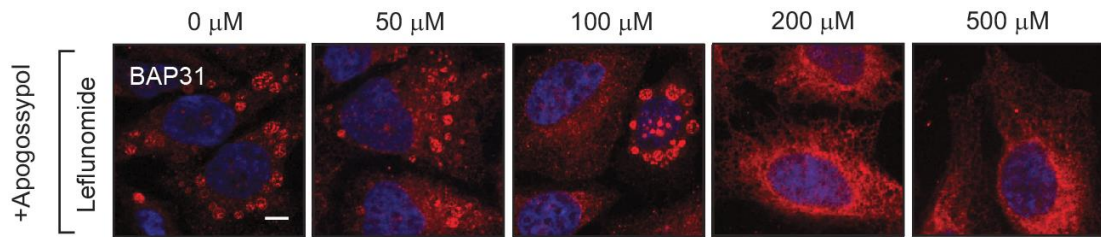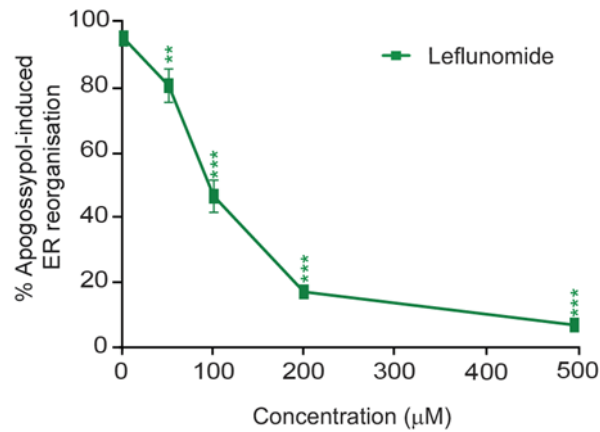
Figure 4.4 Leflunomide abolishes apogossypol-mediated ERMR. a) HeLa cells were exposed to indicated concentrations of leflunomide for 1 h and then exposed to apogossypol (20 μM) for 4 h. The cells were then immunostained for an ER tubule marker (BAP31). Scale bar: 10 μm. b) Quantification of ER membrane reorganisation was performed by counting around 100 cells from 3 independent experiments. Error bars = Mean ± SEM. ** $p \leq 0.005$, *** $p \leq 0.001$.
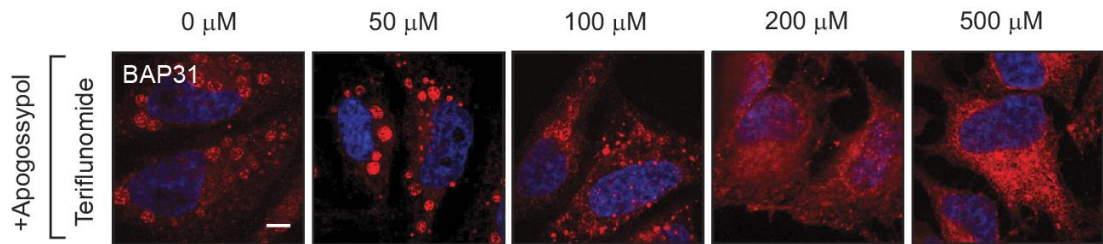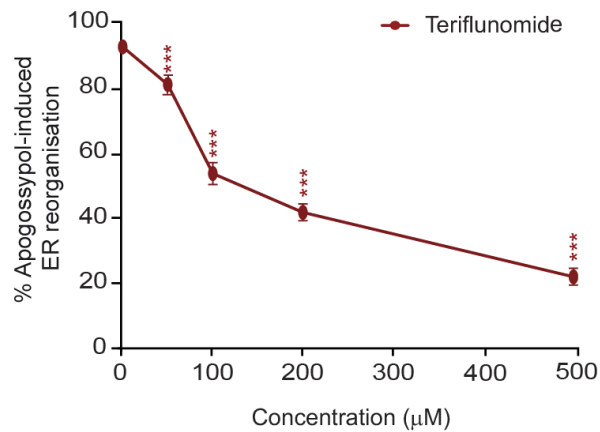
Figure 4.5 Teriflunomide reduces apogossypol-mediated ERMR. a) HeLa cells were exposed to indicated concentrations of teriflunomide for 1 h and then exposed to apogossypol (20 μM) for 4 h. The cells were then immunostained for an ER tubule marker (BAP31). Scale bar: 10 μm. b) Quantification of ER membrane reorganisation was performed by counting around 100 cells from 3 independent experiments. Error bars = Mean ± SEM. *** $p \leq 0.001$.

4.5. DHODH inhibitors alone does not change ER morphology

Although both leflunomide and teriflunomide abolished apogossypol-mediated ERMR, it was necessary to assess if these inhibitors altered ER morphology thus inducing ERMR on their own. In both untreated (DMSO) and treated cells, increasing concentrations of leflunomide and teriflunomide did not result in any marked changes to ER morphology (Figure 4.6).

4.6. DHODH inhibitors induce the UPR in a concentration-and time-dependent manner

It has been reported that DHODH inhibitors induce canonical ER stress and the UPR[79,205]. The UPR is an adaptive response signalling pathway regulated *via* three different stress sensors including inositol-requiring enzyme 1 (IRE1), activating transcription factor 6 (ATF6) and protein kinase RNA-like ER kinase (PERK). Upon ER stress, BiP dissociates from these stress sensors and these eventually activate the adaptive UPR signalling to maintain ER homeostasis. Prolonged ER stress is unable to maintain such ER homeostasis, and as a result, induces apoptosis *via* upregulation of CHOP (CCAAT/enhancer-binding protein homologous protein; a transcription factor)[5,79,163,206]. Since both BiP and CHOP play important roles in ER stress signalling, these are widely used as ER stress markers[79]. Chemical agents like tunicamycin (TU), induce extensive ER stress and as a result are commonly used as positive controls to induce ER stress[197,207,208]. To check whether DHODH inhibitors induce ER stress and the UPR, cells were exposed to increased concentrations of both teriflunomide and leflunomide and protein levels of BiP and CHOP assessed by western blotting. At concentrations higher than 200 µM, teriflunomide induces upregulation of both BiP and CHOP (Figure 4.7 a). Upregulation of BiP was not too edvident in cells exposed to leflunomide, but a drastic increase in CHOP levels were observed at concentrations as low as 50 µM (Figure 4.7 a). Induction of CHOP but not BiP were observed when cells were exposed to leflunomide (200 µM), as early as 4 h (Figure 4.7 b). However, this was not evident in cells exposed to this concentration (200 µM) of teriflunomide even after prolonged exposure (24 h) (Figure 4.7 b).
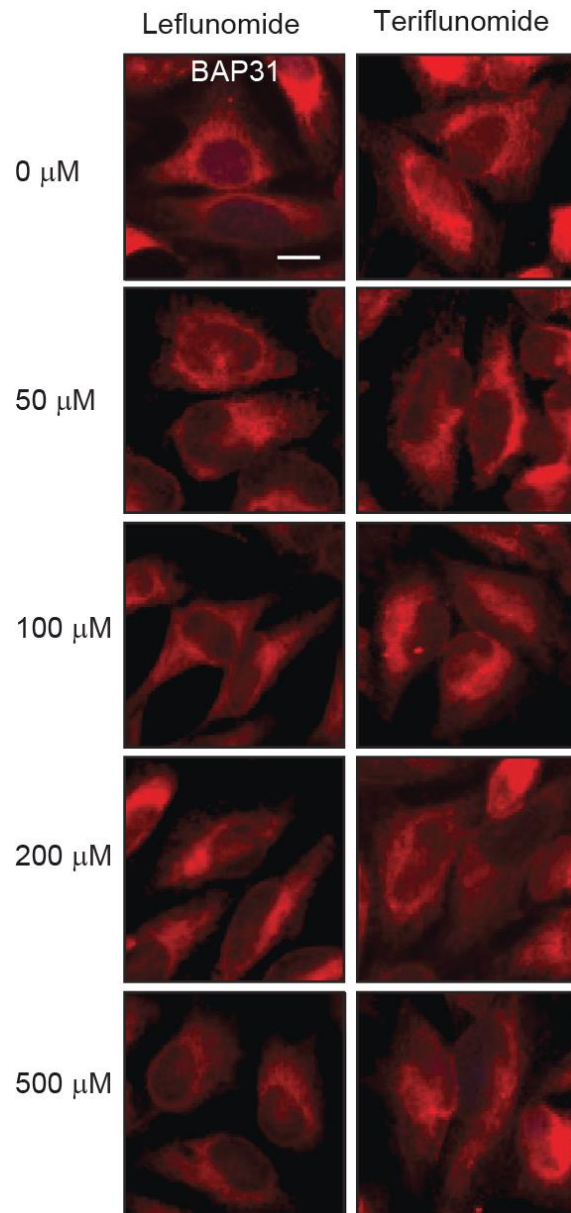
Figure 4.6. Teriflunomide and leflunomide compounds alone do not induce ER membrane reorganisation. HeLa cells were exposed with indicated concentration of DHODH inhibitors including teriflunomide or leflunomide for 1 h then treated with apogossypol (20 μM) for 4 h. The cells were then immunostained for ER tubule marker BAP31. All experiments were independently performed three times. Scale bar: 5 μm.
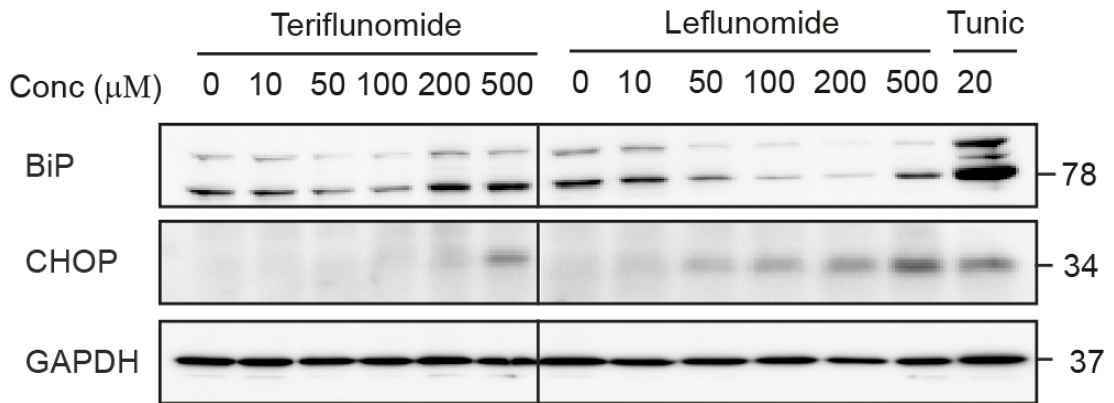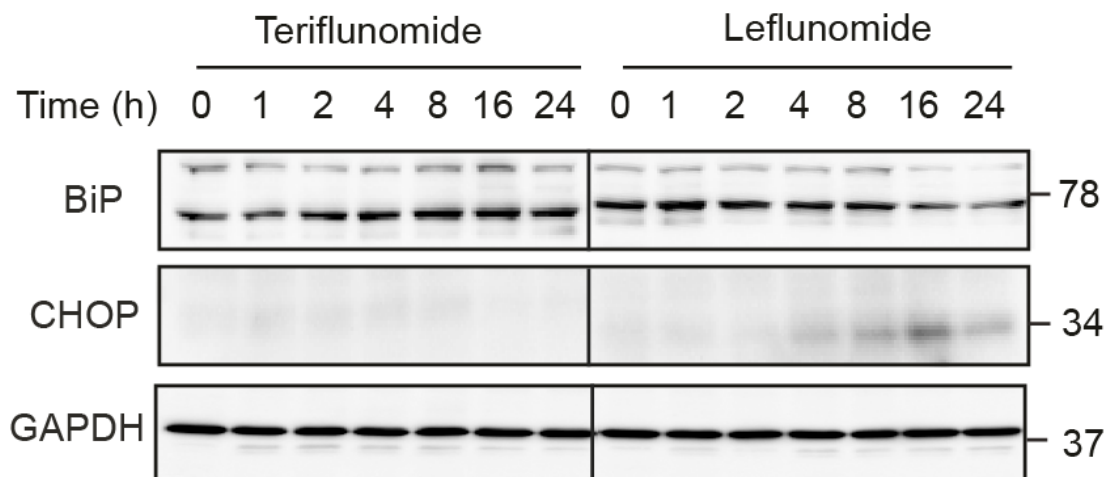
Figure 4.7 Teriflunomide and leflunomide induces UPR in a concentration- and time-dependent manner. a) HeLa cells were exposed to indicated concentrations of teriflunomide and leflunomide for 24 h or b) to fixed concentrations of teriflunomide (200 µM) or leflunomide (200 µM) for the indicated times. After treatment, cells were lysed and subjected to western blot analysis using the indicated antibodies. Conc= concentration; Tunic= tunicamycin.

4.7. DHODH inhibitors trigger apoptosis in a concentration and time-dependent manner

To evaluate whether DHODH inhibitors induce apoptosis, cells were exposed to increasing concentration of inhibitors for 24 and 48 h. Both DHODH inhibitors induced apoptosis in a concentration- and time-dependent manner (Figure 4.8).
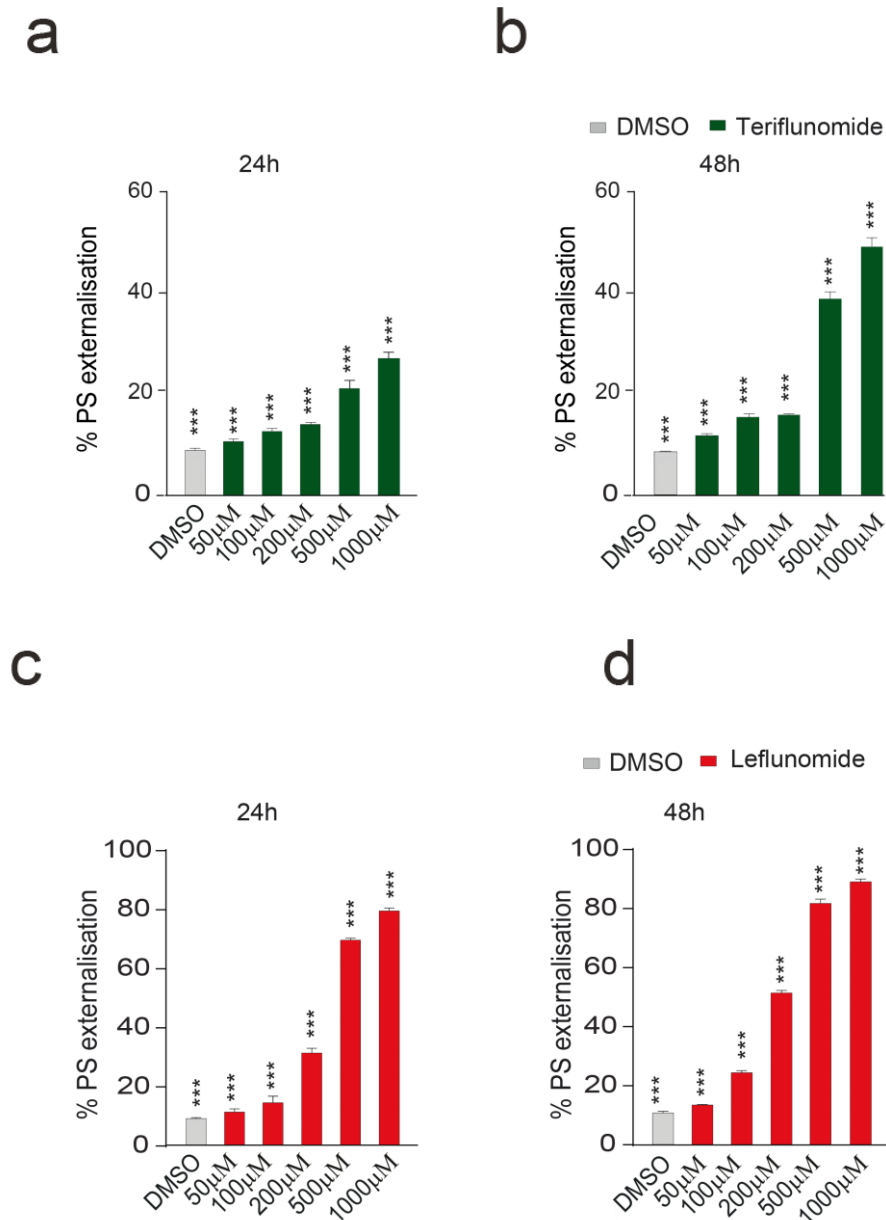
Figure 4.8 DHODH inhibitors induce apotosis in a concentration- and time-dependent manner. HeLa cells were treated with indicated concentrations of DHODH inhibitors for (a and c) 24 h and (b and d) 48 h and assessed for PS externalisation. All experiments were independently performed three times. Error bars = Mean ± SEM. *** $p \leq 0.001$.

4.8. DHODH does not play crucial role in apogossypol-mediated-ERMR

Several studies suggest that leflunomide and teriflunomide modulate *de novo* pyrimidine biosynthesis *via* inhibition of the DHODH enzyme[127,128,137]. To confirm that leflunomide and teriflunomide abolish apogossypol-mediated ERMR by inhibiting DHODH, cells were transiently transfected with two different DHODH siRNAs and then treated with apogossypol. Results showed that silencing the expression levels of DHODH did not affect apogossypol-mediated ERMR (Figure 4.9a). In addition, quantification was performed by counting around 100 cells from 3 independent experiments (Figure 4.9b). The knockdown efficiency of DHODH siRNAs was verified by western blotting from 3 independent experiments (Figure 4.9c). DHODH protein expression levels were marginally reduced following DHODH siRNAs, which was evident from the densitometry analysis that showed that, ~ 40% of DHODH protein expression was reduced following different siRNAs (Figure 4.9d). However, despite this reduction in expression levels, apogossypol-mediated ERMR was not altered, thus suggesting that DHODH might not directly be regulating ERMR.
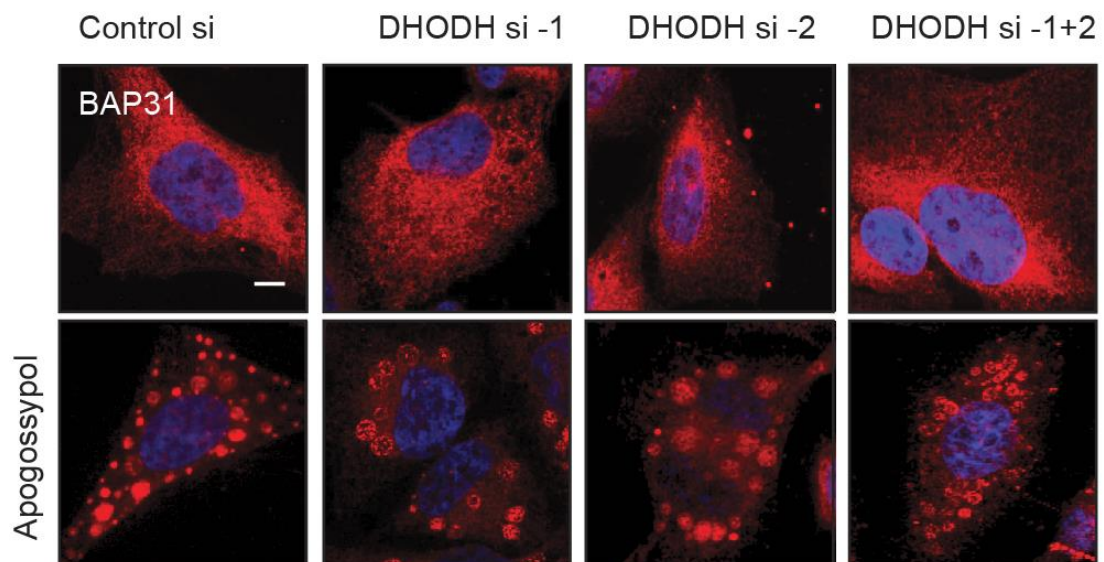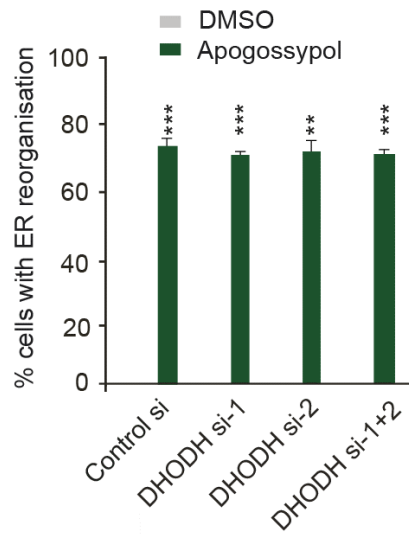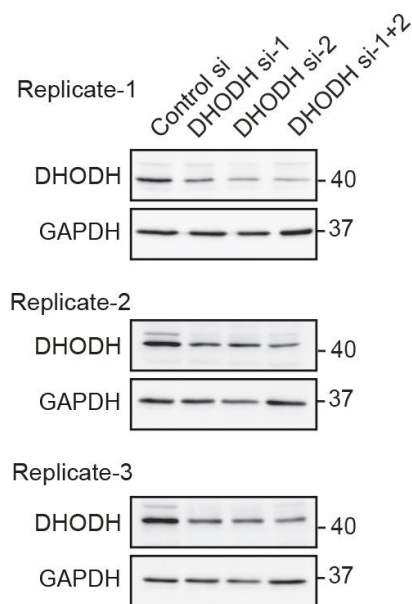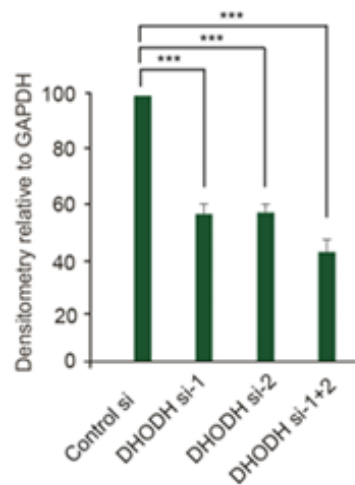
Figure 4.9 DHODH does not play a crucial role in regulating apogossypol-mediated ERMR. a) HeLa cells were transiently transfected with either control siRNA or two different DHODH siRNAs and then exposed to apogossypol (20 μM) for 4 h. The cells were then immunostained with an ER tubule marker (BAP31). Scale bar 10 μm. b) Quantification of ER membrane reorganisation was performed by counting around 100 cells from 3 independent experiments. c) Knockdown efficiency was tested using western blotting. d) Densitometric quantification of DHODH protein versus GAPDH. Error bars = Mean ± SEM. ** $p \leq 0.005$, *** $p \leq 0.001$.

4.9. Metabolic supplementation of orotate or uridine does not alter apogossypol-mediated ERMR

Although the genetic downregulation of DHODH failed to prevent apogossypol-mediated ERMR, it is possible that the residual DHODH (owing to inefficient knockdowns) may still be responsible for the lack of prevention. Therefore, to convincingly rule out an involvement of DHODH in this process, intermediates of pyrimidine synthesis, such as orotate and uridine[123–125] were utilised in the experiments. Orotate is the product of DHODH and orotate is further converted to urdine/ UMP in the presence of UMP synthetase. Cells exposed to orotate or uridine, in the presence of teriflunomide and leflunomide as well as apogossypol still resulted in a significant block in apogossypol-mediated ERMR, which was unaffected by orotate or uridine supplementation (Figures 4.10 and 4.11). Together, these results strongly suggested that teriflunomide and leflunomide mediated anti-ERMR effect most likely *via* a DHODH-independent manner.

4.10. Teriflunomide restores apoptosis antagonised by ERMR

Since, apogossypol prevented BH3 mimetic-mediated apoptosis and teriflunomide prevented apogossypol-mediated ERMR, it is possible that teriflunomide could antagonise the anti-apoptotic effect of ERMR. To test this, cells were exposed to teriflunomide (200 μM) for 1 h and then exposed to apogossypol (20 μM) for 1 h. Finally, cells were exposed to a combination of A-1210477 (10 μM) and A-1331852 (0.1 μM) for 4 h and apoptosis assessed by PS externalisation by flow cytometry. Cells pre-exposed to teriflunomide reversed the anti-apoptotic effects of apogossypol-mediated ERMR on BH3 mimetic-mediated apoptosis (Figure 4.12). In cells exposed to BH3 mimetics, PARP, caspases-9, caspase-3 and caspase-7 were processed (Figure 4.12). Apogossypol prevented this activation, which was efficiently reversed when cells were exposed to teriflunomide (Figure 4.13).
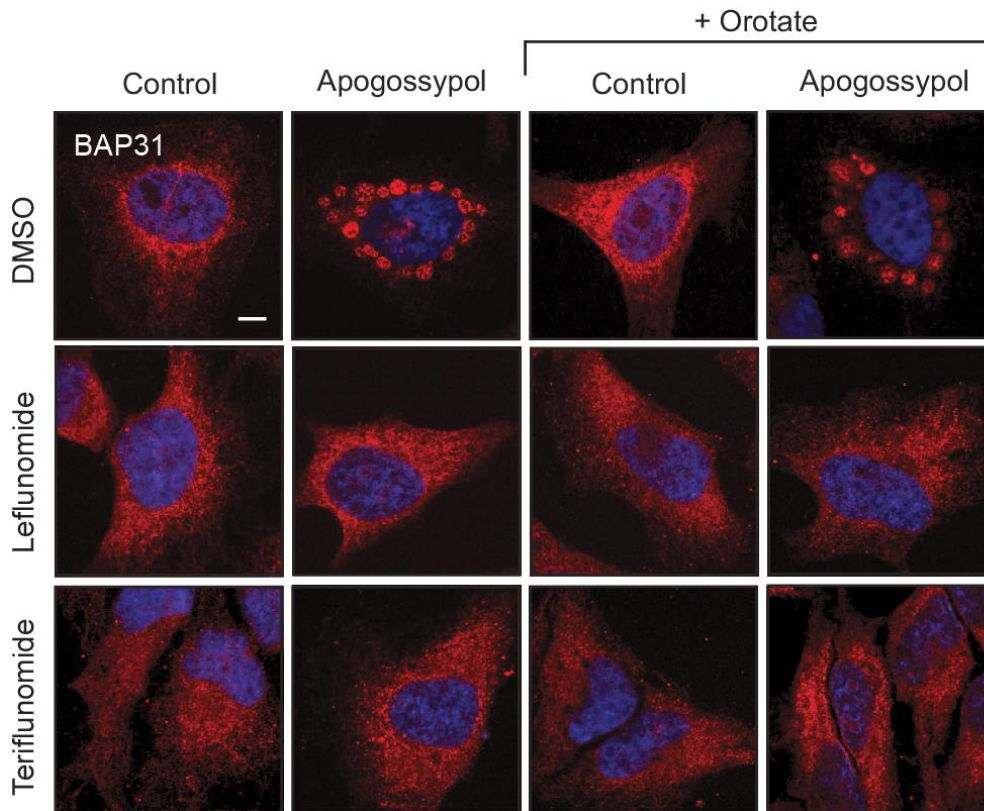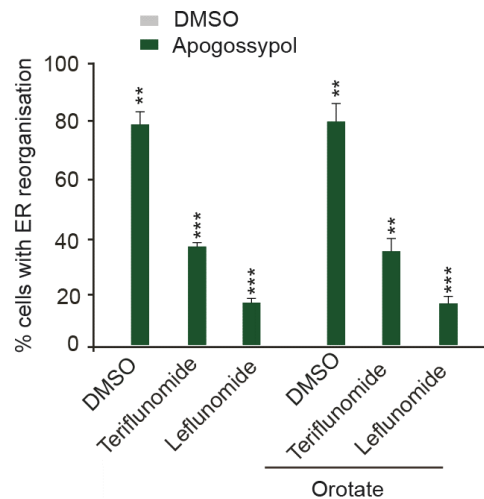
Figure 4.10 Orotate does not alter apogossypol-mediated ERMR. a) HeLa cells were exposed to orotate (1 mM) for 1 h and treated with leflunomide (200 μM) or teriflunomide (200 μM) for 1 h. After treatment, cells were exposed to apogossypol (20 μM) for 4 h. The cells were then immunostained for an ER tubule marker (BAP31). All experiments were independently performed three times. Scale bar: 10 μm. b) Quantification of ERMR was performed by counting around 100 cells from 3 independent experiments. Error bars = Mean ± SEM. ** $p \leq 0.005$, *** $p \leq 0.001$.
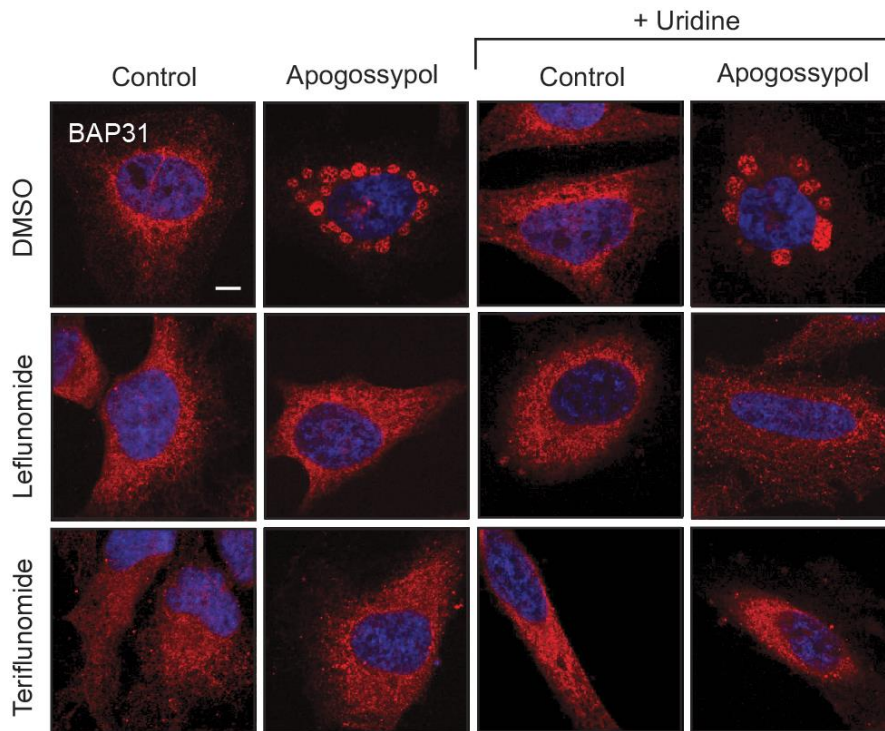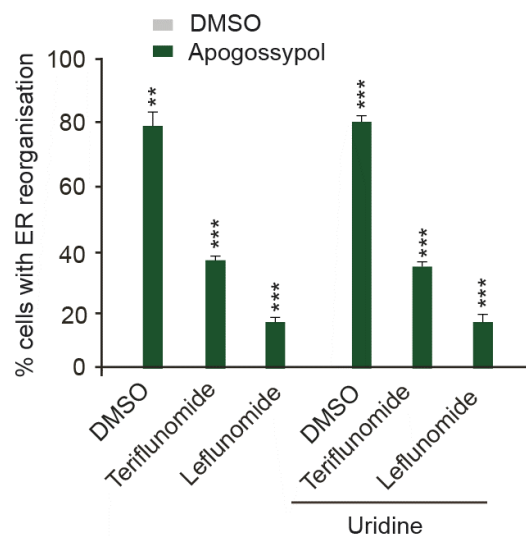
Figure 4.11 Uridine does not alter apogossypol-mediated ERMR. a) HeLa cells were exposed to uridine (1 mM) for 1h and then treated with leflunomide (200 μM) or teriflunomide (200 μM) for 1 h. After that, cells were exposed to apogossypol (20 μM) for 4 h. The cells were then immunostained for an ER tubule marker (BAP31). All experiments were independently performed three times. Scale bar: 10 μm. b) Quantification of ERMR was performed by counting around 100 cells from 3 independent experiments. Error bars = Mean ± SEM. ** $p \leq 0.005$, *** $p \leq 0.001$.

a

DMSO | Apogossypol | Teriflunomide | Teriflunomide + Apogossypol

DMSO

A-1331852 +A-1210477

b

■ DMSO
■ A-1331852+A-1210477

***

% PS externalisation

DMSO   Apogossypol   DMSO   Apogossypol
DMSO   Teriflunomide
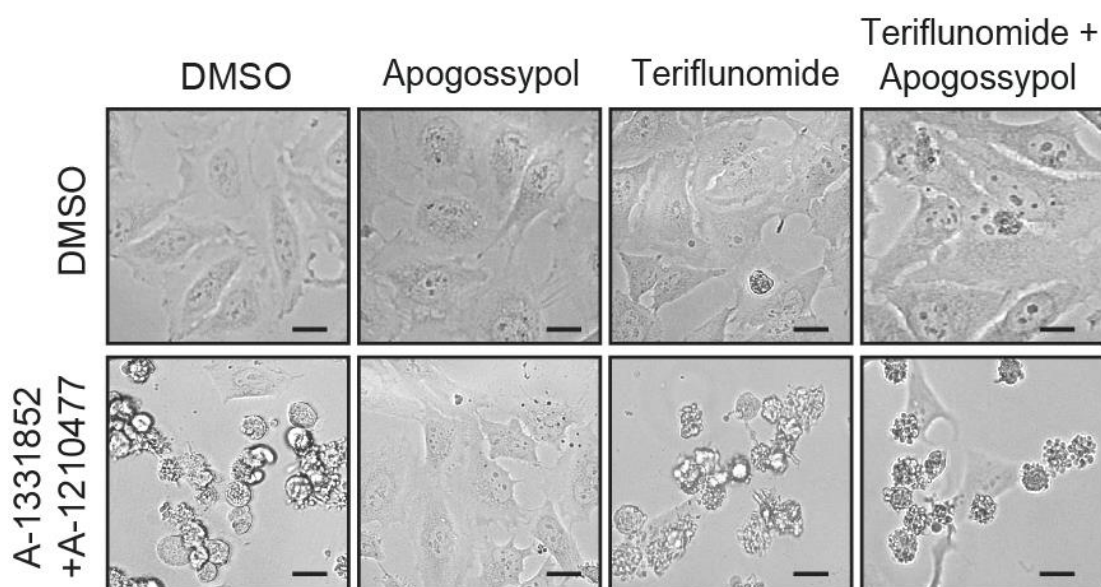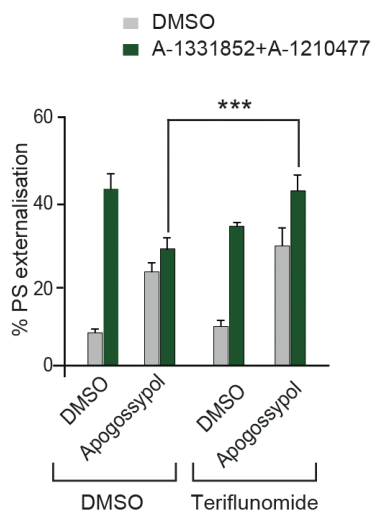
Figure 4.12 Teriflunomide restores apoptosis antagonised by ERMR. HeLa cells were exposed to teriflunomide (200 μM) for 1 h and then treated with apogossypol (20 μM) for 1 h. After treatment, cells were exposed to A-1210477 (10 μM) and A-1331852 (0.1 μM) for 4 h. a) Images were acquired using FLoid® cell imaging station. Scale bar: 2 μm. b) Following treatment, cells were stained with annexin V and PI, and the extent of apoptosis was measured by flow cytometry. All experiments were independently performed three times. Error bars = Mean ± SEM. *** $p \leq 0.001$.
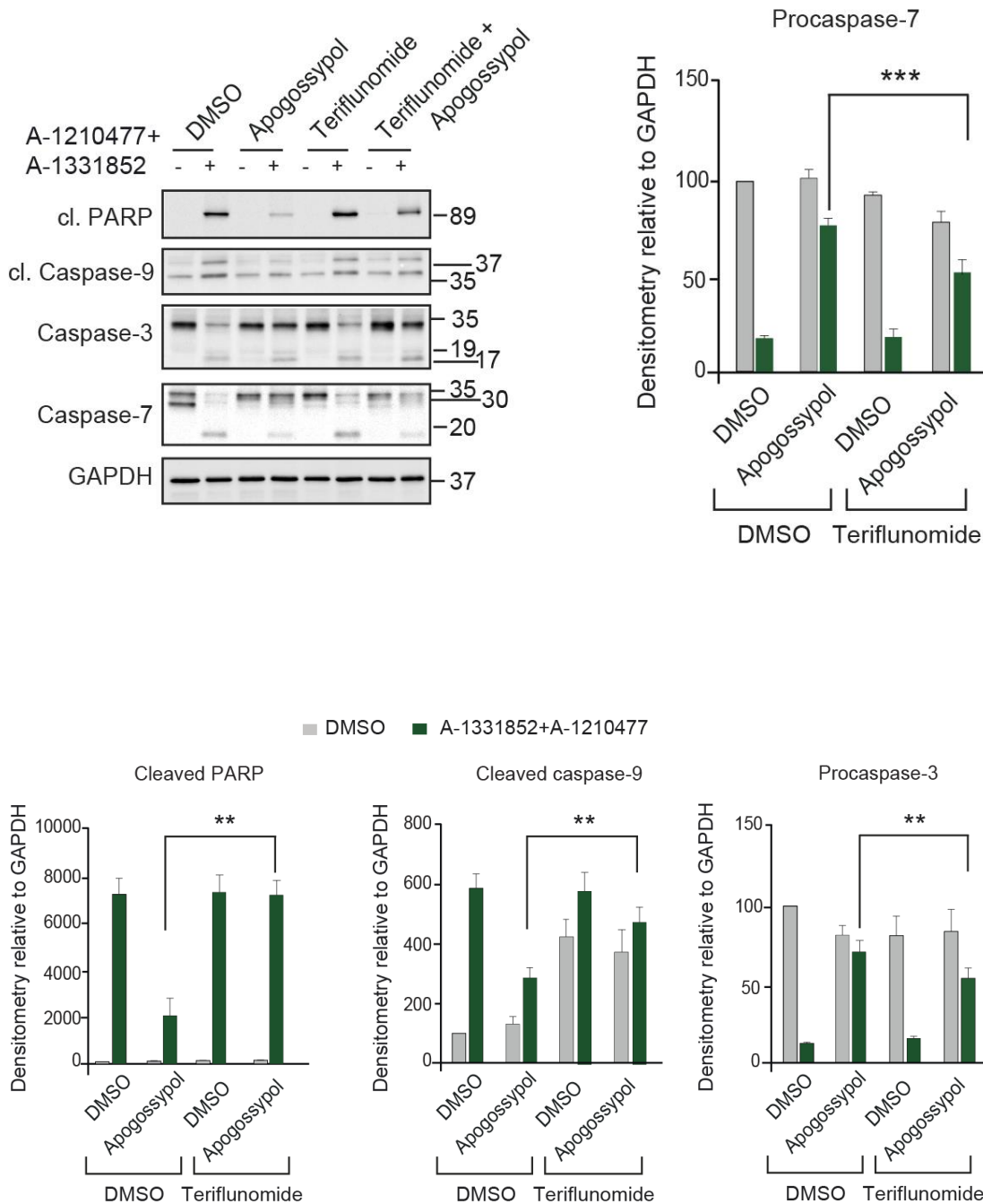
Figure 4.13 Teriflunomide restores apoptosis antagonised by ERMR. HeLa cells were exposed to teriflunomide (200 μM) for 1 h and then treated with apogossypol (20 μM) for 1 h. After treatment, cells were exposed to A-1210477 (10 μM) and A-1331852 (0.1 μM) for 4 h. Following treatment, cells were lysed and subjected to western blot analysis using the indicated antibodies. All experiments were independently performed three times. Densitometric quantification of indicated proteins versus GAPDH. Error bars = Mean ± SEM. ** $p \leq 0.005$, *** $p \leq 0.001$.

4.11. Discussion

Data from the first results chapter demonstrated that apogossypol-mediated ERMR played a regulatory role in mitochondrial fission and apoptosis (Chapter 3). To ensure that the protective effects are due to ERMR and not due to a non-specific effect of apogossypol, modulators of ERMR were used in this chapter to study their roles in BH3 mimetic-mediated apoptosis.

Since 2-APB (SOCE inhibitor) extensively prevented apogossypol-mediated ERMR[11], experiments were performed to assess their effects on apoptosis. However, at concentrations enough to antagonise ERMR, 2-APB was toxic to the cells. This could be because 2-APB is not a specific inhibitor of SOCE. It must be noted that 2-APB has been shown to modulate calcium signalling even at lower concentrations (10-20 µM). Therefore, toxicity associated with a high concentration of 2-APB is most likely due to its non-specific effects that are largely independent of SOCE. This is further strengthened by previous reports in which, silencing the expression levels of SOCE regulators, such as STIM1, ORAI1 and ORAI3 had no effect on apogossypol-mediated ERMR[90]. It has been reported that 2-APB can modulate inositol 1,4,5-trisphosphate (IP_3) channels[209,210]. They are ER calcium efflux channels located on ER membranes and they help in maintaining ER homeostasis[52]. Silencing all three isoforms of IP_3 receptors does not alter apogossypol-mediated ERMR, suggesting that these receptors are not the primary site of action for 2-APB.

Although the current data argues for a SOCE-independent role for 2-APB in antagonising ERMR, two other SOCE modulators, teriflunomide and leflunomide were able to prevent apogossypol-mediated ERMR in a concentration-dependent manner (Figure 4.4 and 4.5). In addition, these agents do not alter ER structure, when used as single agents (Figure 4.6). These findings suggest that teriflunomide and leflunomide alter ERMR without perturbing normal ER morphology. Leflunomide was more potent than teriflunomide in preventing apogossypol-mediated ERMR (Figure 4.4 and 4.5). This was surprising because leflunomide is a pro-drug that gets converted to its active metabolite, teriflunomide[128,143]. Subsequently, teriflunomide can potently inhibit the activity of DHODH. So, for a more potent DHODH inhibitor to have a lesser effect on preventing ERMR, it must mean that the activity of

leflunomide was most likely independent of its ability to inhibit DHODH or toxicity associated with these inhibitors might be preventing ERMR.

DHODH inhibitors have been shown to induce canonical ER stress and the UPR[79,205], which could be confirmed in the current chapter (Figure 4.7). In addition, DHDOH inhibitor exposed cells induces canonical ER stress and UPR at later time points (more than 12 h required) and at higher concentration (more than 500 µM required). Since DHODH inhibitors prevented apogossypol-mediated ERMR within 4 h, at 200 µM concentration suggested that these DHODH mediated anti-ERMR effect regulated independent of UPR.

To assess the function of DHODH in ERMR regulation, DHODH protein levels were reduced following DHODH siRNAs, which failed to modulate apogossypol-mediated ERMR (Figure 4.9). This suggested that DHODH had no role to play in ERMR. However, densitometry analysis of the siRNA blots showed that only ~ 40% of DHODH protein expression was reduced following the different siRNAs. Therefore, it is premature to exclude a role for DHODH in the regulation of ERMR. Further studies aimed at a complete knockdown of DHDOH, possibly using CRISPR (clustered regularly interspaced short palindromic repeats), could offer more insights into this phenomenon. However, DHODH plays a vital role in cell survival, complete silencing of DHODH will certainly be toxic to the cells. DHODH catalyses the fourth step in the *de novo* pyrimidine biosynthesis converting dihydroorotate to orotate, which eventually forms uridine mono phosphate (UMP)[123,125]. Metabolic supplementation of cells with orotate or uridine must thus overcome the effect of DHODH inhibition. The results presented in this chapter demonstrate that neither orotate nor uridine supplementation altered apogossypol-mediated ERMR suggesting that teriflunomide/leflunomide-mediated anti-ERMR effect might be independent of DHODH. The appropriate concentrations of orotate and uridine were determined by an independent experiment that will be discussed later in this thesis in chapter 6.

The major findings from this chapter include the reversal of the anti-apoptotic effects of ERMR by teriflunomide and leflunomide, which appear to exert their effects in a DHODH independent manner (Figure 4.12 and 4.14). Having established a novel role for DHODH inhibitors in membrane dynamics, the next chapter will focus on assessing the therapeutic potential of DHODH in cancer.
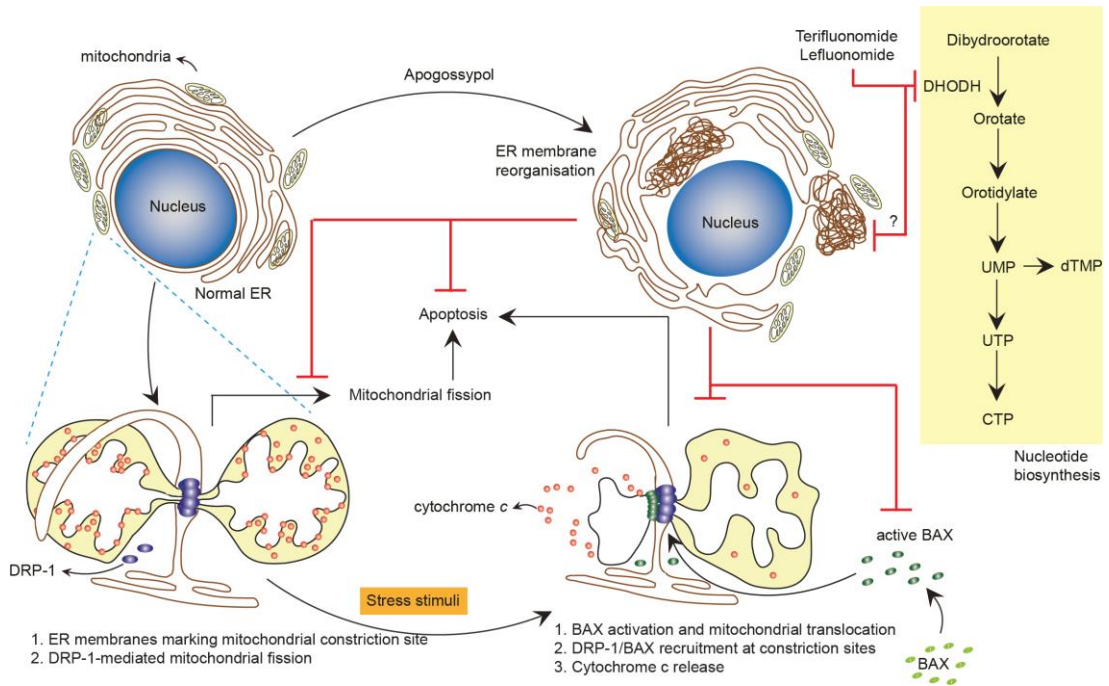
Figure 4.14 Schematic representation of the mitochondrial changes regulated by ERMR. Apogosspypol-mediated ERMR antagonises BH3 mimetic-mediated apoptosis at the level of mitochondrial fission and BAX translocation. Inhibitors of DHODH, teriflunomide and leflunomide, prevent apogossypol-mediated ERMR *via* an unknown mechanism that is independent of DHODH enzyme activity. By antagonising apogossypol-mediated ERMR, teriflunomide also reverts the anti-apoptotic effects of apogossypol.

Chapter 5

DHODH is highly expressed and a potential target in head and neck squamous cell carcinoma

Contents

5.1. Background

DHODH inhibitors play a critical role in the regulation of ER membrane dynamics[211], which appears to regulate mitochondrial fission and apoptosis (Chapter 4). In addition, growing evidence suggests that DHODH inhibitors act as tools for cancer therapy[126,128,132]. These drugs are under investigation for the treatment of acute myeloid leukemia (AML), triple-negative breast cancer (TNBC) therapy, prostate cancer, colon cancer and oral squamous cell carcinoma[212–214]. DHODH is an important enzyme in the *de novo* pyrimidine biosynthesis pathway. It is responsible for converting dihydroorotate to orotate, which eventually converts to uridine monophosphate (UMP) in presence of UMP synthetase[125,127].

Head and neck squamous cell carcinoma (HNSCC) is one of the most common cancer types worldwide[215–219], including the United Kingdom (UK). The incidence of HNSCC in Liverpool is four times the national average[215–217]. HNSCC is often detected in different head and neck regions, including oral cavity (OC), larynx (LX), oropharynx (OP) and hypopharynx (HP)[215]. HNSCC malignancy is highly associated with different risk factors, including tobacco usage and alcohol consumption[215]. Currently, HNSCC is treated either with surgery, radiation or chemotherapy[218,219]. A combination therapy, involving surgery, followed by radiation therapy or chemotherapy is commonly used. Although the current therapies are promising, many patients are prone to develop tumour recurrence and distant metastasis[215]. In addition, these therapeutics frequently cause changes in speech, swallowing, which eventually affects the patient's quality of life and ability to function in society[219]. Therefore, there is a need for improved therapies. Since DHODH inhibitors act as antitumor agents in several cancers, DHODH could be potential candidate for HNSCC therapy.

DHODH is chemically inhibited by several agents, including brequinar, leflunomide, teriflunomide, Bayer (BAY2402234) and ASLAN003 (Figure 5.2)[127,129,137,138]. Brequinar was developed in the mid 1980's and tested in a number of cancers, including head and neck cancer[137,142]. Reports suggested that brequinar has not shown significant effect on early phase clinical trials of head and neck[141,142], breast[212] and ovarian cancer[214]. Leflunomide (Arava) was later designed against DHODH for treating rheumatoid arthritis and this drug successfully gained FDA

approval in 1999[145,146,220]. Several findings report that leflunomide has a short half-life and its treatment often causes severe liver toxicity within 6 months[143]. Due to liver toxicity and weak potency, leflunomide was structurally modified to obtain teriflunomide[146]. Teriflunomide is the active derivative of leflunomide and the only difference between these two drugs is the opening of the isoxazole ring (Figure 5.1). Upon oral administration, the isoxazole ring of leflunomide opens and teriflunomide is formed[146].
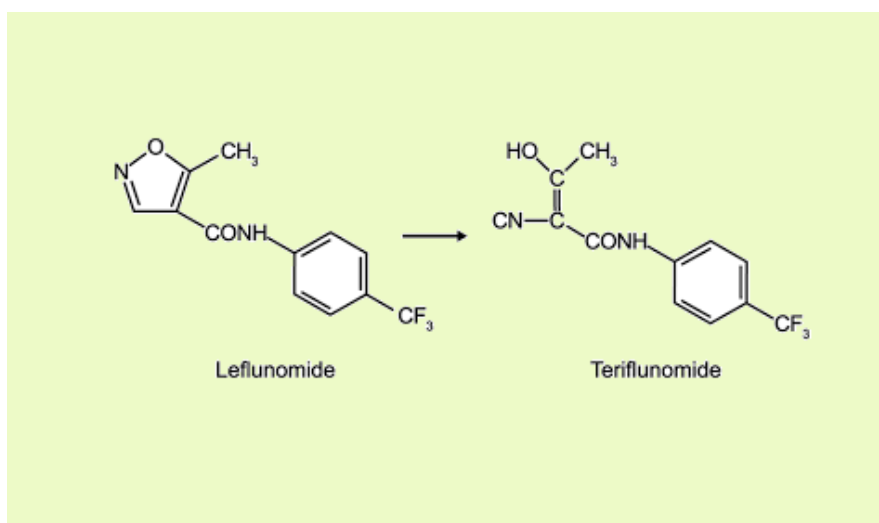
Figure 5.1. chemical structures and conversion of leflunomide to teriflunomide.

Teriflunomide was successfully investigated in clinical trials and received FDA approval in 2012. Since teriflunomide is actively used as a therapeutic agent for treating different cancers, it is used as the primary investigation tool for this study.

The specific questions that will be addressed in this chapter are as follows:

(1) Do the genetic and chemical inhibition of DHODH alter HNSCC cell survival?
(2) Could the pyrimidine intermediates control DHODH-mediated survival effect?
(3) Do DHODH inhibitors demonstrate synergy with current chemotherapeutic agents?
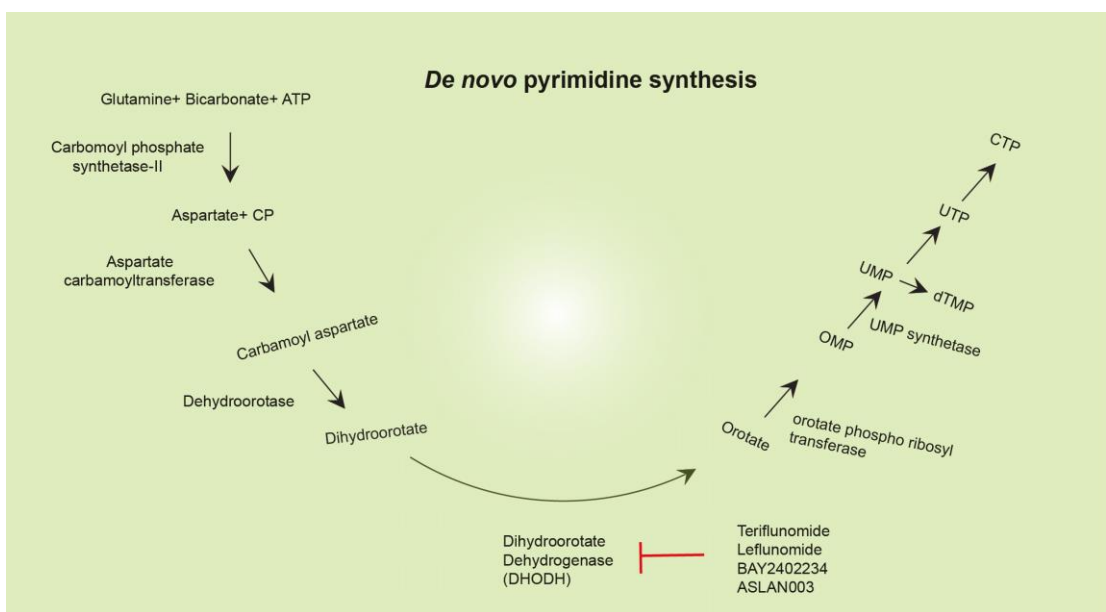
Figure 5.2. Schematic representation of *de novo* pyrimidine biosynthesis. The red line indicates inhibition.

5.2.   DHODH expression in several HNSCC cells.

Since DHODH plays an essential role in ERMR and *de novo* pyrimidine synthesis, it is possible that DHODH may regulate cancer cell survival. To understand the role of DHODH in HNSCC, western blot analysis was performed to check DHODH levels in several HNSCC cell lines. For this, whole cell lysates of UMSCC-1 (derived from oral cavity), UMSCC-11B (derived from larynx), UMSCC-81B (derived from oropharynx) and FaDu (derived from hypopharynx) were collected and subjected to western blot using DHODH antibody. The results indicate that DHODH is highly expressed in several HNSCC cells (Figure 5.3). Since it is highly expressed in several HNSCC cells, DHODH may be useful as a therapeutic target in HNSCC.
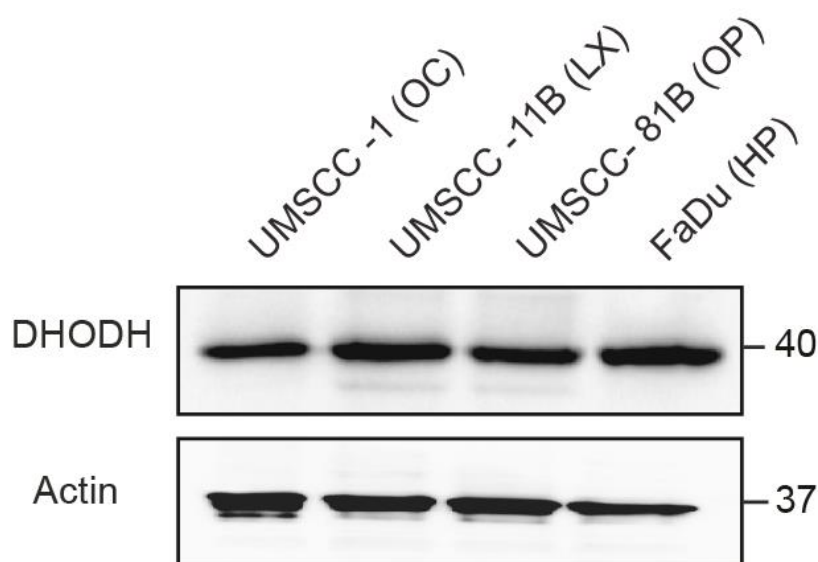
Figure 5.3. DHODH is highly expressed in different HNSCC cells. The indicated cell lines were lysed and subjected to western blot analysis using the DHODH antibody. All experiments were independently performed three times.

5.3. DHODH expression is critical for the clonogenic survival of cell lines derived from oral cavity and larynx

To assess if DHODH expression is important for HNSCC cell survival, cell lines derived from oral cavity and larynx were transiently transfected with either control siRNA or two different DHODH siRNAs, and clonogenic assay was performed. The results of this assay revealed that the colony numbers and sizes were largely reduced upon silencing of DHODH (Figure 5.4), suggesting that DHODH expression is essential for clonogenic survival in these cancer cells.
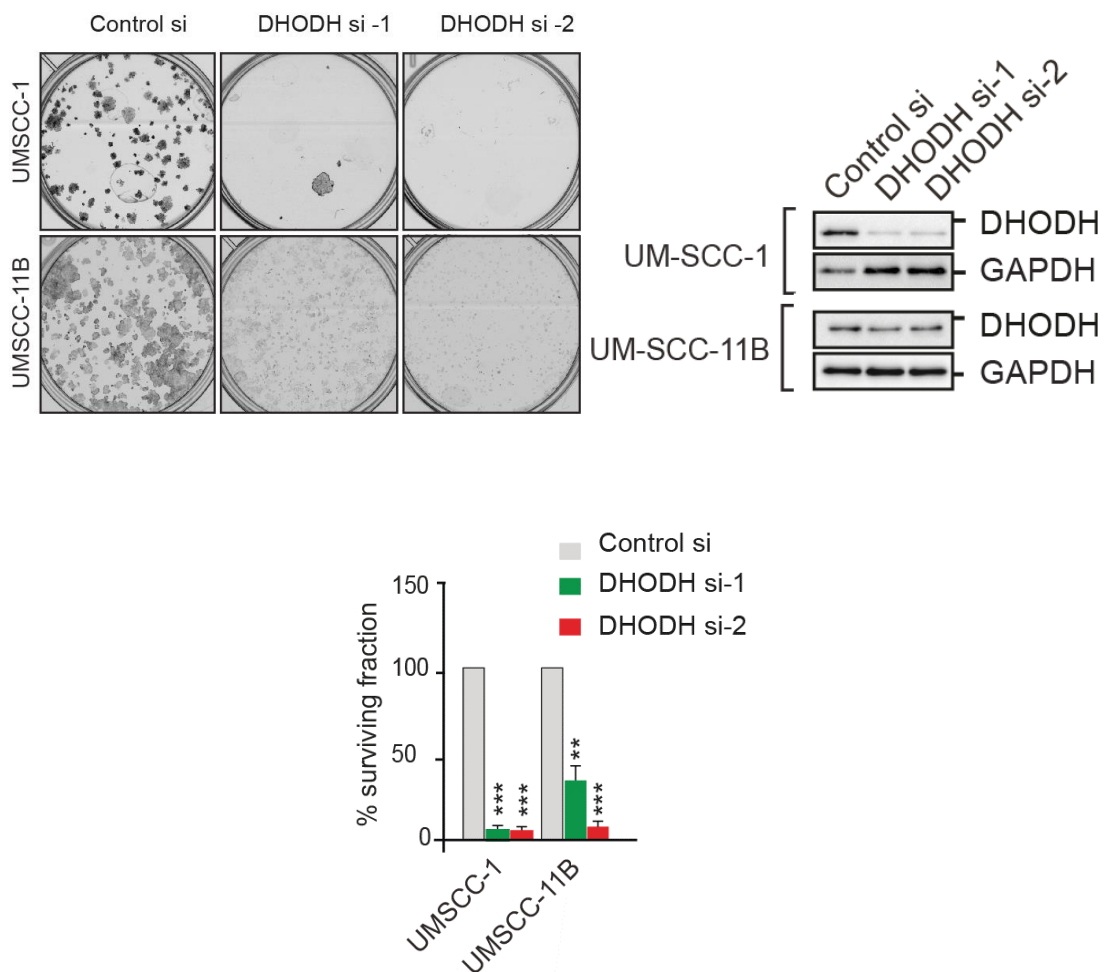
Figure 5.4. DHODH expression is critical for clonogenic survival of cell lines derived from the oral cavity and larynx. UMSCC-1 or UMSCC-11B cells were transiently transfected with either control siRNA or two different DHODH siRNAs. Colonies were grown for ~ 7 days, stained with crystal violet and counted using an automated colony counter. The images represent colony formation assay of indicated cell lines. The graph represents surviving fraction of cells in the colony formation assay. Blots represent knockdown efficiency of siRNAs. All experiments were independently performed three times. Error bars = Mean ± SEM. ** $p \leq 0.005$, *** $p \leq 0.001$

5.4. DHODH expression is critical for the clonogenic survival of cell lines derived from oropharynx and hypopharynx

Similarly, we examined the importance of DHODH for cell survival in other cancer cell lines by transiently transfecting cells, derived from oropharynx and hypopharynx, with either control siRNA or two different DHODH siRNAs and performing clonogenic assay. The results of this assay revealed that the colony numbers and sizes were largely reduced upon silencing of DHODH (Figure 5.5), suggesting that DHODH expression is essential for clonogenic survival in these cancer cells.
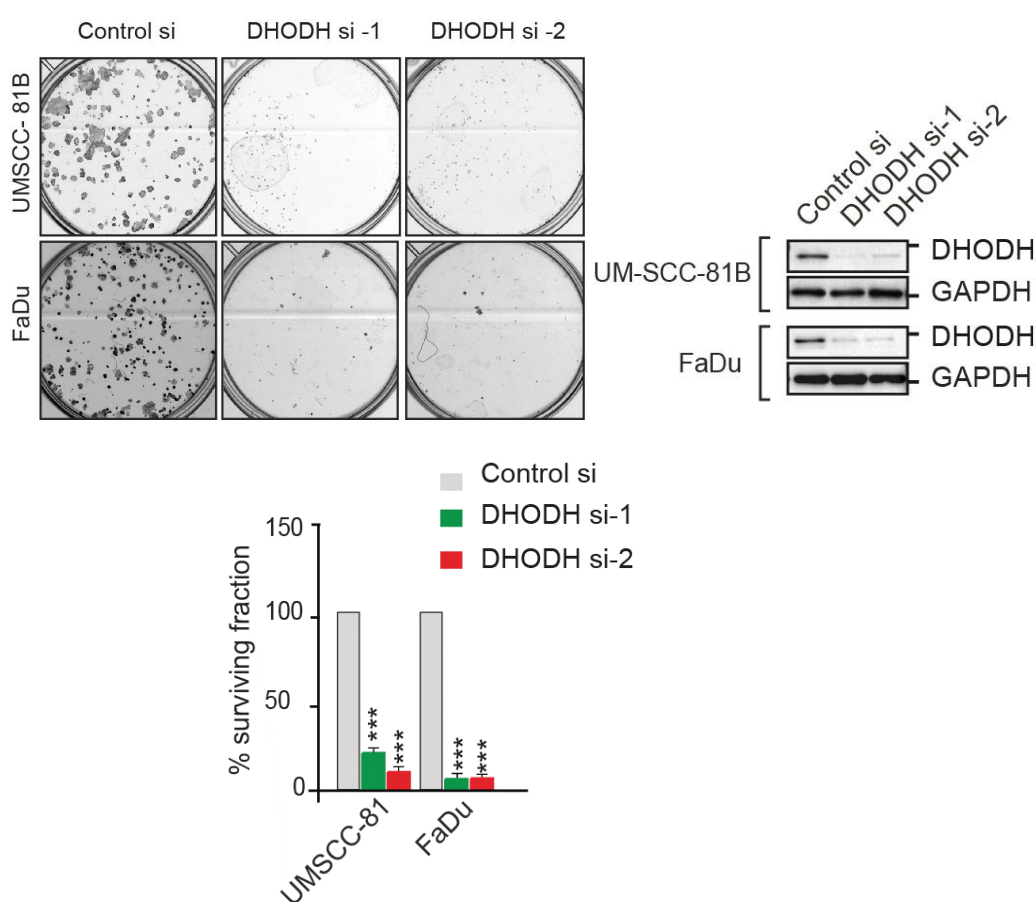
Figure 5.5. DHODH expression is critical for clonogenic survival of cell lines derived from the oropharnx and hypopharaynx. UMSCC-81B or FaDu cells were transiently transfected with either control siRNA or two different DHODH siRNAs. Colonies were grown for ~ 7 days, stained with crystal violet and counted using an automated colony counter. The images represent colony formation assay of indicated cell lines. The graph represents surviving fraction of cells in the colony formation assay. Blots represent knockdown efficiency of siRNAs. All experiments were independently performed three times. Error bars = Mean ± SEM. ** $p \leq 0.005$, *** $p \leq 0.001$

5.5. Teriflunomide significantly reduces clonogenic survival of cell lines derived from oral cavity and larynx

To assess if chemical inhibition of DHODH alters cell survival, cell lines derived from oral cavity and larynx were exposed to teriflunomide (10 μM and 20 μM) and clonogenic assay was performed. The results of this assay revealed that the colony numbers and sizes were largely reduced in a concentration dependent manner (Figure 5.6), suggesting that chemical inhibition of DHODH alters clonogenic survival in these cancer cells.
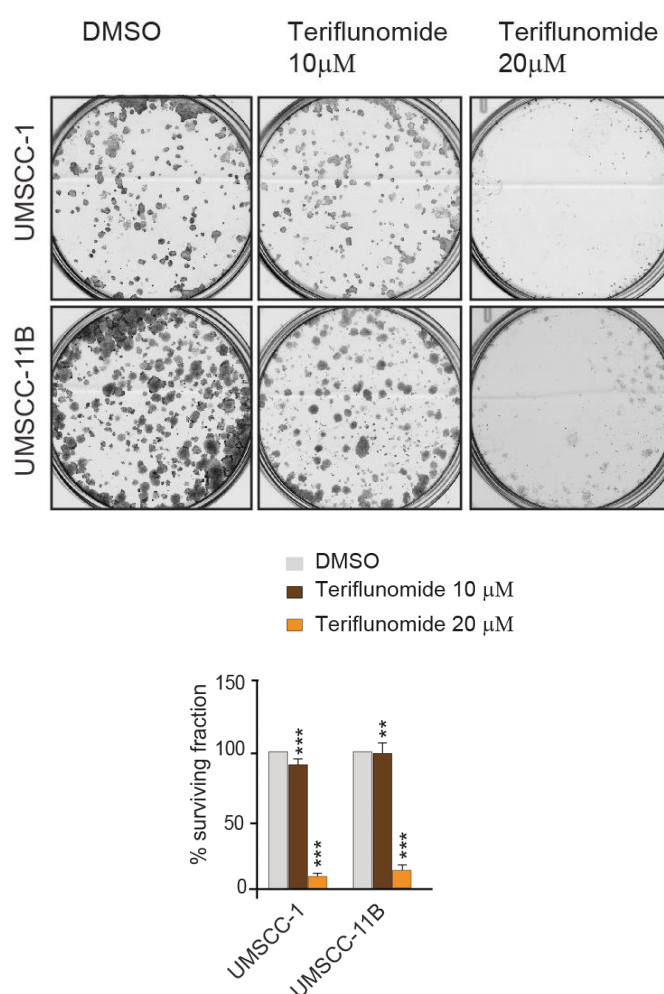
Figure 5.6. Teriflunomide reduces clonogenic survival of cell lines derived from the oral cavity and larynx. UMSCC-1 or UMSCC-11B cells were exposed to teriflunomide (10 μM and 20 μM). Colonies were grown for ~ 7 days, stained with crystal violet and counted using an automated colony counter. The images represent colony formation assay of indicated cell lines. The graph represents surviving fraction of cells in the colony formation assay. All experiments were independently performed three times. Error bars = Mean ± SEM. ** $p \leq 0.005$, *** $p \leq 0.001$.

5.6. Teriflunomide significantly reduces clonogenic survival of cell lines derived from oropharynx and hypopharynx

Similarly, the effect of teriflunomide was examined in other cancer cell lines derived from oropharynx and hypopharynx. Cells were exposed to teriflunomide (10 µM and 20 µM) and clonogenic assay was performed. The results of this assay revealed that the colony numbers and sizes were largely reduced upon teriflunomide exposure in oropharynx cells, but it does not affect the clonogenic survival of FaDu cells (Figure 5.7), suggesting that the chemical inhibition of DHODH exerts its effect only in oropharynx cancer cells.
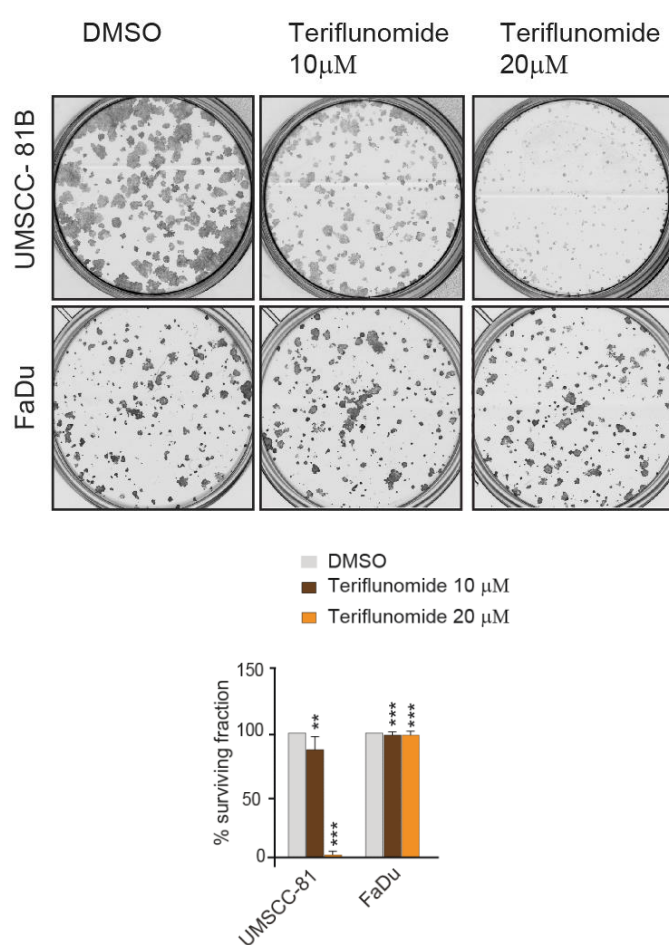
Figure 5.7. Teriflunomide exhibits varying effects on clonogenic survival of cell lines derived from the oropharnx and hypopharaynx. UMSCC-81B or FaDu cells were exposed to teriflunomide (10 µM and 20 µM). Colonies were grown for ~ 7 days, stained with crystal violet and counted using an automated colony counter. The images represent colony formation assay of indicated cell lines. The graph represents surviving fraction of cells in the colony formation assay. All experiments were independently performed three times. Error bars = Mean ± SEM. ** $p \leq 0.005$, *** $p \leq 0.001$

5.7.   Teriflunomide significantly reduces FaDu clonogenic survival

To assess the clonogenic survival ability of FaDu with teriflunomide. Cells were exposed to increasing concentrations of teriflunomide and clonogenic assay was performed. The results of this assay revealed that the FaDu clonogenic survival ability was reduced in a concentration dependent manner (Figure 5.8), suggesting that the FaDu cells needs higher concentration of teriflunomide. It has been reported that FaDu cells inherently associated with multi drug resistance[221], this could be the one of the reasons hypopharyngeal cancer difficult to treat with conventional chemotherapeutic agents. Further studies need to conduct to understand FaDu cells mediated multidrug resistance role in chemotherapy. However, given the absence of data on primary cells/ patient tissues, this theory is largely speculative.
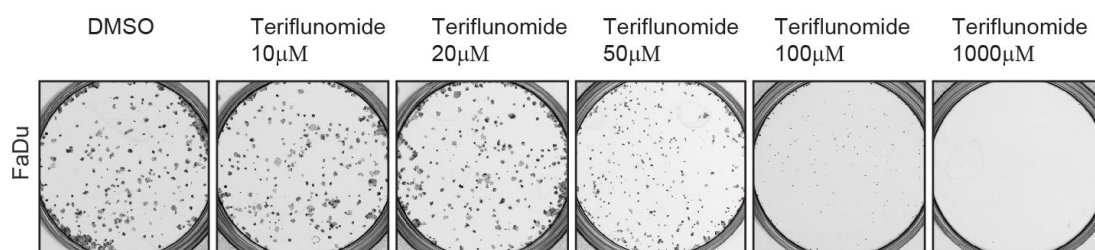
Figure 5.8. Teriflunomide reduces FaDu clonogenic survival in a concentration-deoendent manner. FaDu cells were exposed to indicated concentration of teriflunomide. Colonies were grown for ~ 7 days, stained with crystal violet and counted using an automated colony counter. The images represent colony formation assay of indicated cell lines. All experiments were independently performed three times.

5.8. Orotate supplementation rescues teriflunomide-mediated clonogenic cell survival in most HNSCC cell lines.

Since genetic and chemical inhibition of DHODH significantly alters clonogenic survival ability in several HNSCC, pyrimidine metabolism may be regulating teriflunomide-mediated cell death. It has been reported that orotate is the product of DHODH and orotate is further converted to uridine in the presence of UMP synthetase[126]. Hence it is possible that exogeneous metabolic supplementation of orotate and uridine may alter teriflunomide-mediated cell death. To assess if metabolic supplementation of orotate alters teriflunomide-mediated cell death in cell lines derived from oral cavity and larynx, cells were exposed to orotate (500 µM) and teriflunomide (20 µM) and then clonogenic assay was performed. The results of this assay revealed that teriflunomide-mediated decrease in colony counts was greatly reversed upon exogeneous supplementation of orotate (Figure 5.9), suggesting that orotate alters teriflunomide-mediated reduction in clonogenicity. Similarly, the effect of orotate in teriflunomide-mediated clonogenic cell death was examined in other cell lines derived from oropharynx and hypopharynx. Cells were exposed to orotate (500 µM) and teriflunomide (20 µM) then clonogenic assay was performed. The results of this assay revealed that the colony numbers and sizes were largely reduced upon teriflunomide exposure in oropharynx cells, but it does not affect the clonogenic survival of FaDu cells. In agreement with the findings from UM-SCC-1 and UM-SCC-11B, orotate supplementation reversed the effect of teriflunomide in UM-SCC-81B (Figure 5.9).

5.9. Uridine supplementation rescued teriflunomide-mediated clonogenic cell survival in most cell lines.

Similar to the above experiments, metabolic supplementation of uridine (500 µM) reversed the effect of teriflunomide on UM-SCC-1, UM-SCC-11B (Figure 5.11) and UM-SCC-81B (Figure 5.12) cells. However, rescue following orotate or uridine could not be observed in FaDu cells, as at concentrations tested (20 µM), teriflunomide did not have any effect on the clonogenic survival of FaDu cells.
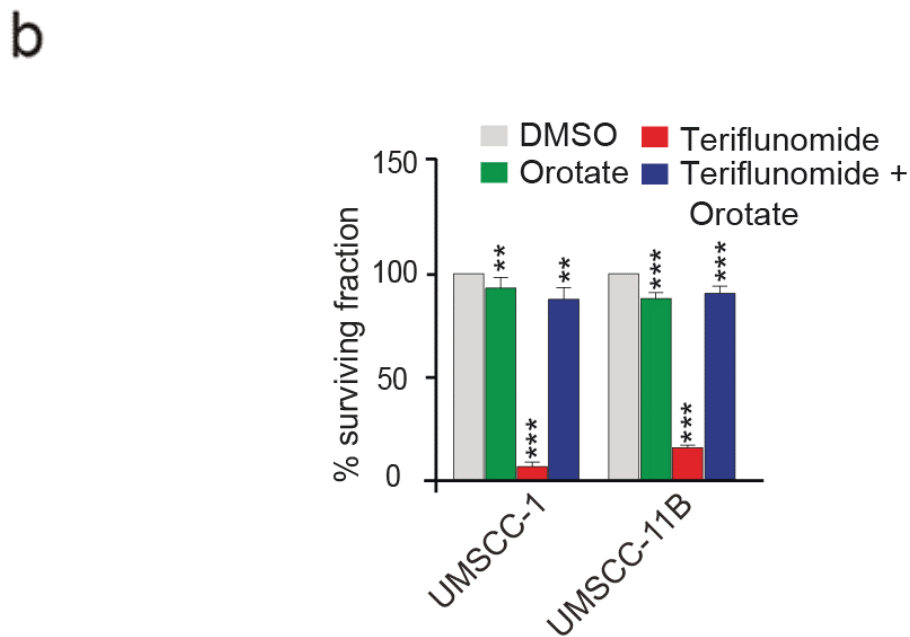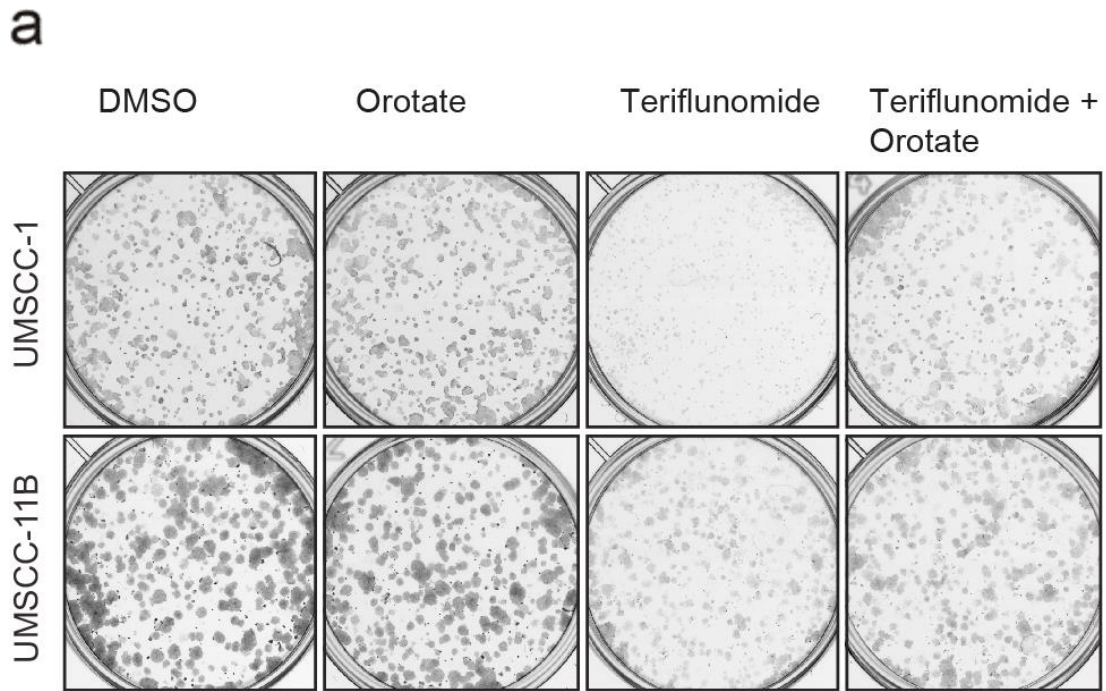
Figure 5.9. Orotate supplementation rescues the effect of teriflunomide in cell lines derived from the oral cavity and larynx. UMSCC- 1 or UMSCC-11B cells were pre-exposed to orotate (500 µM) and then exposed to teriflunomide (20 µM). Colonies were grown for ~ 7 days, stained with crystal violet and counted using an automated colony counter. a) The images represent colony formation assay of indicated cell lines. b) The graph represents surviving fraction of cells in the colony formation assay. All experiments were independently performed three times. Error bars = Mean ± SEM. ** $p \leq 0.005$, *** $p \leq 0.001$.
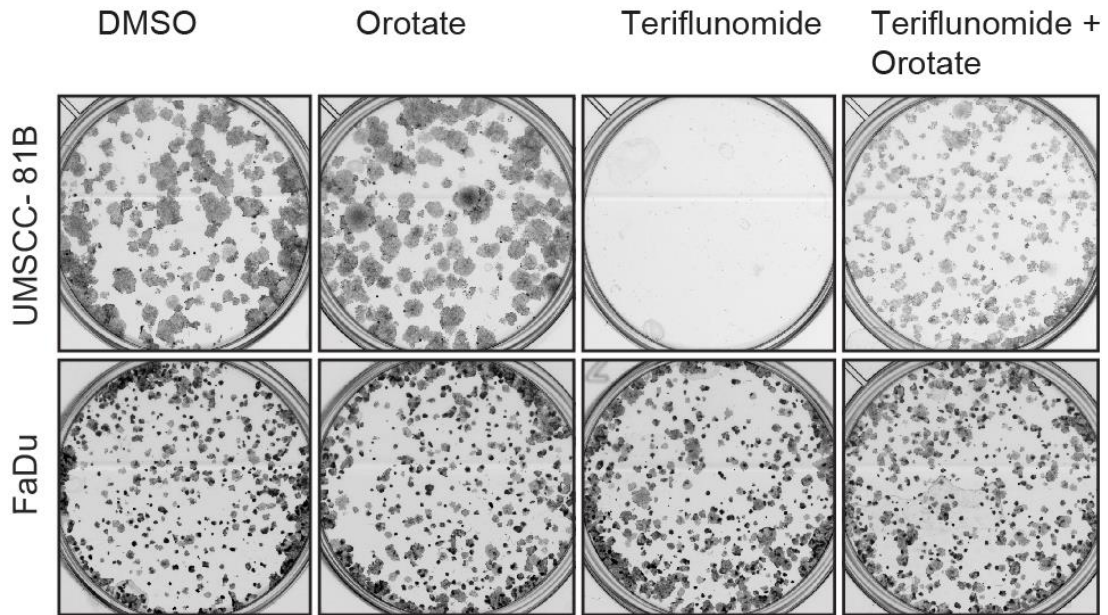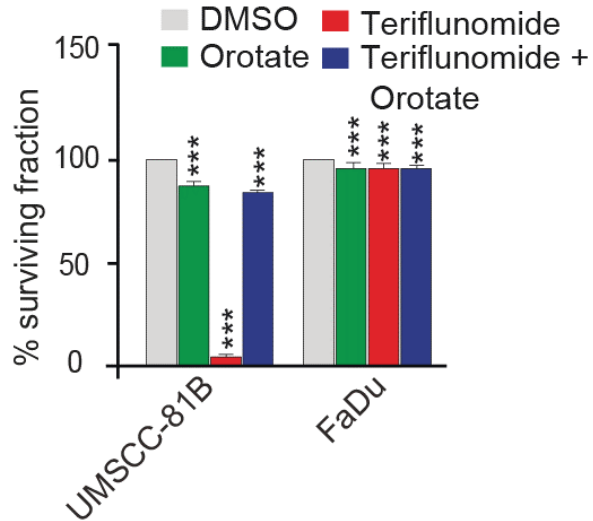
Figure 5.10. Orotate supplementation rescues the effect of teriflunomide in cell lines derived from the oropharnx and hypopharaynx. UMSCC-81B or FaDu cells were pre-exposed to orotate (500 μM) and then exposed to teriflunomide (20 μM). Colonies were grown for ~ 7 days, stained with crystal violet and counted using an automated colony counter. a) The images represent colony formation assay of indicated cell lines. b) The graph represents surviving fraction of cells in the colony formation assay. All experiments were independently performed three times. Error bars = Mean ± SEM. *** $p \leq 0.001$.
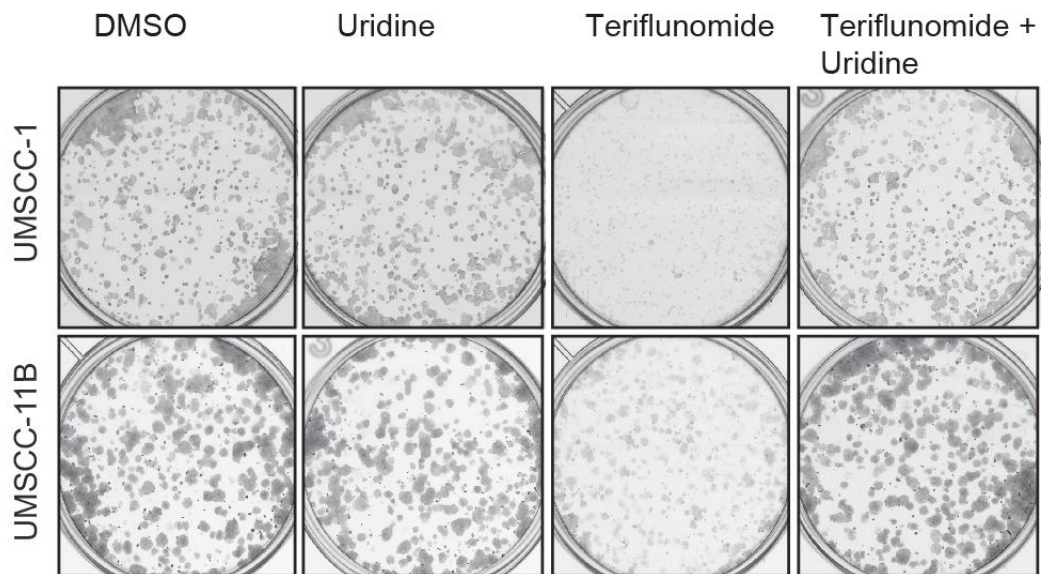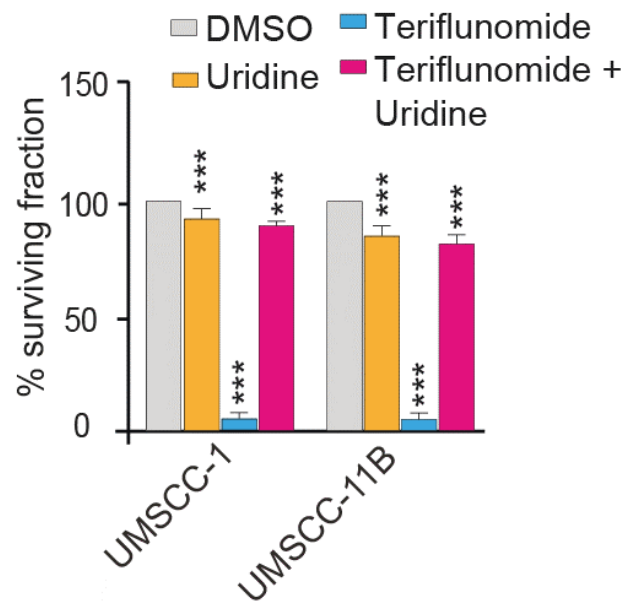
Figure 5.11. Uridine supplementation rescues the effect of teriflunomide in cell lines derived from the oral cavity and larynx. UMSCC- 1 or UMSCC-11B cells were pre-exposed to uridine (500 μM) and then exposed to teriflunomide (20 μM). Colonies were grown for ~ 7 days, stained with crystal violet and counted using an automated colony counter. a) The images represent colony formation assay of indicated cell lines. b) The graph represents surviving fraction of cells in the colony formation assay. All experiments were independently performed three times. Error bars = Mean ± SEM. *** $p ≤ 0.001$.
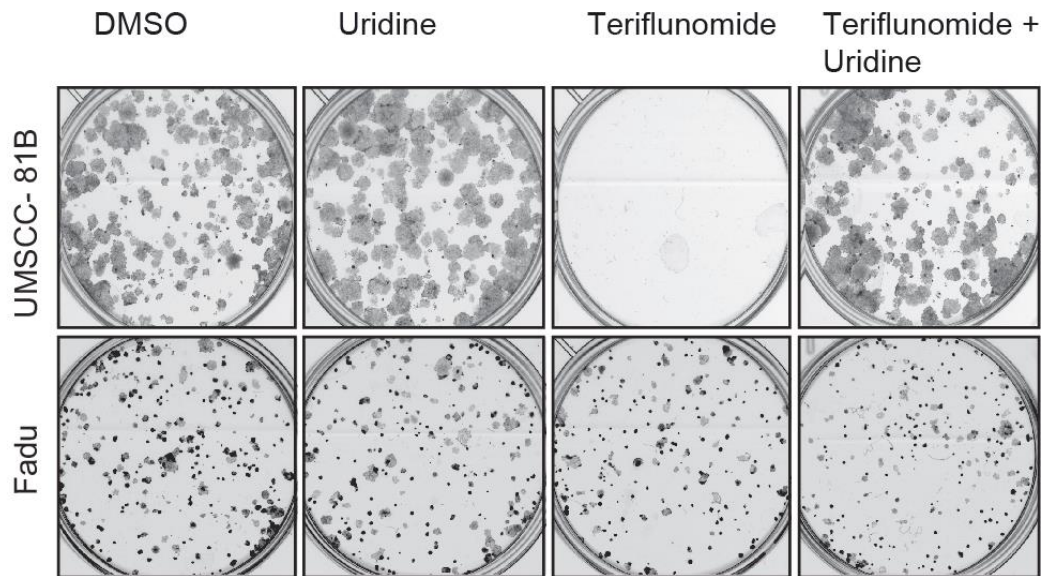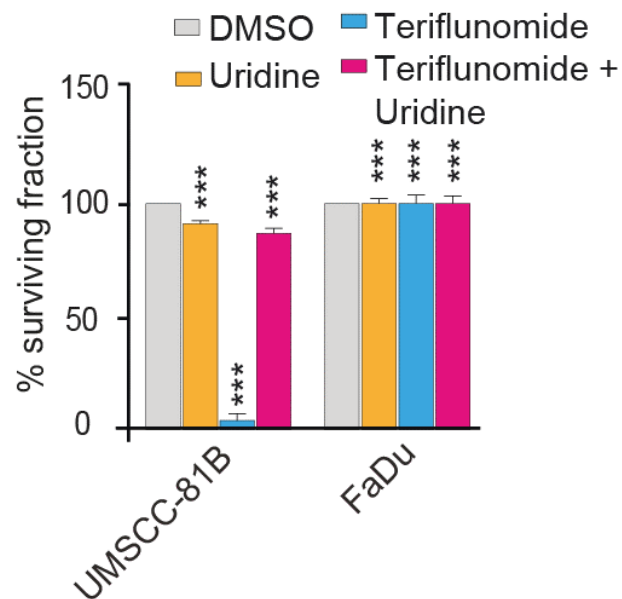
Figure 5.12. Uridine supplementation rescues the effect of teriflunomide in cell lines derived from the oropharnx and hypopharaynx. UMSCC-81B or FaDu cells were pre-exposed to uridine (500 μM) and then exposed to teriflunomide (20 μM). Colonies were grown for ~ 7 days, stained with crystal violet and counted using an automated colony counter. a) The images represent colony formation assay of indicated cell lines. b) The graph represents surviving fraction of cells in the colony formation assay. All experiments were independently performed three times. Error bars = Mean ± SEM. *** $p \leq 0.001$.

5.10. Teriflunomide does not synergise with cisplatin in reducing the clonogenic survival of all HNSCC cell lines

To assess if teriflunomide synergise with cisplatin in the different HNSCC cell lines, cells were exposed to cisplatin (0.5 µM) and teriflunomide (10 µm and 20 µM) and clonogenic assay was performed. Concentrations of cisplatin were calculated based on IC50 measurements, carried out by exposing all the cell lines to increasing concentrations of cisplatin. This data is not shown in this thesis, as this was performed by other members in the Varadarajan lab. All HNSCC cell lines used in this study were sensitive to cisplatin at higher concentrations (1 µM), and therefore, a concentration of 0.5 µM was chosen to ensure that there will be some effect on clonogenicity, which could potentially show synergy with simultaneous exposure to DHODH inhibitors. The results of this assay revealed that the colony numbers and sizes were largely reduced upon increasing concentrations of teriflunomide. However, there was no enhanced reduction in the number of colonies when both cisplatin and teriflunomide were administered together (Figures 5.13 and 5.14).

5.11. Teriflunomide does not synergises with A-1331852 in cell lines derived from oral cavity and larynx.

To assess if teriflunomide synergises with A-1331852 in cell lines derived from oral cavity and larynx. Cells were exposed to A-1331852 (0.1 µM) and teriflunomide (10 µm and 20 µM) then clonogenic assay was performed. The results of this assay revealed that the colony numbers and sizes were largely reduced upon teriflunomide exposure in oral cavity and larynx cells which was not synergised with A-1331852 (Figure 5.15). Suggesting that teriflunomide combination may not require for A-1331852 synergy in these cells. Similarly, the effect of teriflunomide synergy with A-1331852 was examined in other cell lines derived from oropharynx and hypopharynx. Cells were exposed to A-1331852 (0.1 µM) and teriflunomide (10 µm and 20 µM) then clonogenic assay was performed. The results of this assay revealed that the colony numbers and sizes were largely reduced upon teriflunomide exposure in oropharynx cells, but it does not affect the clonogenic survival of FaDu cells. A-1331852 did not show any synergy with teriflunomide in these cells (Figure 5.16).
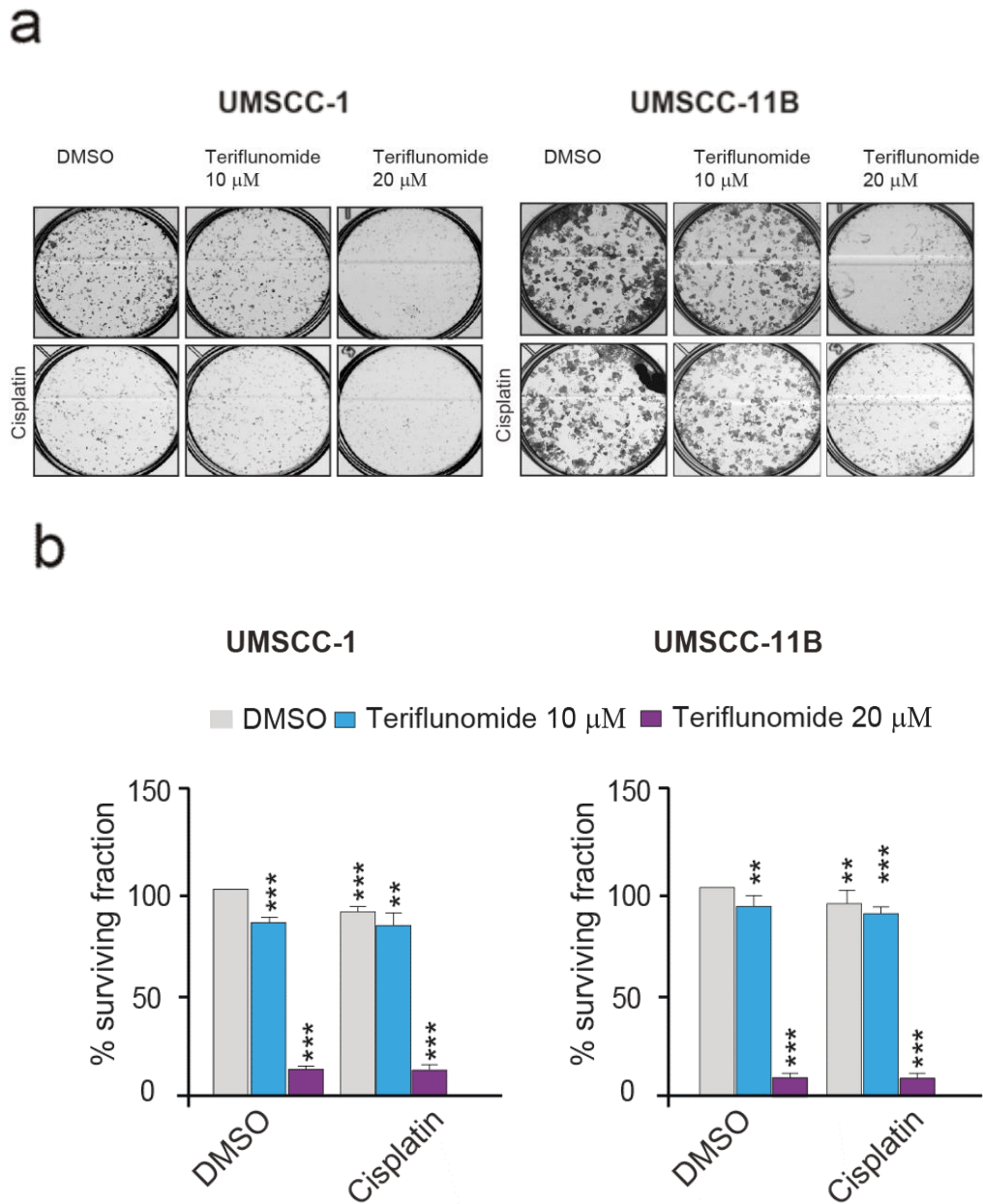
Figure 5.13. Teriflunomide does not synergise with cisplatin in cell lines derived from the oral cavity and larynx. UMSCC- 1 or UMSCC-11, cells were pre-exposed to cisplatin (0.5 µM) and then teriflunomide (10 µM and 20 µM). Colonies grown for ~ 7 days, stained with crystal violet and counted using an automated colony counter. a) The images represent colony formation assay of indicated cell lines. b) The graph represents surviving fraction of cells in the colony formation assay. All experiments were independently performed three times. Error bars = Mean ± SEM. ** $p \leq 0.005$, *** $p \leq 0.001$.
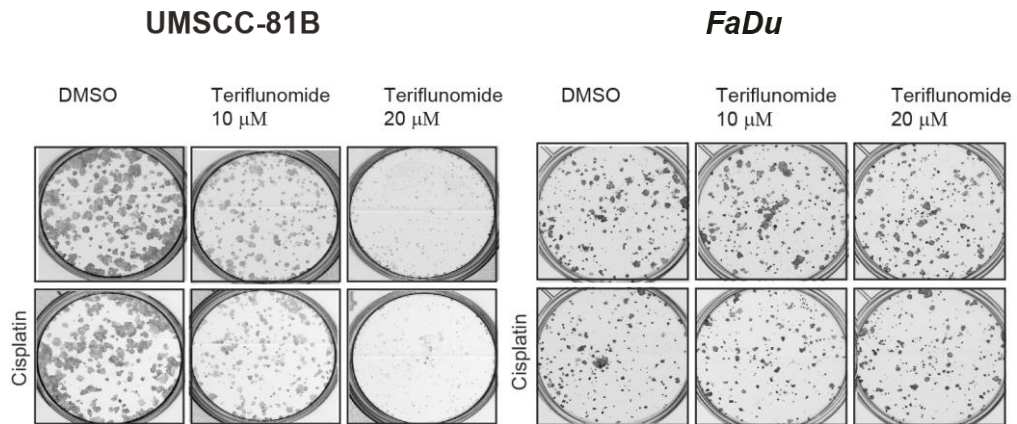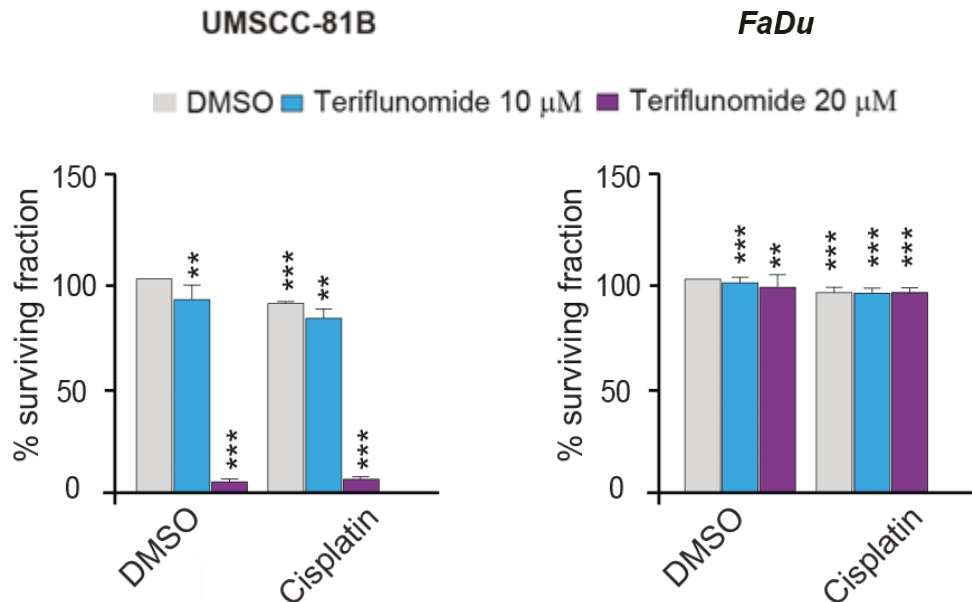
Figure 5.14. Teriflunomide does not synergise with cisplatin in cell lines derived from the oropharnx and hypopharaynx. UMSCC-81B or FaDu, cells were pre-exposed to cisplatin (0.5 µM) then teriflunomide (10 µM and 20 µM). Colonies were grown for ~ 7 days, stained with crystal violet and counted using an automated colony counter. a) The images represent colony formation assay of indicated cell lines. b) The graph represents surviving fraction of cells in the colony formation assay. All experiments were independently performed three times. Error bars = Mean ± SEM. ** $p \leq 0.005$, *** $p \leq 0.001$.
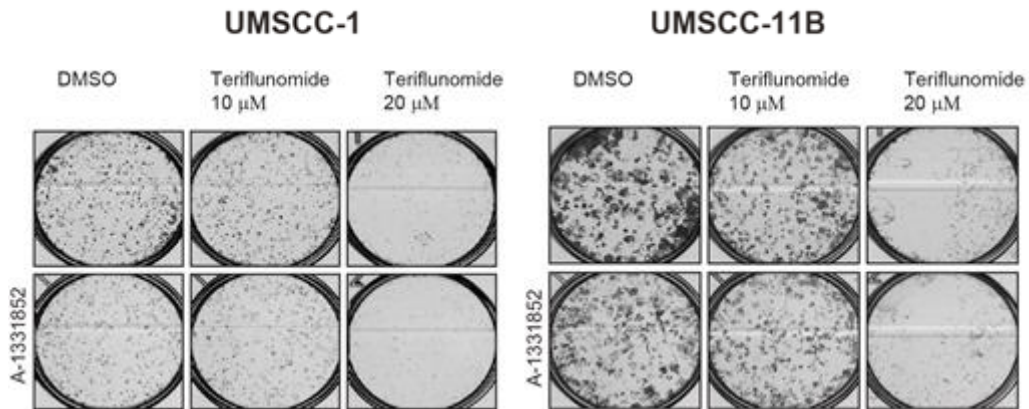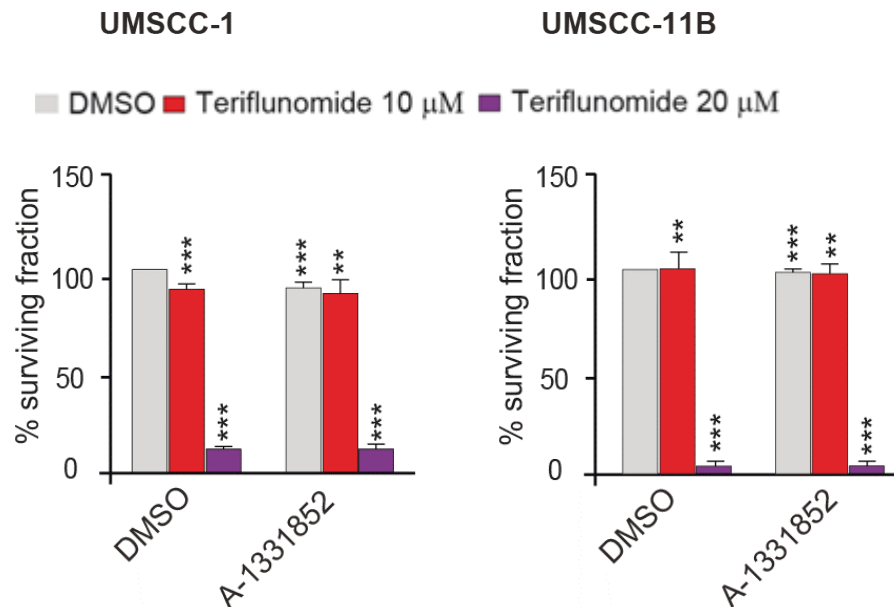
Figure 5.15. Teriflunomide does not synergise with A-1331852 in cell lines derived from the oral cavity and larynx. UMSCC- 1 or UMSCC-11B, cells were pre-exposed to 1331852 (0.1 μM) and then teriflunomide (10 μM and 20 μM). Colonies were grown for ~ 7 days, stained with crystal violet and counted using an automated colony counter. a) The images represent colony formation assay of indicated cell lines. b) The graph represents surviving fraction of cells in the colony formation assay. All experiments were independently performed three times. Error bars = Mean ± SEM. ** $p \leq 0.005$, *** $p \leq 0.001$.

a

UMSCC-81B

FaDu

b
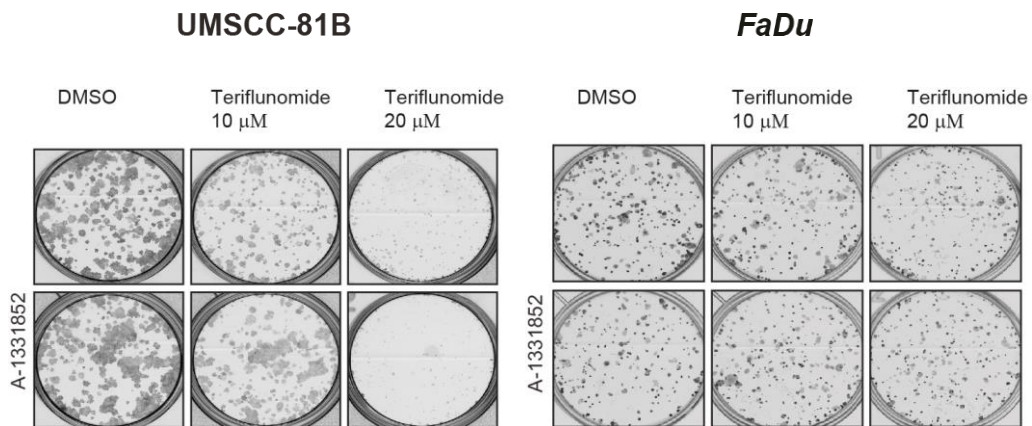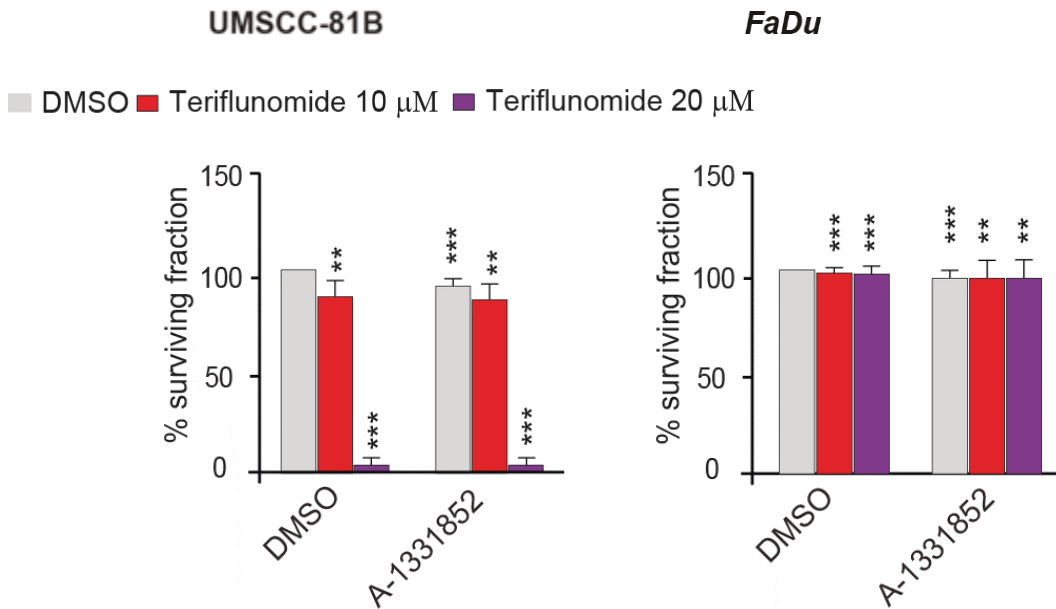
UMSCC-81B

FaDu

Figure 5.16. Teriflunomide does not synergise with A-1331852 in cell lines derived from the oropharnx and hypopharaynx. UMSCC-81B or FaDu, cells were pre-exposed to 1331852 (0.1 μM) and then teriflunomide (10 μM and 20 μM). Colonies were grown for ~ 7 days, stained with crystal violet and counted using an automated colony counter. a) The images represent colony formation assay of indicated cell lines. b) The graph represents surviving fraction of cells in the colony formation assay. All experiments were independently performed three times. Error bars = Mean ± SEM. ** $p \leq 0.005$, *** $p \leq 0.001$.

5.12. Teriflunomide does not synergises with S63845 in cell lines derived from oral cavity and larynx

To assess if teriflunomide synergises with S63845 in cell lines derived from oral cavity and larynx. Cells were exposed to S63845 (0.1 µM) and teriflunomide (10 µm and 20 µM) then clonogenic assay was performed. The results of this assay revealed that the colony numbers and sizes were largely reduced upon teriflunomide exposure in oral cavity and larynx cells which was not synergised with S63845 (Figure 5.17), suggesting that teriflunomide combination may not require for S63845 synergy.

Similarly, the effect of teriflunomide synergy with S63845 was examined in other cell lines derived from oropharynx and hypopharynx. Cells were exposed to S63845 (0.1 µM) and teriflunomide (10 µm and 20 µM) then clonogenic assay was performed. The results of this assay revealed that the colony numbers and sizes were largely reduced upon teriflunomide exposure in oropharynx cells, but it does not affect the clonogenic survival of FaDu cells. S63845 does not show any synergy with teriflunomide in these cells (Figure 5.18).

a

UMSCC-1

DMSO   Teriflunomide 10 μM   Teriflunomide 20 μM

UMSCC-11B

DMSO   Teriflunomide 10 μM   Teriflunomide 20 μM

S63845

b

UMSCC-1   **UMSCC-11B**

▢ DMSO   ▮ Teriflunomide 10 μM   ▮ Teriflunomide 20 μM
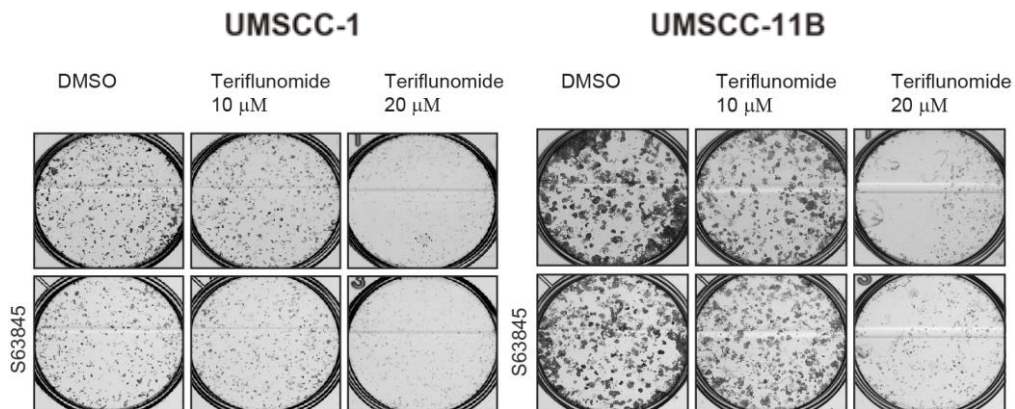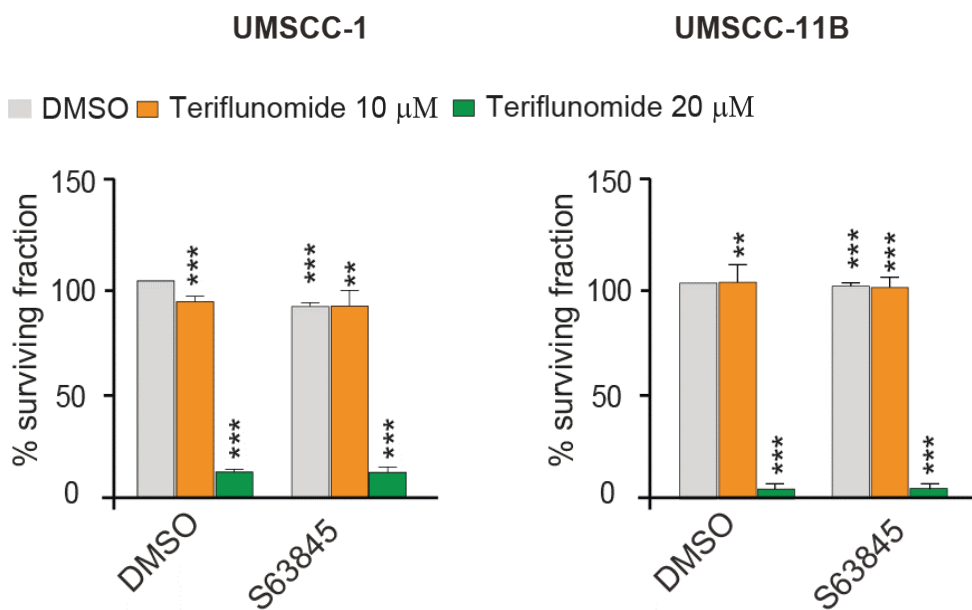
Figure 5.17. Teriflunomide does not synergise with S63845 in cell lines derived from the oral cavity and larynx. UMSCC-1 or UMSCC-11B, cells were pre-exposed to S63845 (0.1 μM) and then teriflunomide (10 μM and 20 μM). Colonies grown for ~ 7 days, stained with crystal violet and counted using an automated colony counter. a) The images represent colony formation assay of indicated cell lines. b) The graph represents surviving fraction of cells in the colony formation assay. All experiments were independently performed three times. Error bars = Mean ± SEM. ** $p \leq 0.005$, *** $p \leq 0.001$.
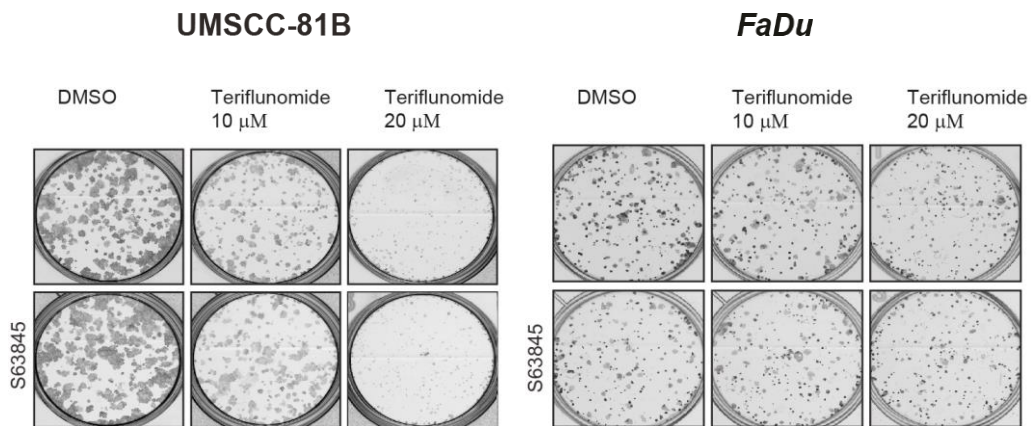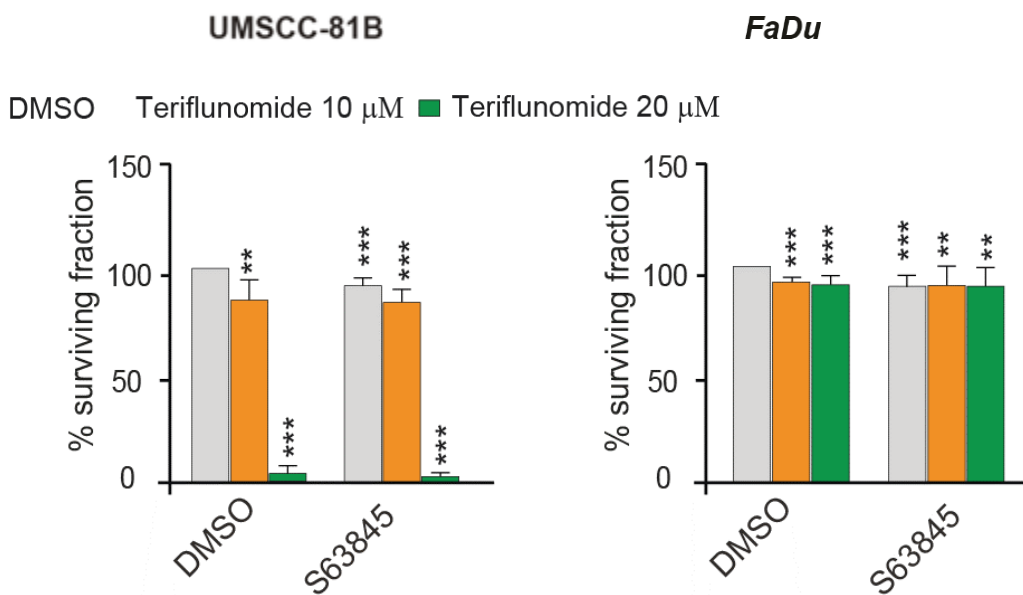
Figure 5.18. Teriflunomide does not synergise with S63845 in cell lines derived from the oropharnx and hypopharaynx. UMSCC-81B or FaDu, cells were pre-exposed to S63845 (0.1 μM) and then teriflunomide (10 μM and 20 μM). Colonies were grown for ~ 7 days, stained with crystal violet and counted using an automated colony counter. a) The images represent colony formation assay of indicated cell lines. b) The graph represents surviving fraction of cells in the colony formation assay. All experiments were independently performed three times. Error bars = Mean ± SEM. ** $p \leq 0.005$, *** $p \leq 0.001$.

5.13. Discussion

Results from the previous chapter (Chapter 4) suggested that DHODH inhibitors played a critical role in ERMR-mediated apoptosis. Growing evidence suggests that DHODH acts as a candidate for several cancers, including AML[128,147]. However, the effect of DHODH is still not well understood in HNSCC, which is one of the most common cancer-type worldwide[217]. Therefore, a more in-depth understanding of the role of DHODH will be useful to improve therapy in HNSCC.

In this chapter, expression levels of DHODH in different HNSCC cell lines were examined. Western blot results showed that several HNSCC cells expressed high levels of DHODH (Figure 5.2). In addition to the 40 kDa band of DHODH that was detected in all cell lines, another band around 38 kDa corresponding to DHODH could be identified in UMSCC-11B and UMSCC-81B, suggesting the presence of multiple isoforms of DHODH in these cell lines. It has been reported that human DHODH exists as two isoforms with molecular weights of 40 kDa and 100 kDa. The additional band at 38 kDa could potentially due to alternative splicing of DHODH. Since HNSCC cells had a high expression of DHODH, it was further examined to assess the requirement of DHODH for cell survival. Upon DHODH silencing, HNSCC clonogenic survival was largely reduced (Figure 5.4-5.5). Similarly, chemical inhibition of DHODH also reduced clonogenicity in most of HNSCC cells (Figure 5.6-5.7), suggesting that DHODH is critical for HNSCC survival. This could be due to a reduction in *de novo* pyrimidine biosynthesis or altered pro survival machinery. Subsequent results suggested that teriflunomide-mediated reduction in clonogenic survival was rescued with metabolic supplementation of pyrimidine (Figure 5.9-5.11), suggesting that DHODH inhibition alters pyrimidine pool and upon supplementation with orotate or uridine (key products of the DHODH reaction), cells regain adequate pyrimidine levels for maintaining cell survival homeostasis. Depletion of pyrimidine levels could cause cell cycle arrest which consequently can induce apoptosis. Together, these results suggested that teriflunomide-mediated reduction in cell survival is downstream of pyrimidine synthesis.

Since currently available chemotherapeutic agents are not effective against HNSCC, teriflunomide could be combined with these drugs to improve therapy. Cisplatin is the one of the widely used chemotherapeutic agent for HNSCC treatment.

It kills cancer cell by damaging DNA and inhibiting DNA synthesis[222–226]. Cisplatin has not been effective in treating HNSCC due to problems arising from toxicity and drug resistance[227]. It is possible that cisplatin combination with teriflunomide may sensitise chemo-resistant cancer cells to undergo apoptosis with less toxicity to surrounding tissues. However, the combination of teriflunomide with cisplatin does not alter cell survival (Figures 5.13 and 5.14), as lower concentrations of cisplatin ($<$ 0.1 µM) was not effective on its own or in combination with teriflunomide. In contrast, higher concentrations of cisplatin ($>$ 0.1 µM) was toxic to the cells even when used to single agents.

It has been reported that BCL-X_L and MCL-1 are highly expressed in HNSCC[102,228–232]. These anti-apoptotic proteins might be playing critical role in teriflunomide-mediated reduction in cell survival. Therefore, cells were exposed to combination of BCL X_L inhibitor (A-1331852) and teriflunomide. However, this combination did not alter cell survival (Figure 5.15- 5.16), suggesting that BCL X_L is not a key regulator for teriflunomide-mediated reduction in cell survival. Similarly, a combination of teriflunomide and MCL-1 inhibitor (S63845) also did not affect the reduction in clonogenic survival (Figure 5.17-5.18), suggested that MCL-1 also may not be the key regulator for teriflunomide-mediated reduction in cell survival. In summary, the present study showed that DHODH played an important role in HNSCC cell survival. However, further studies are required to confirm this observation in HNSCC patient samples.

Chapter 6

General discussion

ER-mitochondrial contacts play essential roles in regulating several cellular processes, including calcium regulation, lipid homeostasis, cell death and cell survival [21,33,47,60,233]. The functions of ER-mitochondrial contacts have been well characterised in calcium regulation and lipid biosynthesis[33]. However, the exact role of ER-mitochondrial communication in apoptosis is still poorly understood. Understanding the intricacies of the apoptosis pathways in cancer is very important, as most of the cancer chemotherapeutic drugs have been designed to target the apoptosis pathway. In addition, the current challenge facing cancer therapy is drug resistance. Cancer cells have been reported to acquire resistance to chemotherapeutic drugs through different mechanisms, which include a failure to undergo apoptosis. This study is aimed at understanding the functional consequences of ER-mitochondrial communication in apoptosis by using ERMR as a tool.

ERMR is a novel cellular stress response characterised by reversible reorganisation of ER membranes, following exposure of cells to a wide variety of drugs, such as apogossypol, ivermectin, terfenadine, suloctidil and other agents[90,91]. ERMR is evolutionary conserved from yeast to humans[91]. In addition, downregulation of anterograde transport protein (αSNAP), retrograde transport protein (syntaxin 18), anti-apoptotic protein (MCL-1) and upregulation of SOCE protein (STIM 1) also resulted in ERMR[90,91]. STIM1 is an ER resident calcium sensor that plays a critical role in SOCE[90]. As STIM 1 is associated with calcium regulation, it is speculated that calcium regulation may essential for ERMR[90]. It has been reported that downregulation of critical calcium regulated SOCE genes, such as STIM1, ORAI1 and ORAI3 had no effect on ERMR[90]. These results suggest that STIM1 may have other functions distinct from calcium regulation. Since ERMR is associated with diverse and specialised functions, including vesicular trafficking defects, mitochondrial fission

and apoptosis, it will be interesting to assess whether downregulation of αSNAP, syntaxin 18 and MCL-1 or an upregulation of STIM 1 would influence mitochondrial fission, MOMP and apoptosis.

In this study, apogossypol is used as a prototype tool to understand functional consequences of ER-mitochondrial communication in apoptosis. Previous studies report that apogossypol regulates ERMR through ionic flux especially, influx of extracellular sodium ions but not calcium ionic flux[90]. Furthermore, apogossypol-induced ERMR modulates ER associated functions, such as the vesicular trafficking between ER exit sites and the Golgi complex[91]. A drastic attenuation of global protein synthesis has also been associated with ERMR[91]. Although these events result in a stress response, ERMR appears to be distinct from classical ER stress pathway and the unfolded protein response (UPR). ERMR occurs even in the absence of transcription and translation and also in cells lacking UPR regulators, such as PERK, IRE1, ATF6, XBP1 and CHOP[91], suggesting that ERMR acts either upstream or independent of UPR.

ERMR is a completely different process from other ER structural alterations, such as such as ER expansion, ER swelling, and ER whorls, which have been reported in the literature[91]. ER expansion has been observed during differentiation of B lymphocytes into plasma cells[234]. During this, ER membranes expand to more than three-fold of their original ER volume, and this expansion has been observed to provide massive space for B-cell differentiation[234]. In contrast, ER swelling is often associated with classical ER stress and the UPR[235]. During UPR, large amounts of misfolded proteins accumulate inside ER lumen[235]. In order to handle such overwhelming accumulation of misfolded proteins, ER lumen often swells to provide the physical space required for protein folding processes, all of which relieves the

extent of ER stress[235]. ER whorls are identified during ER-phagy, during which severely damaged ER membranes are often eliminated through ER-selective autophagy[236]. During this phenomena, large clusters of damaged ER tubules wrap around one another in a circular pattern, which are recognised by the autophagosomes and eventually fuses with lysosomes to digest damaged ER[236]. ERMR noted in this study involves the reversible reorganisation of ER tubules and lack features that resemble ER expansion, ER swelling and ER whorls[90,91].

ER-mitochondrial contacts also play essential roles in mitochondrial fission[237–240]. Growing reports suggest that mitochondrial fission is mediated by a series of events, which begin by the wrapping of ER tubules around mitochondria to mark mitochondrial constriction sites[2,48,239,241]. This later facilitates the recruitment of DRP-1 to the fission site, where DRP-1 binds to its receptors such as MFF, MID49, MID51 – all of which result in mitochondrial fission[31,48,195,242]. DRP-1 has been shown to undergo several post-translational modifications, including phosphorylation, which play regulatory roles in mitochondrial fission[48,243]. Data from this thesis indicates that ERMR prevents DRP-1-mediated mitochondrial fission, most likely by decreasing the phosphorylation status of DRP-1 (at S616, which is associated with mitochondrial fission)[193,194]. This is particularly interesting as similar observations have also been made in dengue virus infected cells[244]. Dengue virus often induces ERMR for replication and survival process[244]. It has been reported that in these cells, viral infection-induced ERMR prevented mitochondrial fission by decreasing the phosphorylation of DRP-1 at Ser 616 to favour viral replication[244]. These results suggested that there could be a strong link between ERMR and phosphorylation, which may affect its translocation from cytosol to mitochondria[211]. The effect of ERMR to prevent mitochondrial fission might be due to the inability of DRP-1 to translocate to

the mitochondrial membranes and this is evidenced by the trapped DRP-1 within the reorganised ER membranes (Figure 3.12). Recent studies suggest that DRP-1 undergoes several post-translational including SUMOylation, which play critical role in DRP-1 stabilisation at mitochondrial fission site[241]. This involves the addition of SUMOs (small ubiquitin-like modifiers) to lysine residues in the target protein. The major key protein involved in SUMOylation of DRP-1 is MAPL[241]. It is a one of the SUMO E3 ligase family proteins, which play an active role in mitochondrial fission[241].

Mitochondrial fission occurs upstream of apoptosis, but the specific mechanisms remain poorly understood. Several sequential events, such as the recruitment of DRP-1 to mitochondrial fission site, BAX and BAK pore formation at OMM, mitochondrial cristae remodelling that is accompanied by OPA1 proteolysis, the release of cytochrome c from IMM to cytosol, and finally the caspase activation cascade, form the distinct stages of the intrinsic apoptotic pathway[101]. OPA1 proteolysis is regulated by YME1L (ATP dependent metalloprotease) and OMA1(zinc endopeptidase), which are responsible for cleaving OPA1 into L-OPA1 and S-OPA1[242,243,245]. Upon OPA1 cleavage, cytochrome c trapped within the mitochondrial cristae releases into the cytosol through BAX and BAK pores in the OMM[48,95,243]. Data from this thesis suggests that ERMR prevented DRP-1-mediated mitochondrial fission, as well as BH3 mimetic-mediated BAX translocation, cytochrome c release and apoptosis (Figures 3.13-3.16). These results clearly suggest that ER tubules play essential roles in regulating BH3-mimetic-mediated apoptosis, by regulating mitochondrial fission. Since ERMR prevented mitochondrial-mediated apoptosis, it may be possible that ERMR may also alter other ER functions, such as structural lipid secretion, drug detoxification, lysosomal and peroxisomal biogenesis[6,8,21,29,33,198,246–248].

Findings from this thesis revealed that DHODH inhibitors, including teriflunomide and leflunomide, prevented ERMR without perturbing normal ER morphology (Figure 4.4-4.5). More specific inhibitors of DHODH have been identified recently such as BAY2402234 and ASLAN003[129,138]. It will be interesting to assess whether these compounds also could prevent ERMR. DHODH inhibitors exhibit dual functions, inhibiting SOCE to prevent extracellular calcium influx into ER lumen, while also inhibiting the enzymatic activity of DHODH to diminish the pyrimidine pool[203]. This suggests that either SOCE-mediated calcium regulation or DHODH enzymatic activity may be regulating ERMR. It has been reported that down regulation of critical SOCE genes such as STIM1, ORAI1 and ORAI3 had no effect on ERMR[90], suggesting that SOCE and its associated calcium regulation had no possible role in ERMR regulation. Findings from this study, involving a genetic knockdown of DHODH demonstrate that DHODH does not regulate ERMR (Figure 4.9). However, it is very hard to rule out an involvement of DHODH in ERMR regulation at this moment, as the siRNAs used in this study failed to completely knockdown DHODH expression (Figure 4.9). Therefore, a complete knockout system, possibly achieved *via* CRISPR, may be necessary to understand the possible role of DHODH in regulating ERMR. However, metabolic supplementation of pyrimidine intermediates, such as orotate and uridine, also failed to alter ERMR, suggesting that a lack of pyrimidine synthesis was not critical for the regulation of ERMR.

High levels of DHODH are observed in a wide range of HNSCC cell lines derived from oral cavity, larynx, oropharynx and hypopharynx (Figure 5.3). In addition, downregulation of DHODH decreases the clonogenic survival of all HNSCC cell lines, suggesting that DHODH might have critical role in HNSCC pathogenesis (Figure 5.3). These results were largely reproducible with DHODH inhibitors in all

HNSCC cell lines, except hypopharyngeal cells, which required a much higher concentration of teriflunomide ($> 100\mu$M). This is not surprising as most hypopharyngeal cells have been shown to inherently possess multi drug resistance[221]. This partly explains why hypopharyngeal cells are hard to treat with chemotherapeutic drugs. Metabolic supplementation of orotate and uridine rescued teriflunomide-mediated clonogenic survival in most HNSCC (Figure 5.9- 5.11), suggesting that orotate and uridine play important roles in regulating clonogenic cell survival. In addition to synthesising pyrimidines for nucleotide biosynthesis, pyrimidine metabolism also results in other end products, such as phosphatidylcholine (PC) and phosphatidylserine (PS)[132]. Further understanding of how PC and PS regulate cell death may give more information towards improving cancer therapy using DHODH inhibitors.

Despite these observations, several important questions remain unanswered. In particular, how is DRP-1 trapped within ERMR? In other words, is there a well-defined molecular machinery that directs DRP-1 to be trapped within ERMR? If ERMR affects BAX translocation and activation but not BAK activation, why is that enough to prevent BH3 mimetic-mediated apoptosis? Can active BAK not induce apoptosis in the absence of BAX? What is the role of other pro-apoptotic proteins in these processes? Further understanding of these points may unveil precise molecular events involving ER-mitochondrial contacts and apoptosis. Collectively, this information will widen our understanding of the ER-mitochondrial communication in apoptosis to improve cancer therapy.

Conclusions

The major findings presented this study are:

- ERMR is restricted to ER tubules

- ERMR does not form in other subcellular organelles

- ERMR prevents DRP-1 mediated mitochondrial fission

- ERMR prevents BH3 mimetic-mediated apoptosis

- ERMR-mediated anti-apoptotic effects can be reversed by DHODH inhibitors

- HNSCC cells express high levels of DHODH

- DHODH inhibitors decrease clonogenic survival of several HNSCC cell lines.

References

1. Hu, J., Prinz, W. A. & Rapoport, T. A. Weaving the web of ER tubules. *Cell* **147**, 1226–1231 (2011).

2. Phillips, M. J. & Voeltz, G. K. Structure and function of ER membrane contact sites with other organelles. *Nat. Rev. Mol. Cell Biol.* (2015). doi:10.1038/nrm.2015.8

3. Yadav, R. K., Chae, S.-W., Kim, H.-R. & Chae, H. J. Endoplasmic Reticulum Stress and Cancer. *J. Cancer Prev.* (2014). doi:10.15430/jcp.2014.19.2.75

4. Urra, H., Dufey, E., Avril, T., Chevet, E. & Hetz, C. Endoplasmic Reticulum Stress and the Hallmarks of Cancer. *Trends in Cancer* (2016). doi:10.1016/j.trecan.2016.03.007

5. Schönthal, A. H. Endoplasmic reticulum stress: its role in disease and novel prospects for therapy. *Scientifica (Cairo).* **2012**, 857516 (2012).

6. English, A. R. & Voeltz, G. K. Endoplasmic Reticulum Structure and Interconnections with Other Organelles. *Cold Spring Harb. Perspect. Biol.* **5**, a013227 (2013).

7. Friedman, J. R. *et al.* ER tubules mark sites of mitochondrial division. *Science* **334**, 358–62 (2011).

8. Goyal, U. & Blackstone, C. Untangling the web: mechanisms underlying ER network formation. *Biochim. Biophys. Acta* **1833**, 2492–8 (2013).

9. Yang, Y. S. & Strittmatter, S. M. The reticulons: A family of proteins with

diverse functions. *Genome Biology* (2007). doi:10.1186/gb-2007-8-12-234

10.   Voeltz, G. K., Prinz, W. A., Shibata, Y., Rist, J. M. & Rapoport, T. A. A class of membrane proteins shaping the tubular endoplasmic reticulum. *Cell* (2006). doi:10.1016/j.cell.2005.11.047

11.   Schwarz, D. S. & Blower, M. D. The endoplasmic reticulum: Structure, function and response to cellular signaling. *Cell. Mol. Life Sci.* (2016). doi:10.1007/s00018-015-2052-6

12.   Kafri, M., Metzl-Raz, E., Jona, G. & Barkai, N. The Cost of Protein Production. *Cell Rep.* (2016). doi:10.1016/j.celrep.2015.12.015

13.   Goldstein, J. L., DeBose-Boyd, R. A. & Brown, M. S. Protein sensors for membrane sterols. *Cell* (2006). doi:10.1016/j.cell.2005.12.022

14.   English, A. R. & Voeltz, G. K. Endoplasmic reticulum structure and interconnections with other organelles. *Cold Spring Harb. Perspect. Biol.* **5**, a013227 (2013).

15.   Vannuvel, K., Renard, P., Raes, M. & Arnould, T. Functional and morphological impact of ER stress on mitochondria. *J. Cell. Physiol.* **228**, 1802–1818 (2013).

16.   Zhao, Y., Zhang, T., Huo, H., Ye, Y. & Liu, Y. Lunapark is a component of a ubiquitin ligase complex localized to the endoplasmic reticulum three-way junctions. *J. Biol. Chem.* (2016). doi:10.1074/jbc.M116.737783

17.   Bian, X. *et al.* Structures of the atlastin GTPase provide insight into homotypic fusion of endoplasmic reticulum membranes. *Proc. Natl. Acad. Sci. U. S. A.* **108**, 3976–81 (2011).

18. Chen, S. *et al.* Lunapark stabilizes nascent three-way junctions in the endoplasmic reticulum. *Proc. Natl. Acad. Sci. U. S. A.* **112**, 418–23 (2015).

19. Chen, S., Novick, P. & Ferro-Novick, S. ER structure and function. *Curr. Opin. Cell Biol.* (2013). doi:10.1016/j.ceb.2013.02.006

20. Phillips, M. J. & Voeltz, G. K. Structure and function of ER membrane contact sites with other organelles. *Nature Reviews Molecular Cell Biology* (2016). doi:10.1038/nrm.2015.8

21. Lebiedzinska, M., Szabadkai, G., Jones, A. W. E., Duszynski, J. & Wieckowski, M. R. Interactions between the endoplasmic reticulum, mitochondria, plasma membrane and other subcellular organelles. *International Journal of Biochemistry and Cell Biology* (2009). doi:10.1016/j.biocel.2009.02.017

22. Prudent, J. & McBride, H. M. The mitochondria???endoplasmic reticulum contact sites: a signalling platform for cell death. *Curr. Opin. Cell Biol.* **47**, 52–63 (2017).

23. Kornmann, B. & Walter, P. ERMES-mediated ER-mitochondria contacts: molecular hubs for the regulation of mitochondrial biology. *J. Cell Sci.* **123**, 1389–1393 (2010).

24. Prudent, J. & McBride, H. M. The mitochondria–endoplasmic reticulum contact sites: a signalling platform for cell death. *Current Opinion in Cell Biology* (2017). doi:10.1016/j.ceb.2017.03.007

25. Periasamy, M. & Kalyanasundaram, A. SERCA pump isoforms: Their role in calcium transport and disease. *Muscle and Nerve* (2007). doi:10.1002/mus.20745

26.   Csordás, G. & Hajnóczky, G. SR/ER-mitochondrial local communication: Calcium and ROS. *Biochimica et Biophysica Acta - Bioenergetics* **1787**, 1352–1362 (2009).

27.   Palmer, C. S. *et al.* MiD49 and MiD51, new components of the mitochondrial fission machinery. *EMBO Rep.* (2011). doi:10.1038/embor.2011.54

28.   Kornmann, B. *et al.* An ER-Mitochondria Tethering Complex Revealed by a Synthetic Biology Screen. *Science (80-.).* (2009). doi:10.1126/science.1175088

29.   Friedman, J. R., DiBenedetto, J. R., West, M., Rowland, A. A. & Voeltz, G. K. Endoplasmic reticulum-endosome contact increases as endosomes traffic and mature. *Mol. Biol. Cell* (2013). doi:10.1091/mbc.E12-10-0733

30.   Krols, M., Bultynck, G. & Janssens, S. ER-Mitochondria contact sites: A new regulator of cellular calcium flux comes into play. *J. Cell Biol.* **214**, 367–70 (2016).

31.   Prudent, J. & McBride, H. M. Mitochondrial Dynamics: ER Actin Tightens the Drp1 Noose. *Curr. Biol.* **26**, R207–R209 (2016).

32.   Flis, V. V. & Daum, G. Lipid transport between the endoplasmic reticulum and mitochondria. *Cold Spring Harb. Perspect. Biol.* (2013). doi:10.1101/cshperspect.a013235

33.   Vance, J. E. MAM (mitochondria-associated membranes) in mammalian cells: Lipids and beyond. *Biochim. Biophys. Acta - Mol. Cell Biol. Lipids* (2014). doi:10.1016/j.bbalip.2013.11.014

34.   Aits, S. & Jäättelä, M. Lysosomal cell death at a glance. *J. Cell Sci.* (2013). doi:10.1242/jcs.091181

35. Boya, P. & Kroemer, G. Lysosomal membrane permeabilization in cell death. *Oncogene* (2008). doi:10.1038/onc.2008.310

36. Guicciardi, M. E., Leist, M. & Gores, G. J. Lysosomes in cell death. *Oncogene* (2004). doi:10.1038/sj.onc.1207512

37. Kirkegaard, T. & Jäättelä, M. Lysosomal involvement in cell death and cancer. *Biochimica et Biophysica Acta - Molecular Cell Research* (2009). doi:10.1016/j.bbamcr.2008.09.008

38. Aston, D. *et al.* High resolution structural evidence suggests the Sarcoplasmic Reticulum forms microdomains with Acidic Stores (lysosomes) in the heart. *Sci. Rep.* (2017). doi:10.1038/srep40620

39. Tabak, H. F., Murk, J. L., Braakman, I. & Geuze, H. J. Peroxisomes start their life in the endoplasmic reticulum. *Traffic* (2003). doi:10.1034/j.1600-0854.2003.00110.x

40. Lahiri, S. *et al.* A Conserved Endoplasmic Reticulum Membrane Protein Complex (EMC) Facilitates Phospholipid Transfer from the ER to Mitochondria. *PLoS Biol.* (2014). doi:10.1371/journal.pbio.1001969

41. Joshi, A. S., Zhang, H. & Prinz, W. A. Organelle biogenesis in the endoplasmic reticulum. *Nature Cell Biology* (2017). doi:10.1038/ncb3579

42. Klecker, T., Böckler, S. & Westermann, B. Making connections: Interorganelle contacts orchestrate mitochondrial behavior. *Trends Cell Biol.* (2014). doi:10.1016/j.tcb.2014.04.004

43. Dimitrov, L., Lam, S. K. & Schekman, R. The role of the endoplasmic reticulum in peroxisome biogenesis. *Cold Spring Harbor Perspectives in Biology* (2013).

doi:10.1101/cshperspect.a013243

44.   Titorenko, V. I. & Rachubinski, R. A. The endoplasmic reticulum plays an essential role in peroxisome biogenesis. *Trends Biochem. Sci.* (1998). doi:10.1016/S0968-0004(98)01226-2

45.   Collins, H. E., Zhu-Mauldin, X., Marchase, R. B. & Chatham, J. C. STIM1/Orai1-mediated SOCE: Current perspectives and potential roles in cardiac function and pathology. *American Journal of Physiology - Heart and Circulatory Physiology* (2013). doi:10.1152/ajpheart.00104.2013

46.   Bartoli, F. & Sabourin, J. Cardiac remodeling and disease: Current understanding of STIM1/Orai1-mediated store-operated Ca2+ entry in cardiac function and pathology. in *Advances in Experimental Medicine and Biology* (2017). doi:10.1007/978-3-319-57732-6_26

47.   Grimm, S. The ER-mitochondria interface: The social network of cell death. *Biochimica et Biophysica Acta - Molecular Cell Research* (2012). doi:10.1016/j.bbamcr.2011.11.018

48.   Tilokani, L., Nagashima, S., Paupe, V. & Prudent, J. Mitochondrial dynamics: Overview of molecular mechanisms. *Essays in Biochemistry* (2018). doi:10.1042/EBC20170104

49.   Helle, S. C. J. *et al.* Organization and function of membrane contact sites. *Biochim. Biophys. Acta - Mol. Cell Res.* (2013). doi:10.1016/j.bbamcr.2013.01.028

50.   Parekh, A. B. & Putney, J. W. Store-operated calcium channels. *Physiological Reviews* (2005). doi:10.1152/physrev.00057.2003

51. English, A. R. & Voeltz, G. K. Endoplasmic reticulum structure and interconnections with other organelles. *Cold Spring Harbor Perspectives in Biology* (2013). doi:10.1101/cshperspect.a013227

52. Amcheslavsky, A., Yeromin, A. V., Penna, A. & Cahalan, M. D. Store-Operated Calcium Channels. in *Encyclopedia of Biological Chemistry: Second Edition* (2013). doi:10.1016/B978-0-12-378630-2.00301-7

53. Verkhratsky, A. & Parpura, V. Calcium signalling and calcium channels: Evolution and general principles. *European Journal of Pharmacology* (2014). doi:10.1016/j.ejphar.2013.11.013

54. Rone, M. B., Fan, J. & Papadopoulos, V. Cholesterol transport in steroid biosynthesis: role of protein-protein interactions and implications in disease states. *Biochim. Biophys. Acta* **1791**, 646–58 (2009).

55. Stoica, R. *et al.* ER–mitochondria associations are regulated by the VAPB–PTPIP51 interaction and are disrupted by ALS/FTD-associated TDP-43. *Nat. Commun.* (2014). doi:10.1038/ncomms4996

56. Ma, Y. & Hendershot, L. M. ER chaperone functions during normal and stress conditions. *J. Chem. Neuroanat.* **28**, 51–65 (2004).

57. Marchi, S. *et al.* Mitochondrial and endoplasmic reticulum calcium homeostasis and cell death. *Cell Calcium* (2018). doi:10.1016/j.ceca.2017.05.003

58. Raffaello, A., Mammucari, C., Gherardi, G. & Rizzuto, R. Calcium at the Center of Cell Signaling: Interplay between Endoplasmic Reticulum, Mitochondria, and Lysosomes. *Trends in Biochemical Sciences* (2016). doi:10.1016/j.tibs.2016.09.001

59.	Remmer, H. The role of the liver in drug metabolism. *Am. J. Med.* (1970). doi:10.1016/S0002-9343(70)80129-2

60.	Flis, V. V & Daum, G. Lipid Transport between the Endoplasmic. *Cold Spring Harb Perspect Biol* (2013). doi:10.1101/cshperspect.a013235

61.	Reiss, A. B. & Wirkowski, E. Role of HMG-CoA reductase inhibitors in neurological disorders: Progress to date. *Drugs* (2007). doi:10.2165/00003495-200767150-00001

62.	Feldman, D., Swarm, R. L. & Becker, J. Ultrastructural Study of Rat Liver and Liver Neoplasms after Long-Term Treatment with Phenobarbital. *Cancer Res.* (1981).

63.	PALADE, G. E. The fine structure of mitochondria. *Anat. Rec.* (1952). doi:10.1002/ar.1091140304

64.	Diab, D. L. *et al.* ER Tubules Mark Sites of Mitochondrial Division. *Science (80-.).* (2011). doi:10.1016/j.cgh.2008.07.016.Cytokeratin

65.	Friedman, J. R. *et al.* ER tubules mark sites of mitochondrial division. *Science (80-.).* (2011). doi:10.1126/science.1207385

66.	Parekh, A. B. & Penner, R. Store depletion and calcium influx. *Physiological Reviews* (1997). doi:10.1152/physrev.1997.77.4.901

67.	Penner, R., Fasolato, C. & Hoth, M. Calcium influx and its control by calcium release. *Curr. Opin. Neurobiol.* (1993). doi:10.1016/0959-4388(93)90130-Q

68.	Berridge, M. J. Inositol trisphosphate and calcium signalling mechanisms. *Biochimica et Biophysica Acta - Molecular Cell Research* (2009). doi:10.1016/j.bbamcr.2008.10.005

69. Fill, M. & Copello, J. A. Ryanodine receptor calcium release channels. *Physiological Reviews* (2002). doi:10.1152/physrev.00013.2002

70. Berridge, M. J., Bootman, M. D. & Roderick, H. L. Calcium signalling: Dynamics, homeostasis and remodelling. *Nature Reviews Molecular Cell Biology* (2003). doi:10.1038/nrm1155

71. Schwarz, P. Calcium homeostasis. *Ugeskrift for laeger* (1994). doi:10.5005/jp/books/13010_5

72. Berridge, M. J. The endoplasmic reticulum: A multifunctional signaling organelle. *Cell Calcium* (2002). doi:10.1016/S0143416002001823

73. Sammels, E., Parys, J. B., Missiaen, L., De Smedt, H. & Bultynck, G. Intracellular Ca2+ storage in health and disease: A dynamic equilibrium. *Cell Calcium* (2010). doi:10.1016/j.ceca.2010.02.001

74. Hogan, P. G., Lewis, R. S. & Rao, A. Molecular Basis of Calcium Signaling in Lymphocytes: STIM and ORAI. *Annu. Rev. Immunol.* (2010). doi:10.1146/annurev.immunol.021908.132550

75. Liou, J. *et al.* STIM is a Ca2+ sensor essential for Ca2+-store- depletion-triggered Ca2+ influx. *Curr. Biol.* (2005). doi:10.1016/j.cub.2005.05.055

76. Derler, I., Jardin, I. & Romanin, C. Molecular mechanisms of STIM/Orai communication. *Am. J. Physiol. - Cell Physiol.* (2016). doi:10.1152/ajpcell.00007.2016

77. Hewavitharana, T. *et al.* Location and function of STIM1 in the activation of Ca2+ entry signals. *J. Biol. Chem.* (2008). doi:10.1074/jbc.M802239200

78. Hetz, C. The unfolded protein response: controlling cell fate decisions under

ER stress and beyond. *Nat. Rev. Mol. Cell Biol.* **13**, 89–102 (2012).

79. Bernales, S., Papa, F. R. & Walter, P. Intracellular Signaling by the Unfolded Protein Response. *Annu. Rev. Cell Dev. Biol.* (2006). doi:10.1146/annurev.cellbio.21.122303.120200

80. Lai, E., Teodoro, T. & Volchuk, A. Endoplasmic reticulum stress: Signaling the unfolded protein response. *Physiology* (2007). doi:10.1152/physiol.00050.2006

81. Blumental-Perry, A. Endoplasmic Reticulum Stress Response, the Future of Cancer Research and a New Designated Journal. *Endoplasmic Reticulum Stress Cancers* **1**, 1–3 (2012).

82. Lai, E., Teodoro, T. & Volchuk, A. Endoplasmic Reticulum Stress: Signaling the Unfolded Protein Response. *Physiology* **22**, 193–201 (2007).

83. Chakrabarti, A., Chen, A. W. & Varner, J. D. A review of the mammalian unfolded protein response. *Biotechnology and Bioengineering* (2011). doi:10.1002/bit.23282

84. Corazzari, M., Gagliardi, M., Fimia, G. M. & Piacentini, M. Endoplasmic reticulum stress, unfolded protein response, and cancer cell fate. *Front. Oncol.* (2017). doi:10.3389/fonc.2017.00078

85. Park, G. Bin *et al.* Endoplasmic reticulum stress-mediated apoptosis of EBV-transformed B cells by cross-linking of CD70 is dependent upon generation of reactive oxygen species and activation of p38 MAPK and JNK pathway. *J. Immunol.* **185**, 7274–7284 (2010).

86. Giampietri, C. *et al.* Cancer microenvironment and endoplasmic reticulum stress response. *Mediators of Inflammation* (2015). doi:10.1155/2015/417281

87.   Puthalakath, H. *et al.* ER Stress Triggers Apoptosis by Activating BH3-Only Protein Bim. *Cell* **129**, 1337–1349 (2007).

88.   Bravo, R. *et al.* Endoplasmic Reticulum and the Unfolded Protein Response. Dynamics and Metabolic Integration. *Int. Rev. Cell Mol. Biol.* (2013). doi:10.1016/B978-0-12-407704-1.00005-1

89.   Oda, T., Kosuge, Y., Arakawa, M., Ishige, K. & Ito, Y. Distinct mechanism of cell death is responsible for tunicamycin-induced ER stress in SK-N-SH and SH-SY5Y cells. *Neurosci. Res.* **60**, 29–39 (2008).

90.   Varadarajan, S. *et al.* Endoplasmic Reticulum Membrane Reorganization Is Regulated by Ionic Homeostasis. *PLoS One* **8**, (2013).

91.   Varadarajan, S. *et al.* A novel cellular stress response characterised by a rapid reorganisation of membranes of the endoplasmic reticulum. *Cell Death Differ.* **19**, 1896–1907 (2012).

92.   Elmore, S. Apoptosis: A Review of Programmed Cell Death. *Toxicologic Pathology* (2007). doi:10.1080/01926230701320337

93.   Fuchs, Y. & Steller, H. Programmed cell death in animal development and disease. *Cell* (2011). doi:10.1016/j.cell.2011.10.033

94.   Robertson, G. S., LaCasse, E. C. & Holcik, M. Programmed Cell Death. in *Pharmacology* (2009). doi:10.1016/B978-0-12-369521-5.00018-X

95.   Parsons, M. J. & Green, D. R. Mitochondria in cell death. *Essays Biochem.* (2010). doi:10.1042/BSE0470099

96.   Yip, K. W. & Reed, J. C. Bcl-2 family proteins and cancer. *Oncogene* (2008). doi:10.1038/onc.2008.307

97. Lessene, G., Czabotar, P. E. & Colman, P. M. BCL-2 family antagonists for cancer therapy. *Nature Reviews Drug Discovery* (2008). doi:10.1038/nrd2658

98. Li, P., Nijhawan, D. & Wang, X. Mitochondrial activation of apoptosis. *Cell* **116**, S57–S61 (2004).

99. Choi, A. M. K. & Wang, X. Apoptosis. in *Encyclopedia of Respiratory Medicine, Four-Volume Set* (2006). doi:10.1016/B0-12-370879-6/00030-2

100. Kumar, S. Caspase function in programmed cell death. *Cell Death and Differentiation* (2007). doi:10.1038/sj.cdd.4402060

101. Danial, N. N. & Korsmeyer, S. J. Cell Death: Critical Control Points. *Cell* **116**, 205–219 (2004).

102. Zhang, L., Ming, L. & Yu, J. BH3 mimetics to improve cancer therapy; mechanisms and examples. *Drug Resist. Updat.* (2007). doi:10.1016/j.drup.2007.08.002

103. Vogler, M. Targeting BCL2-Proteins for the Treatment of Solid Tumours. *Adv. Med.* **2014**, 1–14 (2014).

104. Tait, S. W. G. & Green, D. R. Mitochondria and cell death: Outer membrane permeabilization and beyond. *Nature Reviews Molecular Cell Biology* (2010). doi:10.1038/nrm2952

105. Electron, T. & Chain, T. Electron Transport and Oxidative. *Transport* (1999). doi:10.1007/s00203-011-0785-7

106. Kluck, R. M., Bossy-Wetzel, E., Green, D. R. & Newmeyer, D. D. The release of cytochrome c from mitochondria: a primary site for Bcl-2 regulation of apoptosis. *Science* **275**, 1132–6 (1997).

107. Tuppy, H. & Kreil, G. Cytochrome c. in *Encyclopedia of Biological Chemistry: Second Edition* (2013). doi:10.1016/B978-0-12-378630-2.00374-1

108. Otera, H., Ishihara, N. & Mihara, K. New insights into the function and regulation of mitochondrial fission. *Biochim. Biophys. Acta - Mol. Cell Res.* **1833**, 1256–1268 (2013).

109. Zorzano, A., Liesa, M., Sebastián, D., Segalés, J. & Palacín, M. Mitochondrial fusion proteins: Dual regulators of morphology and metabolism. *Seminars in Cell and Developmental Biology* (2010). doi:10.1016/j.semcdb.2010.01.002

110. Campbell, K. J. & Tait, S. W. G. Targeting BCL-2 regulated apoptosis in cancer. *Open Biology* (2018). doi:10.1098/rsob.180002

111. Grandemange, S., Herzig, S. & Martinou, J. C. Mitochondrial dynamics and cancer. *Seminars in Cancer Biology* (2009). doi:10.1016/j.semcancer.2008.12.001

112. Thomas, S. *et al.* Targeting the Bcl-2 family for cancer therapy. *Expert Opin. Ther. Targets* **17**, 61–75 (2013).

113. Billard, C. BH3 mimetics: status of the field and new developments. *Mol. Cancer Ther.* **12**, 1691–700 (2013).

114. Vaillant, F. *et al.* Targeting BCL-2 with the BH3 Mimetic ABT-199 in Estrogen Receptor-Positive Breast Cancer. *Cancer Cell* (2013). doi:10.1016/j.ccr.2013.06.002

115. Delbridge, A. R. D. & Strasser, A. The BCL-2 protein family, BH3-mimetics and cancer therapy. *Cell Death and Differentiation* (2015). doi:10.1038/cdd.2015.50

116. Elkholi, R., Floros, K. V. & Chipuk, J. E. The role of BH3-only proteins in tumor cell development, signaling, and treatment. *Genes and Cancer* (2011). doi:10.1177/1947601911417177

117. Butterworth, M., Pettitt, A., Varadarajan, S. & Cohen, G. M. BH3 profiling and a toolkit of BH3-mimetic drugs predict anti-apoptotic dependence of cancer cells. *Br. J. Cancer* **114**, 638–641 (2016).

118. Henz, K. *et al.* Selective BH3-mimetics targeting BCL-2, BCL-XL or MCL-1 induce severe mitochondrial perturbations. *Biol. Chem.* (2018). doi:10.1515/hsz-2018-0233

119. Cang, S., Iragavarapu, C., Savooji, J., Song, Y. & Liu, D. ABT-199 (venetoclax) and BCL-2 inhibitors in clinical development. *Journal of Hematology and Oncology* (2015). doi:10.1186/s13045-015-0224-3

120. Fresquet, V., Rieger, M., Carolis, C., García-Barchino, M. J. & Martinez-Climent, J. A. Acquired mutations in BCL2 family proteins conferring resistance to the BH3 mimetic ABT-199 in lymphoma. *Blood* (2014). doi:10.1182/blood-2014-03-560284

121. Lomonosova, E. & Chinnadurai, G. BH3-only proteins in apoptosis and beyond: an overview. *Oncogene* **27 Suppl 1**, S2-19 (2008).

122. L.Omonosova, E. & C.Hinnadurai, G. BH3-only proteins in apoptosis and beyond: An overview. *Oncogene* (2008). doi:10.1038/onc.2009.39

123. Moffatt, B. A. & Ashihara, H. Purine and Pyrimidine Nucleotide Synthesis and Metabolism. *Arab. B.* (2002). doi:10.1199/tab.0018

124. Levine, R. L., Hoogenraad, N. J. & Kretchmer, N. A review: Biological and

clinical aspects of pyrimidine metabolism. *Pediatr. Res.* (1974). doi:10.1203/00006450-197407000-00008

125. Smith, L. H. Pyrimidine Metabolism in Man. *New England Journal of Medicine* (1973). doi:10.1056/NEJM197304122881505

126. D'Eustachio, P. Pyrimidine metabolism. *Reactome - a curated knowledgebase Biol. pathways* (2003). doi:10.3180/react_957.1

127. Reis, R. A. G., Calil, F. A., Feliciano, P. R., Pinheiro, M. P. & Nonato, M. C. The dihydroorotate dehydrogenases: Past and present. *Archives of Biochemistry and Biophysics* (2017). doi:10.1016/j.abb.2017.06.019

128. Madak, J. T., Bankhead, A., Cuthbertson, C. R., Showalter, H. D. & Neamati, N. Revisiting the role of dihydroorotate dehydrogenase as a therapeutic target for cancer. *Pharmacology and Therapeutics* (2019). doi:10.1016/j.pharmthera.2018.10.012

129. Christian, S. *et al.* The novel dihydroorotate dehydrogenase (DHODH) inhibitor BAY 2402234 triggers differentiation and is effective in the treatment of myeloid malignancies. *Leukemia* (2019). doi:10.1038/s41375-019-0461-5

130. Wu, D. *et al.* Pharmacological inhibition of dihydroorotate dehydrogenase induces apoptosis and differentiation in acute myeloid leukemia cells. *Haematologica* (2018). doi:10.3324/haematol.2018.188185

131. Sainas, S. *et al.* DHODH inhibitors and leukemia: An emergent interest for new myeloid differentiation agents. *Drugs Future* (2018). doi:10.1358/dof.2018.043.11.2856492

132. Löffler, M., Fairbanks, L. D., Zameitat, E., Marinaki, A. M. & Simmonds, H.

A. Pyrimidine pathways in health and disease. *Trends in Molecular Medicine* (2005). doi:10.1016/j.molmed.2005.07.003

133. Baumgartner, R. Dual binding mode DHODH inhibitor. *J. Med. Chem.* (2006).

134. Walse, B. *et al.* The structures of human dihydroorotate dehydrogenase with and without inhibitor reveal conformational flexibility in the inhibitor and substrate binding sites. *Biochemistry* (2008). doi:10.1021/bi8003318

135. Baumgartner, R. *et al.* Dual binding mode of a novel series of DHODH inhibitors. *J. Med. Chem.* (2006). doi:10.1021/jm0506975

136. Breedveld, F. C. & Dayer, J. M. Leflunomide: Mode of action in the treatment of rheumatoid arthritis. *Annals of the Rheumatic Diseases* (2000). doi:10.1136/ard.59.11.841

137. Hurt, D. E., Sutton, A. E. & Clardy, J. Brequinar derivatives and species-specific drug design for dihydroorotate dehydrogenase. *Bioorganic Med. Chem. Lett.* (2006). doi:10.1016/j.bmcl.2005.12.029

138. Zhou, J. *et al.* ASLAN003, a Novel and Potent Dihydroorotate Dehydrogenase (DHODH) Inhibitor, Induces Differentiation of Acute Myeloid Leukemia. *Blood* (2018). doi:10.1182/blood-2018-99-114392

139. Bar-Or, A., Pachner, A., Menguy-Vacheron, F., Kaplan, J. & Wiendl, H. Teriflunomide and its mechanism of action in multiple sclerosis. *Drugs* (2014). doi:10.1007/s40265-014-0212-x

140. He, D. *et al.* Teriflunomide for multiple sclerosis. *Cochrane Database of Systematic Reviews* (2016). doi:10.1002/14651858.CD009882.pub3

141. Urba, S. *et al.* Multicenter phase II trial of brequinar sodium in patients with

advanced squamous-cell carcinoma of the head and neck. *Cancer Chemother. Pharmacol.* (1992). doi:10.1007/BF00685106

142. Patrick Dumont, M. & Fiebig, H. H. Phase II Preclinical Drug Screening in Human Tumor Xenografts: A First European Multicenter Collaborative Study. *Cancer Res.* (1992).

143. Oh, J. & O'Connor, P. W. Teriflunomide. *Neurol. Clin. Pract.* (2013). doi:10.1212/CPJ.0b013e318296f299

144. O'Connor, P. W. *et al.* A phase II study of the safety and efficacy of teriflunomide in multiple sclerosis with relapses. *Neurology* (2006). doi:10.1212/01.wnl.0000203121.04509.31

145. Miller, A. E. Teriflunomide in multiple sclerosis: an update. *Neurodegener. Dis. Manag.* (2017). doi:10.2217/nmt-2016-0029

146. Tallantyre, E., Evangelou, N. & Constantinescu, C. S. Spotlight on teriflunomide. *International MS Journal* (2008).

147. Sykes, D. B. *et al.* Inhibition of Dihydroorotate Dehydrogenase Overcomes Differentiation Blockade in Acute Myeloid Leukemia. *Cell* (2016). doi:10.1016/j.cell.2016.08.057

148. Krols, M., Bultynck, G. & Janssens, S. ER-Mitochondria contact sites: A new regulator of cellular calcium flux comes into play. *J. Cell Biol.* (2016). doi:10.1083/jcb.201607124

149. Michel, A. H. & Kornmann, B. The ERMES complex and ER–mitochondria connections. *Biochem. Soc. Trans.* (2012). doi:10.1042/BST20110758

150. Wang, M. & Kaufman, R. J. The impact of the endoplasmic reticulum protein-

folding environment on cancer development. *Nat. Rev. Cancer* **14**, 581–597 (2014).

151. Ron, D. & Walter, P. Signal integration in the endoplasmic reticulum unfolded protein response. *Nat Rev Mol Cell Biol* **8**, 519–529 (2007).

152. Voorhees, R. M. & Hegde, R. S. Structure of the Sec61 channel opened by a signal sequence. *Science (80-.).* (2016). doi:10.1126/science.aad4992

153. Shibata, Y., Hu, J., Kozlov, M. M. & Rapoport, T. A. Mechanisms shaping the membranes of cellular organelles. *Annu. Rev. Cell Dev. Biol.* **25**, 329–54 (2009).

154. English, A. R., Zurek, N. & Voeltz, G. K. Peripheral ER structure and function. *Current Opinion in Cell Biology* (2009). doi:10.1016/j.ceb.2009.04.004

155. Chen, S., Novick, P. & Ferro-Novick, S. ER structure and function. *Curr. Opin. Cell Biol.* **25**, 428–33 (2013).

156. Niu, K. *et al.* BAP31 is involved in T cell activation through TCR signal pathways. *Sci. Rep.* (2017). doi:10.1038/srep44809

157. Schamel, W. W. A. *et al.* A high-molecular-weight complex of membrane proteins BAP29/BAP31 is involved in the retention of membrane-bound IgD in the endoplasmic reticulum. *Proc. Natl. Acad. Sci. U. S. A.* (2003). doi:10.1073/pnas.1633363100

158. Lynes, E. M. & Simmen, T. Urban planning of the endoplasmic reticulum (ER): How diverse mechanisms segregate the many functions of the ER. *Biochimica et Biophysica Acta - Molecular Cell Research* (2011). doi:10.1016/j.bbamcr.2011.06.011

159. Gao, G., Zhu, C., Liu, E. & Nabi, I. R. Reticulon and CLIMP-63 regulate

nanodomain organization of peripheral ER tubules. *PLoS Biol.* (2019). doi:10.1371/journal.pbio.3000355

160. Bertolotti, A., Zhang, Y., Hendershot, L. M., Harding, H. P. & Ron, D. Dynamic interaction of BiP and ER stress transducers in the unfolded-protein response. *Nat. Cell Biol.* **2**, 326–32 (2000).

161. Hatahet, F. & Ruddock, L. W. Protein disulfide isomerase: A critical evaluation of its function in disulfide bond formation. *Antioxidants and Redox Signaling* (2009). doi:10.1089/ars.2009.2466

162. Li, X., Zhang, K. & Li, Z. Unfolded protein response in cancer: the physician's perspective. *J. Hematol. Oncol.* **4**, 8 (2011).

163. Volchuk, A. & Ron, D. The endoplasmic reticulum stress response in the pancreatic ??-cell. *Diabetes, Obes. Metab.* **12**, 48–57 (2010).

164. Appenzeller-Herzog, C. & Hauri, H. P. The ER-Golgi intermediate compartment (ERGIC): In search of its identity and function. *J. Cell Sci.* (2006). doi:10.1242/jcs.03019

165. Hauri, H. P., Kappeler, F., Andersson, H. & Appenzeller, C. ERGIC-53 and traffic in the secretory pathway. *Journal of Cell Science* (2000).

166. Nakamura, N. *et al.* Characterization of a cis-Golgi matrix protein, GM130. *J. Cell Biol.* (1995). doi:10.1083/jcb.131.6.1715

167. Nakamura, N. Emerging new roles of GM130, a cis-Golgi matrix protein, in higher order cell functions. *Journal of Pharmacological Sciences* (2010). doi:10.1254/jphs.09R03CR

168. Rowland, A. A. & Voeltz, G. K. contacts : function of the junction. *Nat. Rev.*

Mol. Cell Biol. **13**, 607–615 (2012).

169. Eskelinen, E. L. Roles of LAMP-1 and LAMP-2 in lysosome biogenesis and autophagy. *Molecular Aspects of Medicine* (2006). doi:10.1016/j.mam.2006.08.005

170. Bukau, B. & Horwich, A. L. The Hsp70 and Hsp60 chaperone machines. *Cell* (1998). doi:10.1016/S0092-8674(00)80928-9

171. Friedman, J. R., Webster, B. M., Mastronarde, D. N., Verhey, K. J. & Voeltz, G. K. ER sliding dynamics and ER-mitochondrial contacts occur on acetylated microtubules. *J. Cell Biol.* **190**, 363–75 (2010).

172. Park, Y. S., Choi, S. E. & Koh, H. C. PGAM5 regulates PINK1/Parkin-mediated mitophagy via DRP1 in CCCP-induced mitochondrial dysfunction. *Toxicol. Lett.* (2018). doi:10.1016/j.toxlet.2017.12.004

173. Thomas, K. J. & Jacobson, M. R. Defects in Mitochondrial Fission Protein Dynamin-Related Protein 1 Are Linked to Apoptotic Resistance and Autophagy in a Lung Cancer Model. *PLoS One* (2012). doi:10.1371/journal.pone.0045319

174. Milani, M. *et al.* DRP-1 is required for BH3 mimetic-mediated mitochondrial fragmentation and apoptosis. *Cell Death Dis.* (2017). doi:10.1038/cddis.2016.485

175. Milani, M., Cohen, G. M. & Varadarajan, S. ER shaping proteins regulate mitochondrial fission, outer membrane permeabilization and apoptosis. *bioRxiv* (2018). doi:10.1101/340448

176. Xu, W. *et al.* Bax-PGAM5L-Drp1 complex is required for intrinsic apoptosis execution. *Oncotarget* (2015). doi:10.18632/oncotarget.5013

177. Martinou, J. C. & Youle, R. J. Mitochondria in Apoptosis: Bcl-2 Family Members and Mitochondrial Dynamics. *Developmental Cell* (2011). doi:10.1016/j.devcel.2011.06.017

178. Karbowski, M., Norris, K. L., Cleland, M. M., Jeong, S. Y. & Youle, R. J. Role of Bax and Bak in mitochondrial morphogenesis. *Nature* (2006). doi:10.1038/nature05111

179. Westphal, D., Dewson, G., Czabotar, P. E. & Kluck, R. M. Molecular biology of Bax and Bak activation and action. *Biochimica et Biophysica Acta - Molecular Cell Research* (2011). doi:10.1016/j.bbamcr.2010.12.019

180. Wei, M. C. *et al.* Proapoptotic BAX and BAK: A requisite gateway to mitochondrial dysfunction and death. *Science (80-.).* (2001). doi:10.1126/science.1059108

181. Hsu, Y. Te & Youle, R. J. Nonionic detergents induce dimerization among members of the Bcl-2 family. *J. Biol. Chem.* (1997). doi:10.1074/jbc.272.21.13829

182. Upton, J. P., Valentijn, A. J., Zhang, L. & Gilmore, A. P. The N-terminal conformation of Bax regulates cell commitment to apoptosis. *Cell Death Differ.* (2007). doi:10.1038/sj.cdd.4402092

183. Nechushtan, A., Smith, C. L., Hsu, Y. Te & Youle, R. J. Conformation of the Bax C-terminus regulates subcellular location and cell death. *EMBO J.* (1999). doi:10.1093/emboj/18.9.2330

184. Souers, A. J. *et al.* ABT-199, a potent and selective BCL-2 inhibitor, achieves antitumor activity while sparing platelets. *Nat. Med.* **19**, 202–8 (2013).

185. Faqar-Uz-Zaman, S. F., Heinicke, U., Meister, M. T., Vogler, M. & Fulda, S. BCL-xL-selective BH3 mimetic sensitizes rhabdomyosarcoma cells to chemotherapeutics by activation of the mitochondrial pathway of apoptosis. *Cancer Lett.* (2018). doi:10.1016/j.canlet.2017.09.025

186. Ferreira, A. *et al.* Cellular and Molecular Life Sciences Mitochondria dynamism: of shape, transport and cell migration. *Cell. Mol. Life Sci* (2014). doi:10.1007/s00018-014-1557-8

187. Westermann, B. Organelle dynamics: ER embraces mitochondria for fission. *Curr. Biol.* **21**, R922–R924 (2011).

188. Rufini, A. & Melino, G. Cell death pathology: The war against cancer. *Biochem. Biophys. Res. Commun.* **414**, 445–450 (2011).

189. Wang, X. Z. *et al.* Signals from the stressed endoplasmic reticulum induce C/EBP-homologous protein (CHOP/GADD153). *Mol. Cell. Biol.* **16**, 4273–80 (1996).

190. Ni, M. & Lee, A. S. ER chaperones in mammalian development and human diseases. *FEBS Lett.* **581**, 3641–3651 (2007).

191. Lee, H. & Yoon, Y. Mitochondrial fission: Regulation and ER connection. *Molecules and Cells* (2014). doi:10.14348/molcells.2014.2329

192. Friedman, J. R. *et al.* ER Tubules Mark Sites of Mitochondrial Division. *Science (80-.).* **334**, 358–362 (2011).

193. Kashatus, J. A. *et al.* Erk2 phosphorylation of Drp1 promotes mitochondrial fission and MAPK-driven tumor growth. *Mol. Cell* (2015). doi:10.1016/j.molcel.2015.01.002

194. Gan, X. *et al.* Inhibition of ERK-DLP1 signaling and mitochondrial division alleviates mitochondrial dysfunction in Alzheimer's disease cybrid cell. *Biochim. Biophys. Acta - Mol. Basis Dis.* (2014). doi:10.1016/j.bbadis.2013.11.009

195. Liesa, M., Palacin, M. & Zorzano, A. Mitochondrial Dynamics in Mammalian Health and Disease. *Physiol. Rev.* **89**, 799–845 (2009).

196. Berridge, M. J. The endoplasmic reticulum: A multifunctional signaling organelle. *Cell Calcium* **32**, 235–249 (2002).

197. Youle, R. J. *et al.* Measuring ER stress and the unfolded protein response using mammalian tissue culture system. *Biochim. Biophys. Acta - Mol. Cell Res.* **7**, 71–92 (2014).

198. Michel, A. H. & Kornmann, B. The ERMES complex and ER-mitochondria connections. *Biochemical Society Transactions* (2012). doi:10.1042/BST20110758

199. Lu, L. *et al.* The small molecule dispergo tubulates the endoplasmic reticulum and inhibits export. *Mol. Biol. Cell* **24**, 1020–9 (2013).

200. Majewski, L. & Kuznicki, J. SOCE in neurons: Signaling or just refilling? *Biochimica et Biophysica Acta - Molecular Cell Research* (2014). doi:10.1016/j.bbamcr.2015.01.019

201. Feske, S. ORAI1 and STIM1 deficiency in human and mice: roles of store-operated Ca2+ entry in the immune system and beyond. *Immunological Reviews* (2009). doi:10.1111/j.1600-065X.2009.00818.x

202. Smyth, J. T. *et al.* Activation and regulation of store-operated calcium entry. *J.*

Cell. Mol. Med. (2010). doi:10.1111/j.1582-4934.2010.01168.x

203. Rahman, S. & Rahman, T. Unveiling some FDA-Approved drugs as inhibitors of the store-operated Ca2+ entry pathway. *Sci. Rep.* (2017). doi:10.1038/s41598-017-13343-x

204. K. Vyas, V. & Ghate, M. Recent Developments in the Medicinal Chemistry and Therapeutic Potential of Dihydroorotate Dehydrogenase (DHODH) Inhibitors. *Mini-Reviews Med. Chem.* (2011). doi:10.2174/138955711797247707

205. Ren, Z. *et al.* Endoplasmic reticulum stress and MAPK signaling pathway activation underlie leflunomide-induced toxicity in HepG2 Cells. *Toxicology* (2017). doi:10.1016/j.tox.2017.10.002

206. Su, H. Y. *et al.* The unfolded protein response plays a predominant homeostatic role in response to mitochondrial stress in pancreatic stellate cells. *PLoS One* **11**, 1–21 (2016).

207. Ohoka, N., Yoshii, S., Hattori, T., Onozaki, K. & Hayashi, H. TRB3, a novel ER stress-inducible gene, is induced via ATF4-CHOP pathway and is involved in cell death. *EMBO J.* (2005). doi:10.1038/sj.emboj.7600596

208. Shen, X., Zhang, K. & Kaufman, R. J. The unfolded protein response - A stress signaling pathway of the endoplasmic reticulum. *Journal of Chemical Neuroanatomy* (2004). doi:10.1016/j.jchemneu.2004.02.006

209. Bootman, M. D. *et al.* 2-Aminoethoxydiphenyl borate (2-APB) is a reliable blocker of store-operated Ca2+ entry but an inconsistent inhibitor of InsP3-induced Ca2+ release. *FASEB Journal* (2002). doi:10.1096/fj.02-0037rev

210. Missiaen, L., Callewaert, G., De Smedt, H. & Parys, J. B. 2-

Aminoethoxydiphenyl borate affects the inositol 1,4,5-trisphosphate receptor, the intracellular Ca2+ pump and the non-specific Ca2+ leak from the non-mitochondrial Ca2+ stores in permeabilized A7r5 cells. *Cell Calcium* (2001). doi:10.1054/ceca.2000.0163

211. Yedida, G., Milani, M., Cohen, G. M. & Varadarajan, S. Apogossypol-mediated reorganisation of the endoplasmic reticulum antagonises mitochondrial fission and apoptosis. *Cell Death Dis.* (2019). doi:10.1038/s41419-019-1759-y

212. Arnould, S. *et al.* Checkpoint kinase 1 inhibition sensitises transformed cells to dihydroorotate dehydrogenase inhibition. *Oncotarget* (2017). doi:10.18632/oncotarget.19199

213. Mathur, D. *et al.* PTEN regulates glutamine flux to pyrimidine synthesis and sensitivity to dihydroorotate dehydrogenase inhibition. *Cancer Discov.* (2017). doi:10.1158/2159-8290.CD-16-0612

214. Miyazaki, Y. *et al.* Selective cytotoxicity of dihydroorotate dehydrogenase inhibitors to human cancer cells under hypoxia and nutrient-deprived conditions. *Front. Pharmacol.* (2018). doi:10.3389/fphar.2018.00997

215. Méry, B. *et al.* Preclinical models in HNSCC: A comprehensive review. *Oral Oncology* (2017). doi:10.1016/j.oraloncology.2016.12.010

216. McCarthy, C. E., Field, J. K., Rajlawat, B. P., Field, A. E. & Marcus, M. W. Trends and regional variation in the incidence of head and neck cancers in England: 2002 to 2011. *Int. J. Oncol.* (2015). doi:10.3892/ijo.2015.2990

217. Taib, B. G. *et al.* Socioeconomic deprivation and the burden of head and neck cancer—Regional variations of incidence and mortality in Merseyside and

Cheshire, North West, England. *Clin. Otolaryngol.* (2018). doi:10.1111/coa.13067

218. Galbiatti, A. L. S. *et al.* Head and neck cancer: Causes, prevention and treatment. *Brazilian Journal of Otorhinolaryngology* (2013). doi:10.5935/1808-8694.20130041

219. Farnebo, L., Malila, N., Mäkitie, A. & Laurell, G. Early death among head and neck cancer patients. *Current Opinion in Otolaryngology and Head and Neck Surgery* (2016). doi:10.1097/MOO.0000000000000236

220. Powers, R. E. *et al.* No Title. *Cell* **5**, 71–92 (2014).

221. Ma, J. *et al.* FaDu cell characteristics induced by multidrug resistance. *Oncol. Rep.* (2011). doi:10.3892/or.2011.1418

222. Galluzzi, L. *et al.* Molecular mechanisms of cisplatin resistance. *Oncogene* (2012). doi:10.1038/onc.2011.384

223. Shaloam, D. & Tchounwou, P. B. Cisplatin in cancer therapy: Molecular mechanisms of action. *Eur. J. Pharmacol.* (2014). doi:10.1016/j.ejphar.2014.07.025.Cisplatin

224. Dasari, S. & Bernard Tchounwou, P. Cisplatin in cancer therapy: Molecular mechanisms of action. *European Journal of Pharmacology* (2014). doi:10.1016/j.ejphar.2014.07.025

225. Bauer, J. A. *et al.* Targeting Apoptosis to Overcome Cisplatin Resistance: A Translational Study in Head and Neck Cancer. *Int. J. Radiat. Oncol. Biol. Phys.* (2007). doi:10.1016/j.ijrobp.2007.05.080

226. Cepeda, V. *et al.* Biochemical Mechanisms of Cisplatin Cytotoxicity.

Anticancer. Agents Med. Chem. (2008). doi:10.2174/187152007779314044

227. Amable, L. Cisplatin resistance and opportunities for precision medicine. *Pharmacological Research* (2016). doi:10.1016/j.phrs.2016.01.001

228. Ow, T. J. *et al.* Optimal targeting of BCL-family proteins in head and neck squamous cell carcinoma requires inhibition of both BCL-xL and MCL-1. *Oncotarget* (2019). doi:10.18632/oncotarget.26563

229. Weeden, C. E. *et al.* Dual inhibition of BCL-XL and MCL-1 is required to induce tumour regression in lung squamous cell carcinomas sensitive to FGFR inhibition. *Oncogene* (2018). doi:10.1038/s41388-018-0268-2

230. Bernier, J., Bentzen, S. M. & Vermorken, J. B. Molecular therapy in head and neck oncology. *Nature Reviews Clinical Oncology* (2009). doi:10.1038/nrclinonc.2009.40

231. Gugić, J. & Strojan, P. Squamous cell carcinoma of the head and neck in the elderly. *Reports of Practical Oncology and Radiotherapy* (2013). doi:10.1016/j.rpor.2012.07.014

232. Voravud, N., Charuruks, N. & Mutirangura, A. Squamous Cell Carcinoma of Head and Neck. *J. Med. Assoc. Thail.* (1997).

233. Perry, S. W., Norman, J. P., Barbieri, J., Brown, E. B. & Gelbard, H. A. Mitochondrial membrane potential probes and the proton gradient: A practical usage guide. *Biotechniques* **50**, 98–115 (2011).

234. Lam, W. Y. & Bhattacharya, D. Metabolic Links between Plasma Cell Survival, Secretion, and Stress. *Trends in Immunology* (2018). doi:10.1016/j.it.2017.08.007

235. Vincenz, L., Jäger, R., O'Dwyer, M. & Samali, A. Endoplasmic reticulum stress and the unfolded protein response: Targeting the achilles heel of multiple myeloma. *Molecular Cancer Therapeutics* (2013). doi:10.1158/1535-7163.MCT-12-0782

236. Schuck, S., Gallagher, C. M. & Walter, P. ER-phagy mediates selective degradation of endoplasmic reticulum independently of the core autophagy machinery. *J. Cell Sci.* (2014). doi:10.1242/jcs.154716

237. Mariotti, F. R., Corrado, M. & Campello, S. *Following mitochondria dynamism: Confocal analysis of the organelle morphology*. *Mitochondrial Regulation: Methods and Protocols* (2014). doi:10.1007/978-1-4939-1875-1-13

238. Mishra, P. & Chan, D. C. Mitochondrial dynamics and inheritance during cell division, development and disease. *Nat. Rev. Mol. Cell Biol.* **15**, 634–46 (2014).

239. Jonathan R. Friedman, 1 *et al.* ER Tubules Mark Sites of Mitochondrial Division. *Science* (2009). doi:10.1126/science.1176921

240. Senft, D. & Ronai, Z. A. Regulators of mitochondrial dynamics in cancer. *Current Opinion in Cell Biology* (2016). doi:10.1016/j.ceb.2016.02.001

241. Prudent, J. *et al.* MAPL SUMOylation of Drp1 Stabilizes an ER/Mitochondrial Platform Required for Cell Death. *Mol. Cell* (2015). doi:10.1016/j.molcel.2015.08.001

242. Samangouei, P. *et al.* MiD49 and MiD51: New mediators of mitochondrial fission and novel targets for cardioprotection. *Cond. Med.* (2018).

243. Kasahara, A. & Scorrano, L. Mitochondria: From cell death executioners to

regulators of cell differentiation. *Trends in Cell Biology* (2014). doi:10.1016/j.tcb.2014.08.005

244. Tuiskunen Bäck, A. & Lundkvist, Å. Dengue viruses – an overview. *Infect. Ecol. Epidemiol.* (2013). doi:10.3402/iee.v3i0.19839

245. Milani, M. *et al.* DRP-1 functions independently of mitochondrial structural perturbations to facilitate BH3 mimetic-mediated apoptosis. *Cell Death Discov.* (2019). doi:10.1038/s41420-019-0199-x

246. Kornmann, B. The molecular hug between the ER and the mitochondria. *Curr. Opin. Cell Biol.* (2013). doi:10.1016/j.ceb.2013.02.010

247. Griffing, L. R. Networking in the endoplasmic reticulum. in *Biochemical Society Transactions* (2010). doi:10.1042/BST0380747

248. Crib, A. E., Peyrou, M., Muruganandan, S. & Schneider, L. The endoplasmic reticulum in xenobiotic toxicity. *Drug Metabolism Reviews* (2005). doi:10.1080/03602530500205135